1-1-2012

Performance analysis of a two-stage variable capacity air source heat pump and a horizontal loop coupled ground source heat pump system

Amir Alizadeh Safa
Ryerson University

PERFORMANCE ANALYSIS OF A TWO-STAGE VARIABLE CAPACITY AIR SOURCE HEAT PUMP AND A HORIZONTAL LOOP COUPLED GROUND SOURCE HEAT PUMP SYSTEM

By

Amir Alizadeh Safa
Bachelor of Engineering (Mechanical Engineering)
Ryerson University, Toronto, 2009

A Thesis

Presented to Ryerson University

In partial fulfillment of the

requirements for the degree of

MASTER OF APPLIED SCIENCE

In the program of

Mechanical Engineering

Toronto, Ontario, Canada, 2012

Author's Declaration

I hereby declare that I am the sole author of this thesis.

I authorize Ryerson University to lend this thesis to other institutions or individuals for the purpose of scholarly research.

Amir Alizadeh Safa

I further authorize Ryerson University to reproduce this thesis by photocopying or by other means, in total or in part, at the request of other institutions or individuals for the purpose of scholarly research.

Amir Alizadeh Safa

PERFORMANCE ANALYSIS OF A TWO-STAGE VARIABLE CAPACITY AIR SOURCE HEAT PUMP AND A HORIZONTAL LOOP COUPLED GROUND SOURCE HEAT PUMP SYSTEM

Amir Alizadeh Safa
Master of Applied Science
Mechanical Engineering
Ryerson University, Toronto, Ontario, Canada, 2012

Abstract

The thermal performance of a new two-stage variable capacity air source heat pump (ASHP) and a horizontal ground loop ground source heat pump (GSHP) was investigated side-by-side at the Archetype Sustainable Twin Houses located in Toronto, Canada. The heat pumps were tested in cooling mode, as well as heating mode under extreme winter conditions. In cooling mode, the ASHP COP ranged from 4.7 to 5.7 at an outdoor temperature of 33°C and 16°C respectively, while the GSHP COP ranged from 4.9 (at an ELT of 8.5°C and EST of 19.2°C) to 5.6 (at an ELT of 12.4°C and EST of 17.8°C). In heating mode, the ASHP COP ranged from 1.79 to 5.0 at an outdoor temperature of -19˚C and 9˚C respectively, while the GSHP COP ranged from 3.05 (at an ELT of 44.4°C and an EST of 2.7°C) to 3.44 (at an ELT of 41.5°C and an EST of 5.48°C) during the earlier winter test period. Data extrapolation and energy simulation was also performed to predict annual heat pump performance in Toronto as well as other Canadian regions.

Acknowledgements

This thesis would not have been possible without the kind support of my supervisor Dr. Alan Fung. Dr. Fung's guidance and encouragement from the initial to the final level of the thesis enabled me to finish this great task. I would also like to thank Dr. Wey Leong for his assistance with my thesis. I am grateful to my colleagues Dahai Zhang and Rupayan Barua for their support in this project. The financial support of Regional Municipality of Peel, Regional Municipality of York, City of Toronto, Building Industry and Land Development (BILD) Association, Toronto and Region Conservation Authority (TRCA), MITACS Accelerate, Reliance Home Comfort and Union Gas Ltd. in implementing this project is greatly appreciated. I would finally like to thank David Nixon and Warren Yates of the Toronto and Region Conservation Authority for implementing the monitoring system at the Archetype Houses.

Table of Contents

List of Tables

List of Figures

List of Appendices

Abbreviations

ASHP: Air-Source Heat Pump

ASHRAE: American Society of Heating Refrigeration Air conditioning Engineers

AHU: Air Handling Unit

BILD: Building Industry and Land Development

COP: Coefficient of Performance

DAQ: Data Acquisition System

DB: Dry Bulb

DHW: Domestic Hot Water

DHWT: Domestic Hot Water Tank

EST: Entering Source Temperature

ELT: Entering Load Temperature

GSHP: Ground-Source Heat Pump

GPM: Gallon per Minute

HVAC: Heating, Ventilation & Air Conditioning

kW: Kilowatt

kWh: Kilowatt Hour

LEED: Leadership in Energy and Environmental Design

NRCan: Natural Resources Canada

PG: Propylene Glycol

SEER: Seasonal Energy Efficiency Ratio

SCOP: Seasonal Coefficient of Performance

TRCA: Toronto and Region Conservation Authority

PSIa: Pound-Force Per Square Inch Absolute

WB: Wet Bulb

Nomenclature

AT	Air temperature (^{o}C)
COP_{Heat}	Heating coefficient of performance (kW/kW)
COP_{Cool}	Cooling coefficient of performance (kW/kW)
c_{pa}	Specific heat capacity of air (kJ/kg^{o}C)
c_{pw}	Specific heat capacity of water vapour (kJ/kg^{o}C)
FL16	Water/propylene glycol flow rate in ground loop (gal/min)
H	Altitude (Ft)
h_w	Specific enthalpy of water vapour (kJ/kg)
h_{we}	Evaporation heat of water (kJ/kg)
h	Specific enthalpy of moist air (kJ/kg)
h_a	Specific enthalpy of dry air (kJ/kg)
$\dot{m}_w$	Mass flow rate of water (kg/s)
M_w	Mass of moist air (kg)
M_{da}	Mass of dry air (kg)
P_a	Atmospheric pressure (Pa)
Ps	Saturation vapour pressure (Pa)
P_{da}	Pressure of dry air (Pa)
P_w	Pressure of water vapour (Pa)
$\dot{Q}_{Heat}$	Heating delivered from heat pump (kW)
$\dot{Q}_{Cool}$	Cooling delivered from heat pump (kW)
$\dot{Q}_{Extraction}$	Heat extracted from ground (kW)
$\dot{Q}_{Desuperheater}$	Heat supplied by desuperheater (kW)

$\dot{Q}_{Electrical}$	Electrical power (kW)
R_{da}	Gas constant of dry air (287.05 J/kg.K)
RH	Relative humidity (%)
R_w	Gas constant of water vapour (461.495 J/kg.K)
t	Dry bulb temperature (^oC)
T	Dry bulb temperature (^oC)
V	Total volume (m^3)
$\dot{V}$	Volumetric flow rate (GPM)
w	Humidity ratio (kg water vapour/kg dry air)
x	Humidity ratio (kg/kg)

Greek Symbols:

ρ	Density of air (kg/m^3)

Chapter 1

Introduction and Objectives

Buildings significantly contribute to overall energy use and electricity consumption. Energy use by the building sector continues to increase mainly due to fast construction of new buildings. In Canada, buildings consume 33% of total energy production, and use 1.46 ExaJoules of energy per year (Marrone, 2007). According to the Natural Resources Canada, by 2030 all new homes will be built to net-zero energy standards (CanmetENERGY , 2009). To lower energy consumption associated with buildings and reach the net zero energy goal, a number of smart strategies can be employed. Besides the strategy of decreasing energy demand within buildings, another approach is to focus on energy efficiency. One area of energy efficiency that can be considered is the use of highly efficient mechanical equipment, such as advanced air-source heat pumps (ASHP) and ground source heat pumps (GSHP) for space heating and cooling. The use of such mechanical equipment can greatly lower primary energy use within buildings.

For the purpose of efficient residential heating and cooling, air-source heat pumps are more widely used than ground-source heat pumps mainly due to lower installed costs. ASHP systems use ambient air as a heat source in winter and pump heat inside the home using refrigerant filled coils. In heating mode, the liquid refrigerant absorbs heat through an outdoor evaporator changing into a vapour. This vapour is then compressed by the compressor resulting in a high temperature and high pressure gas. The gas is then delivered into the condenser where usually a fan blows indoor air over the coils to deliver hot air to the zone while condensing the refrigerant. In cooling mode, the cycle is reversed where heat inside the building is released to the ambient using the same principle. One great disadvantage of the air-source heat pump is the decrease of heat output and coefficient of performance (COP) in colder climates (Bertsch & Groll, 2008). As a result, most systems are often coupled with an auxiliary heating source. Heating requirements in climates like Canada provide a challenge to the air source heat pump because of outdoor temperatures that can reach below -25˚C. Also, because of such cold winter temperatures in the heating season, to meet the required building heating demand, a large sized heat pump will often be used. Due to such large capacity heat pump, the compressor will often operate at part load to meet the building demand at milder winter temperatures. This causes a reduction in efficiency and comfort due to the need of heat pump cycling. Multiple or modulating compressors address mismatched loads by sizing compressor capacity to meet heating loads at full capacity, and part load operation with a lower stage compressor to satisfy cooling loads and dehumidification. However, the problem of reduced heating cycle efficiency as ambient temperature decreases still remains (Roth, Dieckmann, & Brodrick, 2009). Variable speed ASHPs however offer potential improvements in the efficiency and reliability of operation. These improvements are due to reduction in cyclic operating time, and improved performance at lower operating speeds (Erbs, Bullock, & Voorhis, 1986).

Ground source heat pump systems are increasingly implemented for heating and air-conditioning in residential, commercial, and institutional buildings as well. This system consists of buried pipe loops in the ground, connected to a heat pump through which a fluid is circulated. Due to efficient space savings, the ground-loop heat exchangers are mostly constructed to a vertical borehole configuration rather than a horizontal one. The coefficient of performance of ground source heat pumps are generally higher than the air source heat pump mainly because of relatively stable source/sink temperatures (Kavanaugh & Raffferty, 1997). The GSHP uses the ground as a heat source in heating mode and a heat sink in cooling mode. In heating mode, heat is absorbed from the ground and used to evaporate the refrigerant. In cooling mode, the heat is absorbed from the conditioned space and transferred to the ground through the heat exchangers. Due to stable ground temperatures associated with the use of GSHP's, in colder climates such as Canada, the capacity of the system is not reduced in the same manner as the air source heat pump. One common issue with GSHP's however is an overall reduction of performance due to a reduction of ground temperature in the vicinity of the buried pipe during the end of the heating season. This is due to the significant amount of heat that is extracted from the ground from the beginning to the end of the heating season. As a result, in heating mode the GSHP is at times coupled with solar collectors for the purpose of recharging the ground temperature in cold climates (Enyu, Fung, Qi, & Leong, 2012), (Kjellsson, Hellstrom, & Perers, 2010), (Rad, Fung, & Leong, 2009)

Often with the use of heat pumps for space heating and cooling, a heat exchanger called a desuperheater is used to deliver some hot water for domestic hot water (DHW) use. The desuperheater is a heat exchanger used preferably in cooling mode placed after the compression stage to recover heat from the high pressure and high temperature superheated refrigerant exiting the compressor. This system takes some of the heat out of the discharge gas and delivers it for DHW heating. In cooling mode this process is known to enhance heat pump efficiency because it allows the refrigerant to be further condensed at the condenser heat exchanger. In heating mode however the heat transfer to the DHW is taken from the overall heat produced by the heat pump. (Biaoua & Bernier, 2008)

In an effort to demonstrate sustainable housing technologies in Ontario, the Toronto and Region Conservation Authority (TRCA) along with the Building Industry and Land Development (BILD) Association have implemented the "Archetype Sustainable House" project at the Living City Campus at Kortright Centre in Vaughan, Ontario, Canada. This prototype twin house is designed to demonstrate sustainable housing technologies through research, education, training, market transformation and partnership programs. Amongst a variety of sustainable technologies within the twin houses, two pieces of equipment are studied in this thesis: Two-stage variable capacity air source heat pump in House A, and a horizontal loop coupled ground source heat pump with an optional desuperheater in House B. A long term monitoring system has been implemented to monitor both the equipment using a data acquisition (DAQ) system, and analysed using LabVIEW platform. Data from various sensors installed in the system are collected every 5 seconds. (Zhang, Barua, & Fung, 2011).

1.1 Objectives

In order to investigate the two pieces of mechanical equipment, it is necessary to carry out comprehensive monitoring on most aspects of thermal performance of the heat pumps. To better understand the performance of these heat pumps, a combination of detailed monitoring, performance extrapolation, and energy modeling has been conducted. The detailed objectives of this thesis are given below.

1) Collection of data from sensors installed on both equipment

There are various sensors used to evaluate the performance of the two equipment. For the ASHP, the goal is to obtain 3-4 weeks of data in the cooling season, and 3-6 weeks in the heating season depending on weather conditions. Similarly, it is desirable to collect 3-4 weeks of data in the cooling season, and 3-4 weeks of data in the heating season for the GSHP.

2) Analysis of performance of the ASHP system using data collected

The ASHP system tested has the capability to control its capacity using a two stage variable speed compressor. This system also claims to perform well in cold ambient temperatures. The aim here is to develop cooling and heating performance curves for the ASHP as well as develop cooling and heating part load performance curves. Points of interest are the efficiency of the heat pump at the coldest outdoor temperatures, efficiency of the heat pump when the system is operating at part loads, and the two stage compressor operating characteristics.

3) Analysis of performance of the GSHP system using data collected

The GSHP system tested in the Archetype House has a horizontal coupled ground loop, and an optional desuperheater for water heating. The aim is to develop cooling and heating performance curves based on entering load and source temperatures. Points of interest are the efficiency of the heat pump at different load/source temperatures, and the cycling characteristics of the compressor.

4) The investigation of improvements and potential problems of control systems of equipment

Potential problems and improvements of control system within the overall systems will be investigated. The aim is to identify issues with the current as installed system and determine methods of improving the overall efficiency of the system through the use of data extrapolation.

5) The annual performance of the heat pumps and a comparison of the two systems using TRNSYS energy modeling

TRNSYS 16 will be used to model the twin houses as well as the heat pump systems including all conditioning equipment. The heat pumps will be modeled using the performance curves obtained from the data collection. The TRNSYS house model will be validated using the daily thermal output of the heat pumps at different average daily temperatures. The objective is to simulate the annual performance of each system in each house. The systems will then be simulated in different Canadian regions. Finally, a payback analysis will be investigated using the results of the simulation.

Chapter 2

Literature Review

2.1 Heat Pump Systems

Many studies in the literature have investigated the performance of heat pump systems using various methods. In all cases seen in literature, the heat pump system is mainly composed of the compressor, the indoor heat exchanger or condenser in heating mode, and the outdoor unit or the evaporator (in heating mode). The performance of the tested heat pump systems is generally given by the coefficient of performance (COP) which is defined as the output thermal energy over the input electricity consumption.

A study by the Technical University of Nova Scotia (Ugursal, Ma, & Li, 1992) studied the thermal performance of an air-to-air heat pump installed in an R-2000 house. A one year monitoring system was implemented to study the performance of the house and the air source heat pump system. Data was gathered from the installed sensors every three minutes using a micro-processor based data acquisition system. The results of the study showed that the heating COP (including indoor and outdoor units) of the air source heat pump peaked at 1.8 at an outdoor temperature of 4-6˚C while at -15˚C the COP turned out to be close to 1.1. In terms of part load performance, the research group noticed the heating COP fell sharply when the outdoor temperature was above 6˚C, this was because the heating requirement of the house was lower than the heating capacity of the heat pump and caused the heat pump to operate with short cycles in a less efficient part load mode.

A two-stage coupled heat pump system coupling an air source heat pump and a water source heat pump has been investigated for cold climates in Beijing, China (Wang, Ma, Jiang, Yang, Xu, & Yang, 2005). This system operates in two ways where the single stage operates in moderate outdoor temperatures supplying hot water at a temperature of 10°C – 20°C as a low temperature heat source for the WSHP, and the second stage operates in cold outdoor temperatures supplying hot water at a temperature of 20°C – 50°C. This system is installed in a 2200 m^2 building complex consisting of 17 guest rooms and 12 offices. The heating system consists of the two-stage coupled heat pump and in-floor radiant heating. The nominal heating capacity and power of each compressor is 118 kW and 37 kW respectively. The evaporator consists of 12 fans each having a nominal air flow rate of 10,500 m^3/hr. Measurements of hot water supply and return temperature, water flow rate, outdoor and indoor air temperature, intake and discharge temperature of compressor, condenser and evaporative pressure, and power consumption of the entire system were gathered. The test period was from December 16, 2003 to January 13, 2004 and the minimum and maximum ambient temperatures were -5˚C and 5˚C respectively. The findings of the experiment indicated that the average COP during this period was 3.2 while the minimum and maximum COP was obtained as 2.5 and 4.4 respectively.

A research group from the Istanbul Technical University (Kent, 1995) studied the performance of a compact air-to-air heat pump unit used for heating a small office. Using temperature, pressure, and power sensors, the group monitored the heat pump in heating mode and came up with a performance curve that summarized the COP of the heat pump with respect to ambient temperature. Due to the milder climate of the test location, the lowest temperature the heat pump encountered was 4˚C with a heating COP of 1.7.

Part-load performance analysis has been conducted on air-to-water heat pump systems to investigate the losses associated with compressor cycling and the use of backup heating (Tassou, Marquand, & Wilson, 1984). Experimental results have been obtained from an air-to-water heat pump designed for a maximum output of about 8 kW. The performance of the heat pump is monitored by comprehensive instrumentation linked to a single board microprocessor. The test house was considered to have a design heat loss of 7.86 kW at a temperature difference of 20 Kelvin. The results of the study indicated that even when heat pump sizing was performed at an optimal level, the losses due to on/off cycling reduced the efficiency of the system by about 6%, and backup resistant heating caused another decrease of efficiency by about 4% at low ambient temperatures.

A variable capacity compressor heat pump system was tested in Japan under winter temperatures between 0˚C and -10˚C and summer temperatures ranging from 25˚C to 35˚C (Umezu & Suma, 1984). The findings of this research suggest that the variable capacity compressor results in energy savings of 15%. They conclude that energy savings are achieved because 1) the system has a two-stage capacity without an electric heater enabling the output thermal energy to better meet the heating and cooling demand, 2) the heating to cooling ratio is 1.5 which is ideal for a two-stage system because the single stage can be mostly utilized for cooling while the second stage for heating, and 3) a smaller compressor can be used in the system.

Ten residential air-to-air heat pump systems were used to heat a 151.2 m^2 experimental greenhouse, and the performance under various temperatures was investigated (Tong, Kozai, Nishioka, & Ohyama, 2010). The ten heat pumps were identical each having a heating capacity of 2.8 kW and a rated heating COP of 5.4 at an indoor temperature of 20˚C and an outdoor temperature of 7˚C. Sensors were used to measure operating characteristics of the heat pumps to compute the COP. Air temperature and relative humidity in the greenhouse was measured using sensors with accuracy of ± 0.4˚C and ±3% respectively, while the outdoor temperature and relative humidity was measured with sensors having accuracy of ± 0.3˚C and ±2% respectively. Data was collected with a recorder every minute. The outdoor temperature during the experiment ranged from -4.5˚C to 5.6˚C while the indoor temperature was maintained at 16˚C. At an outdoor temperature of 5.6˚C the COP turned out to be 5.8 while at an outdoor temperature of -4.5˚C the COP was measured to be 2.9.

The monitored performance of an air to water heat pump in a well insulated experimental house has been investigated under part load operation (Mountford & Freund, 1981). The heat pump was installed as a split unit with a heat output of 4.4 kW at 0˚C ambient air temperature, with a water outlet temperature of 45˚C and 930 l/h flow rate. During compressor operation, measurements of water flow rate, temperature, and energy consumption were made every 3 seconds. The air temperatures in the zones as well as the ambient temperature were collected every 30 seconds. The sensor accuracy was estimated to be ± 2% in power consumption, ± 4 %

in heat flow, and ± 0.25˚C in temperature. The performance of the heat pump included the electricity consumption of the fan and circulation pump. The test was done during November 14 – March 24, 1980 with an average outdoor temperature of 6.4˚C. During this period the heat pump outputted 6269 kWh of heat while consuming 2745 kWh of electricity resulting in an average heating COP of 2.28. It was also concluded that the part load operation resulted in a 15% reduction in COP while compared to the steady state COP.

An ASHP was tested for the purpose of operating efficiently in cold winter temperatures of Beijing, China (Guoyuan, Qinhu, & Yi, 2003). In this system, a fan coil unit was used for the condenser. Operating conditions such as supply and return flow rate and temperature of water in the condenser, along with the system energy consumption was measured. The measured efficiency values were estimated to have an uncertainty of approximately 2.6%. The results of the study indicated that the heating capacity decreased linearly with a decrease of evaporation temperature however the rate of decrease was less than the conventional ASHP. It was noted that the heating capacity was approximately 5.5 kW when the condensing temperature was 45 ˚C and the evaporation temperature was -25˚C proving sufficient for the -15˚C lowest ambient temperatures of Beijing.

An enhanced ASHP system was built and experimentally tested in Wuxi, China for cold climate performance (Wang, Xie, Wu, Wu, & Yuan, 2011). The ASHP system uses a bypass refrigerant circuit to increase the density of the refrigerant at the inlet of the compressor thus improving the efficiency. The prototype ASHP was investigated in a temperature and humidity controlled test chamber. Various sensors were used to obtain the performance of the system. Sensors used included temperature sensors with an accuracy of ±0.1°C, pressure transducer sensors with an accuracy of ±0.2%, air velocity transducers with an accuracy of ±0.5%, watt-hour meter with an accuracy of ±1%, and a data logger with sampling intervals of 30 seconds. The findings of the test period suggest that at an indoor temperature of 20°C and an outdoor temperature of 9°C the COP turned out to be 3.5, while at an indoor temperature of 20°C and an outdoor temperature of -15°C the COP was 2.35.

A three year study on the performance of a ground source heat pump system in Northern Greece (Michopoulos, Bozis, Kikidis, Papakostas, & Kyriakis, 2007) uses a data acquisition system (DAQ) to collect data from sensors installed on the heat pump unit. This study looks at the basic parameters and the energy flows of a ground source heat pump system used for air conditioning a City Hall building. The building is a public space with an air-conditioned area of 1350 m^2 and is considered to be the largest GSHP installation in all of Greece. This ground source heat pump system consists of 7 groups of water-to-water heat pumps, 21 boreholes with 80 m depth and fan-coil units. The basic operational characteristics are constantly monitored over a three year period. The data logging system monitors the ground heat exchanger inlet and outlet temperatures using a film type 4 wire Pt-100 temperature sensors, and the ambient air temperature using a 3-wire Pt-100 temperature sensor every 10 minutes. The results of the monitored system indicate that the primary energy required by the system for heating is estimated to be lowered by 45% and 97% (period average) as compared to that of air-to-water heat pump based and conventional oil boiler respectively. In cooling mode the relevant differences are estimated at 28% and 55% for air-to-water and air-to-air heat pump based systems. The seasonal COP of the system has not yet been stabilized, as it is gradually increasing just as expected due to the operation of the ground heat exchanger.

The cooling performance of a vertical ground-coupled heat pump system for a school building in Korea is studied (Hwang, Lee, & Jeong, 2008). The evaluation of the cooling performance has been conducted from actual heat pump operation over a summer period. In this study, ten heat pump units with the capacity of 10 hp each were installed in the school building with a closed vertical type ground heat exchanger with 24 boreholes of 175 m depth. To investigate the cooling performance of the GSHP system, various operating conditions were monitored over the summer period with a data acquisition system. These operating conditions include the ambient temperature, the ground temperature, the water inlet and outlet temperatures of the ground heat exchanger, and the power consumption rate of the heat pump system. The findings of this study indicate that the overall COP of the GSHP system was found to be 5.9 at

65% partial load condition. While the air source heat pump (ASHP) system, which has the same capacity as the GSHP system, was found to have an overall COP of 3.4.

The effect of cyclic operation of a horizontal ground loop coupled heat pump performance is studied using a finite element numerical model (Wibbels & Braven, 1994). The results show that cyclic operation will decrease the COP of the heat pump. The numerical model shows a larger penalty on heat pump efficiency with frequent cyclic operation. Also, it was noticed that as the percent capacity decreases, the cyclic penalty increases.

A ground coupled heat pump system is monitored using a data acquisition system to obtain data on instantaneous measurements of temperature, flow rate and power consumption (Magranera, Monterob, Quilis, & Urchueguíac, 2010). The GSHP performance results are then compared to a numerical prediction using TRNSYS software. The GSHP system consists of a reversible water-to-water heat pump with 15.9 kW of nominal cooling capacity and 19.3 kW of nominal heating capacity with a vertical borehole heat exchanger. There are 6 boreholes of 50 m depth in a rectangular configuration that make up the ground heat exchanger. Sensors are used to measure source and load supply and return temperatures and flow rates as well as the system power consumption. Four-wire PT100 sensors with an accuracy of ± 0.1˚C are used for temperature measurements while the mass flow rate and power meters are measured with Danfoss Coriolli meter with an accuracy of less than 0.1% and Gossen Metrawatt with an accuracy of ± 0.5% respectively. The system was then modeled and simulated using TRNSYS software comprising of four components: the water-to-water heat pump, the vertical ground model, circulation pumps, and the required loads. The major findings of this study suggest that the simulation results based on manufacturer supplied data overestimates the energy performance of the ground coupled system by 15-20%.

A GSHP system has been tested with various ground loop configurations at the Eco House in the University of Nottingham (Doherty, Al-Huthaili, Riffat, & Abodahab, 2004). The GSHP was installed in the house to provide heating and cooling, and a natural gas-fired condensing boiler is added to provide supplementary heating when required. The heat pump unit had a heating capacity of 8 kW using R-22 as the refrigerant and included a desuperheater to provide hot water at low flow rates. The results of the test indicate that the difference between the entering water temperature to the evaporator and the exiting temperature of the condenser significantly affects the heat pump COP. In heating mode the COP was obtained to be 3.5 at a 30 °C difference in entering source temperature and an exit load temperature, while the COP was obtained to be 3 at a 40°C difference between entering source temperature and an exit load temperature.

The performance of a GSHP with a vertical ground heat exchanger was investigated experimentally using monitored data from a data acquisition system in Erzurum, Turkey (Bakirci, 2010). The system consists of an 8 kW heating capacity heat pump with vertical ground heat exchanger, a water-cooled evaporator and condenser, and a water circulation pump. The ground loop fluid consists of 50% antifreeze-water mixture while refrigerant 134a was used as the working fluid. The ground heat exchanger unit is a single U-tube placed in two vertical boreholes that are 53 m deep. Data collection of source and load temperature, flow rate, and power consumption of the system is obtained. The findings of the experimental study indicate that at an average entering source temperature of 1.6˚C and an entering load temperature of 47˚C the average heating COP was obtained to be 2.89.

An experimental heating performance evaluation of a GSHP system with a ground coupled heat exchanger and a fan coil air delivery system was studied in China from December 25, 2007 to February 6, 2008 (Wang, Ma, & Lu, 2009). The system uses R134a refrigerant as the working fluid and comprises of three single U-tube ground heat exchangers placed in three 30 m vertical boreholes. The 6.43 kW capacity heat pump supplies hot water to a AHU at a temperature of around 50.4˚C. Flow rate, pressure, temperature, and power consumption were measured every half hour during the experiment. Power sensors with an uncertainty of 0.1% were used to measure the consumption of the compressor, AHU fan, and the ground loop pump. A flow meter with an accuracy of 0.5% was used to measure the load and source flow rate while four-wire PT100 sensors with an accuracy of 0.1% were used to gather information on fluid temperature. Pressure transducers with an estimated accuracy of 0.1% were used to obtain information on suction and discharge pressure of the compressor and inlet and outlet pressures of the three parallel ground heat exchangers. The entire measurement process was controlled by a data acquisition unit connected to a data logger. The findings of this experiment indicate that the heating COP (only including the consumption of the heat pump compressor) turned out to be 3.55 at an evaporative temperature of 3.14˚C and a condensing temperature of 53.4˚C.

2.2 Desuperheater

The GSHP system in House B of the twin-houses also has an optional desuperheater installed into the system for the purpose of providing hot water to the domestic hot water tank. The advantage of having an optional desuperheater installed in the system is to recover heat from the high pressure and high temperature refrigerant after the compression stage during cooling mode. In cooling mode, this process allows a lower refrigerant condensing temperature resulting in improved operational efficiency. In heating mode, the heat transfer to the domestic hot water actually causes a reduction in space heating capacity, thus the compressor must operate longer to meet the heating demand. However, since the GSHP system operates with a much higher efficiency than electrical coils for domestic water heating, the use of a desuperheater can still be beneficial in heating mode as well. A few studies have investigated the performance of heat pumps in cooling and heating mode with a desuperheater.

An air-to-air heat pump with a COP of 3.11 at an outdoor temperature of 8.3˚C was evaluated alternately with an electric-resistance water heater and a desuperheater for water heating (Baxter, 1984). In terms of heat pump performance, it was noticed that the overall efficiency in heating mode was not changed by the desuperheater however the space heating capacity reduced by about 20%. The desuperheater on the other hand improved the cooling COP by 35%. The research results also indicated that the desuperheater was a good option in the heating season as it generates hot water with a higher efficiency than electric-resistance heating.

A study on an air-to-air heat pump system with a desuperheater for water heating (D'Valentine & Goldschmidt, 1990) was completed to analyze the cooling and heating efficiency. Their data demonstrated that the use of a desuperheater increased the COP during cooling mode and decreased the COP in heating mode. The results showed that at a desuperheater capacity of 1.46 kW and an outdoor temperature of 1.7˚C, the heating COP decreases by 17%. However in cooling with a desuperheater capacity of 1.46 kW and an outdoor temperature of 28˚C, the COP increased by 5%.

An air-cooled heat pump system was retrofitted with a desuperheater for providing year round hot water service and was investigated for operating performance and energy efficiency (Deng, Song, & Tant, 1998). The COP of the retrofitted air cooled heat pump system was much higher than that of an air-cooled chiller under the same operating conditions. During heating mode, although the COP was half of the cooling COP, the desuperheater system proved to be more economical than electrical water heating. At an outdoor temperature of 28˚C the cooling COP ranged from 4.3-6.2; while at a temperature of 15˚C, the heating COP ranged from 3.2-3.6.

Various methods of producing domestic hot water using renewable energy systems were examined for a net zero energy house (Biaoua & Bernier, 2008). One of the systems used is the desuperheater of a GSHP system with electric backup for DHW heating. The results of the study indicated that in a house requiring 4605 kWh of electricity use for domestic hot water, a desuperheater can reduce this consumption by 36% to 2940 kWh. It was also noted that during the heating season, part of the heat is taken from space heating causing the GSHP to operate for longer periods to meet the heating load. As a result, the space conditioning needs for a GSHP with a desuperheater was higher (4712 kWh) than the base case (4222 kWh).

2.3 Energy Modeling

There are only a couple of methods to evaluate the accuracy of energy simulation programs (Judkoff & Neymark, 1995). One of those methods is using empirical validation where calculated results from the program are compared to monitored data from a real system. Judkoff & Neymark developed a procedure for systematically testing whole building energy simulation models using a comparative testing method. A procedure called Building Energy Simulation Test and Diagnostic Method (BESTEST) is used to compare several state-of-the-art whole building energy simulation programs in terms of annual loads, annual maximum and minimum temperature, peak loads, and hourly data. The results from this study indicate that the range of uncertainty represented by the current generation of detailed building energy simulation programs is still fairly large.

Today's building energy simulations can be categorized in two ways. The first way is simulation mainly of the building envelope with a simplified method for HVAC operations. The second way is using detailed transient simulation of the building envelope, HVAC equipment, and controls. Due to the complexity of the second method, most studies use a simplified assumption for their HVAC system performance (Zogou & Stamatelos, 2007). The annual performance of a three zone residential building in Greece, with a conventional chiller-boiler system is compared to an alternative horizontal loop GSHP using TRNSYS 16 (Zogou & Stamatelos, 2007). The first simulation consists of a boiler and an air-cooled chiller model that use a fan coil system to distribute heating and cooling. The alternative system uses a water-source heat pump with a horizontal looped ground heat exchanger and also uses a fan coil to distribute heating and cooling to different zones. The TRNSYS simulation indicates that a detailed model of the HVAC system operation provides a more realistic assessment of the effects of HVAC sizing, control system, and design parameters of the two configurations.

The effect of smart control strategies on domestic low temperature heat pump heating systems have been investigated using TRNSYS (Sakellari, Forse, & Lundqvist, 2006). A reference system is developed in TRNSYS consisting mainly of a well insulated single family house, an exhaust air heat pump and an in-floor radiant heating system. Some of the control strategies used include predictive climate control, increased ventilation rates when suitable, proper sizing and matching capacity and loads, and the ability to respond to rapid load changes. The results of the TRNSYS simulation indicate that a proper control system can potentially save up to 60% in HVAC energy consumption.

A group at the Georgia Institute of Technology (Fadel, Cowden, & Dymek, 1986) studied the performance of a variable speed drive heat pump through simulation. The heat pump compressor can change speed by changing the frequency of the current by means of an inverter. The simulation results demonstrate that the variable speed heat pump has improved COP at reduced frequency and higher heating capacities at high frequencies. The improved COP is desirable for enhancing the part load performance of the heat pump. It was also noted that the efficiencies of the heat pump deteriorate at higher frequencies because the heat exchangers are more heavily loaded requiring the condenser to operate at a higher temperature and pressure, and similarly forcing the evaporator to a lower pressure. Due to this higher pressure ratio, the work to the compressor increases resulting in a decrease of COP.

TRNSYS simulations have been performed to investigate different configurations of ground source heat pumps and solar collectors for space heating and domestic hot water (Kjellsson, Hellstrom, & Perers, 2010). The options considered were 1) GSHP with no solar heat, 2) GSHP with solar heat recharging boreholes only, 3) GSHP with solar heat used for domestic hot water only, and 4) GSHP with solar heat recharging the boreholes from November to February, and the rest of the year for domestic hot water. The simulation used the Stockholm weather file with a house having 29 400 kWh/yr of heating and DHW demand, while a heat pump power of 7 kW and a flat plate solar collector with 10 m^2 area was used in the simulation. The findings from the simulation suggest that the best option is to have the solar collector recharge the borehole during the winter because the ground temperature tends to be lower due to significant heat extraction from the ground, and use the solar collector for domestic hot water in the summer. Due to low irradiation during the winter months, the hot water produced using the solar collector would be better suited for recharging the ground rather than being delivered to domestic hot water. However, during the cooling season the solar collector can provide sufficient hot water for DHW heating, and the ground heat can be naturally recharged for the next heating season.

A 4000 m^2 greenhouse utilizing liquid petroleum gas as the fuel for heating is planned to be modified with an additional air-to-water heat pump in Melbourne, Australia (Aye, Fuller, & Canal, 2010). Before the heat pump system is added to the boiler system, a TRNSYS model was developed to simulate the performance. The current system uses a 1 MW liquid petroleum gas fired boiler that produces hot water stored in an 80 m^3 un-insulated concrete storage tank and is delivered using in-floor radiant heating. The proposed heat pump configuration has two 32 kW air-to-water heat pumps to provide heating between 11pm and 7am to utilize off-peak electricity rates thus resulting in a financially alternative heating option. When there is insufficient heat in the storage tank, the boiler is used to provide the remaining hot water. The findings of the TRNSYS simulation suggest that the heat pump system is found to have a simple payback period of six years and will lower the liquid petroleum consumption by 16%.

The use of simulation tools for performance validation and energy analysis of HVAC systems is used to benchmark actual collected data from monitoring systems (Salsbury & Diamond, 2000). The study looks at developing a Matlab model to represent a dual-duct air handling unit. A three year data collection is gathered and compared with the simulation model. The final result of the study showed how the use of validating simulation models with actual gathered data can be used to predict HVAC system performance in the future under various conditions.

As evident from the literature, there have been quite a few studies on air source and ground source heat pump experimental and numerical investigations. However there still remain some potential improvements and gaps in this area of research that will be addressed by this study. For instance, most ASHP systems investigated in the literature have been tested at mild winter temperatures and fail to provide a good understanding of the heat pump performance in cold climates such as Canada. The performance of using such systems in ambient temperatures below -20˚C is one of the questions this thesis will address. As well, due to a wide range of ambient temperatures within the ASHP testing period, along with a high frequency data logger collecting data every 5 seconds, the part load efficiency of the ASHP is also investigated within this study. Similarly, there are fewer experimental studies on ground source heat pumps that use horizontal ground heat exchangers for residential applications. Due to the availability of land at the Kortright Center in Vaughan, this ground loop configuration was possible and the performance of such heat exchanger on heat pump operation was studied. Also, the effect of a desuperheater on the heating performance of ground source heat pump systems is not often seen in the literature. Both equipment are tested and investigated simultaneously in the same location, allowing a direct comparison of performance. Testing of two side-by-side HVAC equipment under similar conditions is uncommon in the literature. Lastly, because an energy model of the entire system will be created using the performance results of the data collection, the performance of these systems can be simulated under various cases, i.e. different locations, various heat pump capacities, different building envelope or orientation etc.

Chapter 3

House and System Description

3.1 House Description

The TRCA Archetype Sustainable Twin-Houses demonstrate sustainable housing technologies through experimentation and research. The houses are one of the first Canadian projects to achieve a LEED for Homes Platinum Certification (Dembo, NG, Pyrka, & Fung, 2009). The first house called A (house to the left in Figure 1) is designed to demonstrate current best practise sustainable technologies while the second house (house to the right in Figure 1) called B is designed to demonstrate experimental sustainable technologies for the future. House A uses a two-stage variable capacity air-source heat pump for space heating and cooling, while House B has a horizontal-loop coupled ground source heat pump for space heating and cooling and an optional desuperheater for water heating.

Figure 1 South-West Side of Twin Houses

Both houses are made to have an air-tight building envelope according to the standards of ASHRAE 90.1. Table 1 lists the structural features of the twin houses. The major difference between the twin houses is the window type where House B has triple glazed windows with aluminum-clad wood frames while House A has double glazed windows with fibreglass frames. Table 2 and Table 3 list the floor areas and volumes of the Twin Houses respectively.

Table 1 Structural features of the Twin Houses

Features	House-A	House-B
Basement walls	RSI 3.54 (R20)	RSI 3.54 (R20)
Basement Slab	RSI 1.76 (R10)	RSI 1.76 (R10)
Above Grade Walls	RSI 5.64 (R32)	RSI 5.64 (R32)
Windows	2.19 W/m^2K (0.39 $Btu/hr\text{-}ft^2\text{-}^{\circ}F$)	1.59 $W/m^2 K$ (0.28 $Btu/hr\text{-}ft^2\text{-}^{\circ}F$)
Roof	RSI 7 (R40)	RSI 7 (R40)
Overall UA Value*	160 W/K	172 W/K

*Heating at -7˚C outdoor and 21˚C indoor air based on TRNSYS House model

Table 2 Floor area of Twin Houses

Floor Area	House A - m^2 (ft^2)	House B - m^2 (ft^2)
Basement	86.95 (936)	86.95 (936)
First Floor	86.95 (936)	86.95 (936)
Second Floor	86.95 (936)	60.19 (636)
Third Floor	83.6 (900)	86.95 (936)
Total	344.45 (3708)	321.04 (3444)

Table 3 Zone volumes of Twin Houses

Zone Volume	House A – m^3 (ft^3)	House B – m^3 (ft^3)
Basement	234.03 (8264)	234.03 (8264)
First Floor	291.54 (10296)	291.54 (10296)
Second Floor	238.53 (8424)	238.53 (8424)
Third Floor	222 (7840)	271.83 (9600)
Total	932.57 (34824)	1035.94 (36584)

3.2 Internal Gains

The internal heat gains from electrical appliances and occupants influence both the comfort level as well as the overall building consumption, which also controls the sizing of heating and cooling equipment (Aydinalp, Ferguson, Fung, & Ugursal, 2001). Accurate load profiles allow researchers to represent heat gains and thus present more precise results in their simulation. The Twin Houses were assumed to have four occupants (2 adults and 2 children). Load profiles in House A and B were created using incandescent light bulbs with schedules to represent the occupant internal gains. Other gains within the twin houses were measured depending on the type of equipment used. Table 5 and Table 6 list the House A and B equipment internal gains respectively.

Occupants (House A & B)

2 adults for 50 % of the time

2 children for 50% of the time

Sensible Internal Heat Gain: 2.4 kWh/day

Equipment/Appliance/Lighting House A

Table 4 House A Equipment/Appliance/Lighting Internal Gains

	kWh/day	Annual kWh	kJ/hr
Interior Lighting	3	1095	450
Major Appliances	6	2190	900
Other	3	1095	450

Equipment/Appliance/Lighting House B

Table 5 House B Equipment/Appliance/Lighting Internal Gains

	kWh/day	Annual kWh	kJ/hr
Interior Lighting	3	1095	450
Major Appliances	6	2190	900
Other	3	1095	450

3.3 Mechanical Systems

House A uses a two-stage variable capacity air-to-air heat pump with a direct expansion coil AHU for delivery of conditioned air. House B uses a horizontal-loop coupled ground source heat pump with an optional desuperheater for water heating, and provides heating with a radiant in-floor system, and cooling using a fan coil AHU system. The technical information on the heat pump systems and air handling units are given in Table 6, while the equipment manufacturer and model are given in Table 7.

Table 6 Mechanical System Technical Information

Equipment	Technical Information
Air Source Heat Pump (ASHP)	HEATING CAPACITIES: COP: 3.27, Heating capacity: 11.06 kW (38 MBH) at 21.1˚C (70˚F) DB and 15.6˚C (60˚F) WB indoor and 8.3˚C (47˚F) DB and 6.1˚C (43˚F) WB outdoor COOLING CAPACITIES: COP: 3.52, Cooling capacity: 9.82 kW (33.5 MBH), at 26.7 ˚C (80˚F) DB and 19.4˚C (67˚F) WB indoor and 35˚C (95˚F) DB and 23.9˚C (75˚F) WB outdoor
Ground Source Heat Pump (GSHP)	HEATING CAPACITIES: COP: 4.16, Heating Capacity: 12.66 kW (43.2 MBH) at -1.1˚C (30˚F) Entering Source Temperature (EST), 37.7 ˚C (100˚F) Entering Load Temperature (ELT) and 1.04 Liters/sec (16.5 GPM) source flow rate COOLING CAPACITIES: COP: 3.54, Cooling Capacity: 13.04 kW (44.5 MBH) at 26.6˚C (80˚F) Entering Source Temperature (EST), 14.65 ˚C (50˚F) Entering Load Temperature (ELT), and 1.04 Liters/sec (16.5 GPM) source flow rate LENGTH OF HORIZONTAL LOOP: 152.39m (500'), Number of loop: 2, Depth of ground level: 1.83m (6')
Air Handling Unit – A	Multi Speed Fan, Airflow Dry: 705-810-920 CFM, Airflow Wet: 635-730-830 Cooling capacity: 8.73 kW (2.5 tons) Heating capacity: 16.73 kW (57.48 MBH) at 800 CFM and 82 °C (180°F) EWT
Air Handling Unit – B	Multi-Zone Air Distribution, Multi Speed Fan Cooling capacity: 12.3 kW (3.5 tons) Heating capacity: 28 kW (95 MBH) at 1400 CFM and 82°C (180°F) EWT

Table 7 Manufacturer and Model of Equipment

Equipment	**Manufacturer/Distributor**	**Model**
Air Source Heat pump	Mitshubishi Electric	PUZ-HA36NHA
AHU-A	Mitshubishi Electric	PKA-A36KA(L)
Ground Source Heat Pump	Water Furnace International, Inc.	EW 042 R12SSA
Buffer Tank	GSW Water Heating	CST-80
AHU-B	Ecologix Heating Technologies Inc.	C3-06

Chapter 4

Methodology

The implementation of a long-term monitoring system within the Archetype Houses was completed by a former Master of Applied Science student (Barua, 2010). Sensors were installed on the ASHP and GSHP system and were calibrated after installation. To ensure accurate data was being collected, a data test period initially took place where the collected data was compared to manufacturer equipment specification. Once the data was validated, further comprehensive analysis on the two heat pumps was done. Both the two-stage air source heat pump within House A and the ground source heat pump within House B were studied simultaneously. While the data collection was taking place, a TRNSYS model of the Archetype House and the two pieces of equipment was developed and later validated using the actual collected data. Finally once the model was fully developed, it was used to investigate the thermal performance of the Archetype House and the heat pumps in different Canadian locations.

4.1 Monitoring Systems: Two-Stage Air Source Heat Pump

To analyze the thermal performance of the ASHP system using the monitoring systems, data for various operating conditions was obtained. Data such as outdoor temperature and relative humidity, supply/return temperature and relative humidity to the zones, supply/return air flow rate, and the power consumption of the system was collected. Table 8 lists the air temperature, relative humidity, and air velocity sensors required for the ASHP analysis. These sensors provide output signals in milliamps. Table 9 lists the electricity consumption sensors of the ASHP that provide output signals in pulses.

Table 8 ASHP Relative Humidity and Air Temperature Sensors

Module: AI-111 (Output signal: mA)			
Address of sensors	**Sensors**	**Sensors type**	**Location**
A-CFP1-M4-CH9	RH12	Relative Humidity	Main return air from zone to AHU
A-CFP1-M4-CH10	AT12	Air Temperature	
A-CFP1-M4-CH11	RH7	Relative Humidity	Main supply air AHU to zone
A-CFP1-M4-CH12	AT7	Air Temperature	
A-CFP1-M4-CH15	AV1	Air Velocity Meter	Supply air duct from AHU

Table 9 ASHP Power Sensors

Module: CTR-502 (Output signal: Pulse) Watt-node				
Sl. No	**Address of sensors**	**Sensors**	**Sensors type**	**Location**
3	A-CFP3-M1-CH3	3-P-1	Watt-node	Two stage ASHP (compressor + outdoor Fan)
7	A-CFP3-M4-CH4	1	Watt-node	AHU fan and HEPA filter fan

The first task taken was to examine the collected data and ensure the values are within an acceptable range. One way of validating the ASHP data is to compare it with the manufacturer's performance data. The data obtained from the manufacturer for the heat pump performance is divided into cooling performance and heating performance. The cooling performance curve of the ASHP requires the total cooling output, the sensible cooling, and the cooling power consumption at operating conditions of indoor dry bulb temperature, indoor wet bulb temperature, outdoor dry bulb temperature, and the flow rate of air in the air handling unit. The heating performance curve of the ASHP requires output heating and power consumption at operating conditions of indoor dry bulb temperature, outdoor dry bulb temperature, and the AHU flow rate.

The data were collected for a 20 – 45 day period in the summer and winter using a program called LabVIEW, and stored using Microsoft SQL Server. During the test period, there were points where the data were out of the normal range, and obtaining an average of all the values could cause discrepancy in the results. Out of range data points were eliminated from the regular data points to obtain steady accurate results. Due to the transient nature of the heat pumps, data was used only when steady state conditions were reached. Since the data is collected for a 3 – 6 week period, extrapolation of data will be utilized to predict the typical yearly performance of the heat pumps.

4.2 Air Source Heat Pump Equations

A schematic of House A AHU is given in Figure 2 depicting the return air, the supply air, and the connection with the ASHP and the corresponding sensors and their locations.

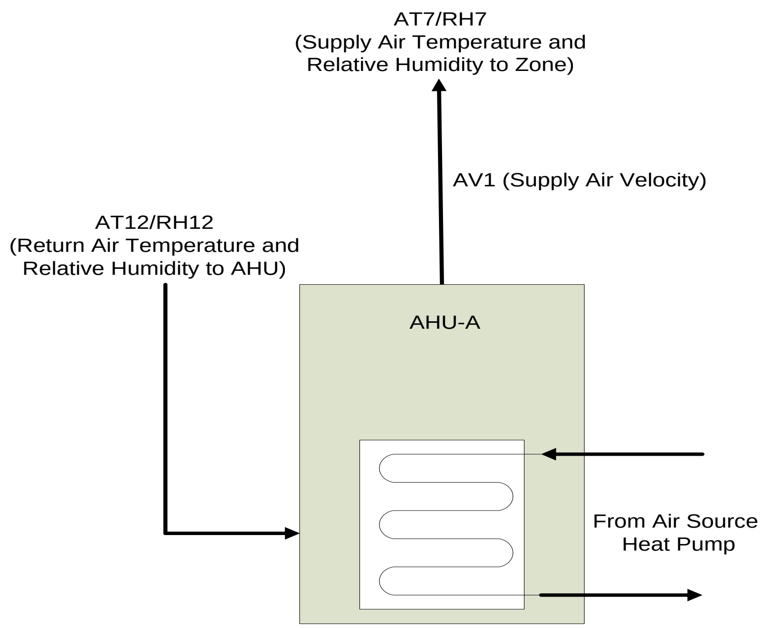

Figure 2 AHU-A Schematic

From the study by Bertsch and Groll (2008), the equations that represent the air source heat pump performance are given below in Equations 1-5:

$$\dot{Q}_{Heat} = \dot{m}_{air}(h_{a,o} - h_{a,i}) \quad (1)$$

$$\dot{Q}_{Cool} = \dot{m}_{air}\left(h_{a,o} - h_{a,i}\right) \quad (2)$$

$$COP_{Heat} = \frac{\dot{Q}_{Heat}}{\dot{Q}_{Electrical}} \quad (3)$$

$$COP_{Cold} = \frac{\dot{Q}_{Cool}}{\dot{Q}_{Electrical}} \quad (4)$$

$$\dot{Q}_{Electrical} = W_{Compressor} + W_{Outdoor\ fan} \quad (5)$$

where:

$\dot{Q}_{Heat/Cool}$: Thermal output (kW)

$\dot{m}_{air}$: Mass flow rate of air through the AHU (kg/s)

$h_{a,o}$: Enthalpy of air leaving the AHU (kJ/kg)

$h_{a,i}$: Enthalpy of air entering the AHU (kJ/kg)

COP: Coefficient of performance

$\dot{Q}_{Electrical}$: Electricity consumption of the system (kW)

Specific Enthalpy of Moist Air

Using the equation for the specific enthalpy of moist air, the enthalpy of air going into and exiting the system are given as follows:

$$\boldsymbol{h = h_a + x h_w} \tag{6}$$

where:

h = Specific enthalpy of moist air (kJ/kg)

h_a = Specific enthalpy of dry air (kJ/kg)

x = Humidity ratio (kg/kg)

h_w = Specific enthalpy of water vapour (kJ/kg)

$$\boldsymbol{h = C_{pa} t + x(C_{pw} t + h_{we})} \tag{7}$$

where:

c_{pa} = Specific heat capacity of air (kJ/kg^{o}C)

t = Air temperature (^{o}C)

c_{pw} = Specific heat capacity of water vapour (kJ/kg^{o}C)

h_{we} = Latent heat of evaporation at 0^{o}C (kJ/kg)

For air temperature between -100˚C and 100˚C the specific heat capacity (c_p) can be set to c_{pa} = 1 (kJ/kg^{o}C) [I]. For water vapour, the specific heat capacity can be set to c_{pw} = 1.86 (kJ/kg^{o}C)[I]. The evaporation heat of water at 0^{o}C can be set to h_{we} = 2501.3 (kJ/kg)[I]. Substituting the constants into Equation (7) the following equation for enthalpy is derived.

$$\text{Enthalpy } (h) = 1\, t + w(1.86\, t + 2501.3) \qquad (8)$$

where:

w = Humidity ratio (kg water vapour/kg dry air)

t = Dry bulb temperature (^{o}C)

The expression for humidity ratio in Equation 9 is obtained from the ASHRAE 2009 Handbook (ASHRAE, 2009).

$$w = 0.6219 * p\, /(P_a - p)) \qquad (9)$$

Where:

p = Water Vapour Pressure (Pa)

P_a= Atmospheric Pressure (Pa)

The Atmospheric Pressure is obtained using Equation 10 from ASHRAE 2009 Handbook (ASHRAE, 2009). The atmospheric pressure is given with respect to the altitude of the location, in this case the altitude of Toronto.

Altitude of Toronto: H = 347 ft[II]

$$p_a = 14.696 * (1 - 6.8754\, x\, 10^{-6} * H)^{5.2559} \qquad (10)$$

p_a = 14.513 psia (100063.6 Pa)

Water vapour pressure is obtained using Equation 11 from the saturation vapour pressure, and relative humidity:

$$p = p_s * RH\%/100 \qquad (11)$$

I Retrieved from Heating, Ventilating, and Air Conditioning, 6th Edition (McQuiston, Parker, & Spitler, 2005)

II: http://www.aviewoncities.com/toronto/torontofacts.htm

III: http://www.conservationphysics.org/atmcalc/atmoclc1.php

where:

$$p_s = 610.78 * e^{\frac{t*17.2694}{t+238.3}}\text{III}$$

Substituting Equations 10 and 11 into 9, the resulting expression is obtained for the humidity ratio as shown in Equation 12.

$$w = 0.6219 * 610.78 * RH\%/100 * e^{\frac{t*17.2694}{t+238.3}} / \left(100063.6 - 610.78 * RH\%/100 * e^{\frac{t*17.2694}{t+238.3}}\right)$$

$$w = \frac{379.84*RH\%/100*e^{\frac{t*17.2694}{t+238.3}}}{100063.6 - 610.78*RH\%/100*e^{\frac{t*17.2694}{t+238.3}}} \tag{12}$$

Equation 12 is then substituted into Equation 8 to obtain the expression for enthalpy. This is given in Equation 13.

$$\text{Enthalpy } (h) = 1\,t + \frac{379.84*RH\%/100*e^{\frac{t*17.2694}{t+238.3}}}{100063.6 - 610.78*RH\%/100*e^{\frac{t*17.2694}{t+238.3}}}(1.86\,t + 2501.3) \tag{13}$$

Now substituting Equation 13 back into Equations 1 and 2 to get the heating/cooling output for the heat hump, Equation 14 is derived.

$$\dot{Q}_{Heat} = \dot{m}_{air}([\boldsymbol{AT7} + \frac{379.84*RH7\%/100*e^{\frac{AT7*17.2694}{AT7+238.3}}}{100063.6 - 610.78*RH7\%/100*e^{\frac{AT7*17.2694}{AT7+238.3}}}(\boldsymbol{1.86\,AT7 + 2501.3})] -$$

$$[\boldsymbol{AT12} + \frac{379.84*RH12\%/100*e^{\frac{AT12*17.2694}{AT12+238.3}}}{100063.6 - 610.78*RH12\%/100*e^{\frac{AT12*17.2694}{AT12+238.3}}}(\boldsymbol{1.86\,AT12 + 2501.3})]) \tag{14}$$

The mass flow rate of air can be expressed using the density of the inlet air, the velocity of air entering the system, and the cross sectional area of the supply air handling unit (AHU). Data collection of inlet velocity can be used along with a temperature dependent density function and a constant cross sectional supply duct area of 0.164 m^2 for this portion of the calculation. The density of air can be approximated either by using standard atmospheric conditions, and assuming the air is dry, or can be approximated at a certain altitude and moisture content. The density of moist air can be obtained using the following equation from the ASHRAE 2009 handbook (ASHRAE, 2009).

$$\rho = \frac{M_{da} + M_w}{V} \tag{15}$$

$$\rho = \frac{P_{da}}{R_{da}T} + \frac{P_w}{R_w T} \tag{16}$$

where:

M_{da}: Mass of dry air (kg)

M_w: Mass of moist air (kg)

V: Total volume (m^3)

P_{da}: Pressure of dry air (Pa)

P_w: Pressure of water vapour (Pa)

R_{da}: Gas constant of dry air (287.05 J/kg.K)

R_w: Gas constant of water vapour (461.495 J/kg.K)

T: Temperature (˚K)

Using Equation 16, the density of moist air is plotted as shown in Figure 3, where the relative humidity is taken as a constant at 50% and the pressure of dry air (100063.6 Pa) is taken at the altitude of Toronto using Equation 10. As well, the density at standard atmospheric condition and dry air [IV] is also shown on the same plot. As evident from the plot, standard atmospheric dry air condition can be used to approximate the density of air for obtaining the mass flow rate. The average percentage difference of the two methods is about 1 % (refer to Table A 1 in Appendix A).

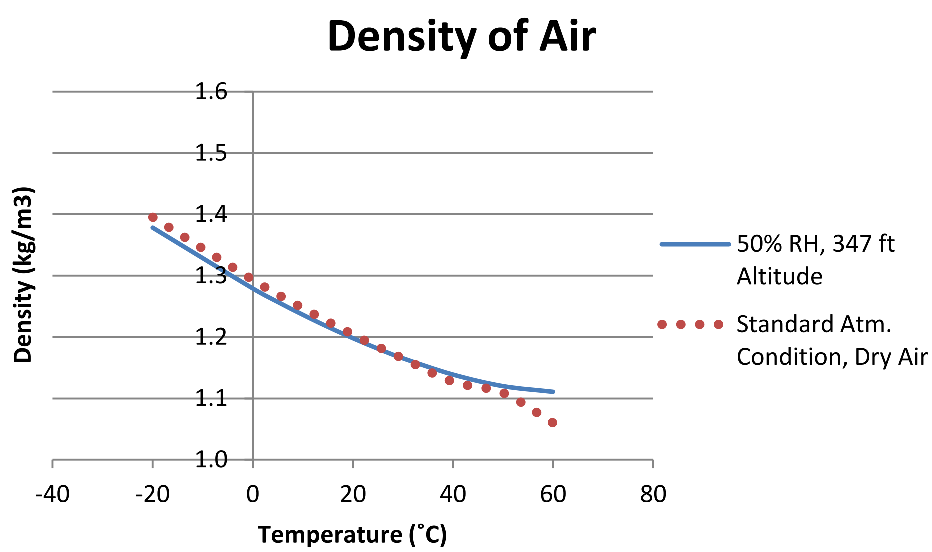

Figure 3 Density of Air

From the standard atmospheric density curve in Figure 3, a function of density with temperature is derived and presented below where AT is the air temperature

$$\rho = 2x10^{-5}(AT)^2 - 0.0047(AT) + 1.293 \tag{17}$$

The mass flow rate of air can now be calculated by: $\dot{m}_{air} = \rho AV$ where A is the cross sectional area of the supply duct[V], and V is the average air velocity in m/s.

The final equation for heating and cooling output is represented by Equation 18 and 19:

$$\dot{Q}_{Heat} = \rho(0.164)AV1\left(\left[\boldsymbol{AT7} + \frac{379.84*RH7\%/100*e^{\frac{AT7*17.2694}{AT7+238.3}}}{100063.6 - 610.78*RH7\%/100*e^{\frac{AT7*17.2694}{AT7+238.3}}}(\mathbf{1.86}\ \boldsymbol{AT7} + \mathbf{2501.3})\right] - \right.$$

$$\left.\left[\boldsymbol{AT12} + \frac{379.84*RH12\%/100*e^{\frac{AT12*17.2694}{AT12+238.3}}}{100063.6 - 610.78*RH12\%/100*e^{\frac{AT12*17.2694}{AT12+238.3}}}(\mathbf{1.86}\ \boldsymbol{AT12} + \mathbf{2501.3})\right]\right) \tag{18}$$

IV: http://www.engineeringtoolbox.com/air-desity-specific-weight-d_600.html

V cross sectional area of supply air duct (0.164 m^2)

$$\dot{Q}_{Cool} = \rho(0.164)AV1\left(\left[\boldsymbol{AT12} + \frac{379.84*RH12\%/100*e^{\frac{AT12*17.2694}{AT12+238.3}}}{100063.6 - 610.78*RH12\%/100*e^{\frac{AT12*17.2694}{AT12+238.3}}}(\mathbf{1.86}\ \boldsymbol{AT12} + \mathbf{2501.3})\right] -\right.$$

$$\left.\left[\boldsymbol{AT7} + \frac{379.84*RH7\%/100*e^{\frac{AT7*17.2694}{AT7+238.3}}}{100063.6 - 610.78*RH7\%/100*e^{\frac{AT7*17.2694}{AT7+238.3}}}(\mathbf{1.86}\ \boldsymbol{AT7} + \mathbf{2501.3})\right]\right) \tag{19}$$

4.3 Monitoring Systems: Ground Source Heat Pump

A schematic of the GSHP in House B is shown in Figure 4, depicting the ground loop line, the buffer tank line, and the desuperheater line with the corresponding sensors and their locations.

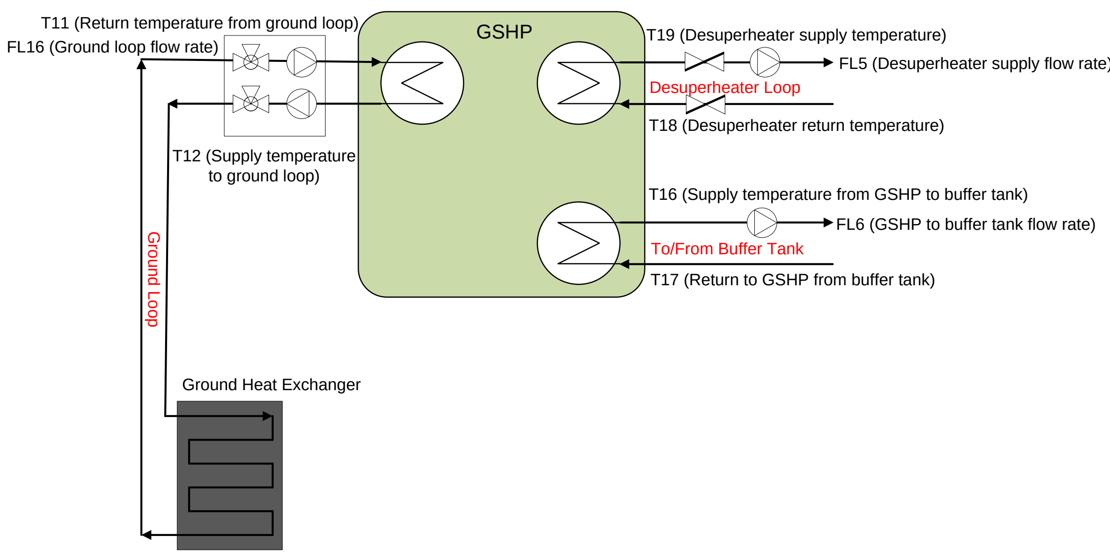

Figure 4 GSHP Schematic

To analyze the thermal performance of the GSHP system using the monitoring system, data for various operating conditions was obtained. Data such as outdoor temperature and relative humidity, supply and return temperature and flow rate of water to the buffer tank, supply and return glycol-water temperature and flow rate to the ground loop, supply temperature and flow rate of the desuperheater loop, and the power consumption of the compressor, ground loop pump, pump to the buffer tank, and the desuperheater pump. Tables 10-14 list the sensors utilized in gathering the required data for the GSHP.

Table 10 GSHP Outdoor Temperature and Relative Humidity Sensors

Module: AI-111 (Output signal: mA)			
Address	**Sensors**	**Sensors type**	**Location**
B-CFP2-M3-CH15	RH24	RH	Outdoor air RH (North side)
B-CFP2-M3-CH16	AT24	Air Temp.	Outdoor air temperature (North side)

Table 11 GSHP Temperature Sensors

Module: RTD-122 (Output signal: RTD)			
Address	**Sensors**	**Sensors type**	**Location**
B-CFP1-M2-CH5	T18	Pt. 500	Desuperheater return
B-CFP1-M2-CH6	T19	Pt. 500	Desuperheater supply
B-CFP1-M1-CH1	T12	Pt. 500	Supply to ground loop
B-CFP1-M1-CH2	T11	Pt. 500	Return from ground loop
B-CFP2-M6-CH3	T16	Pt. 500	Supply from GSHP to buffer tank
B-CFP2-M6-CH4	T17	Pt. 500	Return from GSHP to buffer tank

Table 12 Desuperheater Flow Rate Sensor

Module: CTR-502 (Output signal: Pulse)			
Address	**Sensors**	**Sensors type**	**Location**
B-CFP1-M3-CH7	FL5	Flow rate	Desuperheater

Table 13 Ground Loop and GSHP to Buffer Tank Flow Rate Sensor

Module: AI-110 (Output signal: mA or mV)			
Address	**Sensors**	**Sensors type**	**Location**
B-CFP2-M7-CH4	FL16	Liquid flow rate	Ground loop
B-CFP2-M7-CH7	FL6	Water flow rate	GSHP to buffer tank

Table 14 GSHP Power Sensors

Module: CTR-502 (Output signal: Pulse), Sensor type: Watt node			
Address	**Sensors**	**Sensors type**	**Location**
B-CFP7-M1-CH7	3-P-1	GSHP compressor: 50 Amps	GSHP
B-CFP7-M2-CH1	5-P3-1	GSHP to buffer tank: 5 Amps	Supply to buffer tank
B-CFP7-M2-CH2	5-P3-2	Desuperheater pump: 5 Amps	GSHP
B-CFP7-M2-CH3	5-P3-3	Earth loop of GSHP: 5 Amps	GSHP

4.4 Ground Source Heat Pump Equations

Similar to the equations for the air source heat pump, the ground source heat pump performance can be determined using the following equations:

$$\dot{Q}_{Heat} = \dot{m}_w CP_w (T_{w,o} - T_{w,i}) \tag{20}$$

$$\dot{Q}_{Cool} = \dot{m}_w CP_w (T_{w,o} - T_{w,i}) \tag{21}$$

Where:

$\dot{Q}_{Heat/Cool}$: Thermal output (kW)

$\dot{m}_w$ = Mass flow rate of water (kg/s)

CP_w = Specific heat of water (kJ/kg.K)

$T_{w,o}$: Water temperature leaving the system (˚C)

$T_{w,i}$: Water temperature entering the system (˚C)

The flow rate sensors provide output in gallons per minute, thus Equations 20 and 21 were expressed in terms of volumetric flow rate $\dot{V}$ (GPM), and density ρ (kg/m^3). The mass flow rate of water in kg/s can be expressed as:

$$\dot{m}_w = \dot{V} * \left(\frac{1 \text{ min}}{60\text{S}}\right) * \left(\frac{3.7854 \text{ L}}{1 \text{ Gallon}}\right) * \left(\frac{1\text{m}^3}{1000 \text{ L}}\right) * \rho \tag{22}$$

$$\dot{m}_w = 6.309x10^{-5} * \dot{V} * \rho \tag{23}$$

The density of water is given as a function of temperature in the Fundamentals of Engineering Thermodynamics textbook (Moran & Shapiro, 2004). An equation was created from the density versus temperature plot (see Figure A 1 in Appendix A) for a temperature range of 2˚C to 77˚C. This equation is given below as

$$\rho = -0.0041(T)^2 - 0.0333\,(T) + 1000.1 \tag{24}$$

Where:

ρ: Density of Water (kg/m^3)

T: Water Temperature (˚C)

The specific heat of water does not significantly change with temperature from 0˚C to 100˚C as evident from Moran and Shapiro's Fundamentals of Engineering Thermodynamics (See Table A2 in Appendix A), thus a constant value of 4.187 kJ/kg K was used. Substituting Equation 23 into Equation 20 and 21, along with a constant specific heat, the flow rate to the buffer tank in GPM (FL6), the supply temperature to the buffer tank (T16), and the return temperature from the buffer tank to the GSHP (T17), the following equation for output heating and cooling in kW from the GSHP to the buffer tank is obtained as follows:

$$\dot{Q}_{Heat} = 6.309x10^{-5} * \mathrm{FL6} * \rho * 4.187 * (T16 - T17) \quad (25)$$

$$\dot{Q}_{Cool} = 6.309x10^{-5} * \mathrm{FL6} * \rho * 4.187 * (T17 - T16) \quad (26)$$

Once the output heating and cooling is obtained, Equation 27 and 28 can be used to investigate the coefficient of performance of the system using the thermal heat output and the electricity consumption of the unit which includes the compressor and ground loop circulation pump.

$$COP_{Heat} = \frac{\dot{Q}_{Heat}}{\dot{Q}_{Electrical}} \quad (27)$$

$$COP_{Cold} = \frac{\dot{Q}_{Cool}}{\dot{Q}_{Electrical}} \quad (28)$$

Where:

$$\dot{Q}_{Electrical} = W_{Compressor} + W_{Ground\ Loop\ Pump} \quad (29)$$

4.5 Heat Extraction/Rejection from/to ground

Similar to the heating/cooling output to the buffer tank, the heat extraction and rejection from and to the ground via the ground loop is calculated in units of kW using the following equations:

$$\dot{Q}_{Extraction} = 6.309x10^{-5} * \mathrm{FL16} * \rho * \mathrm{Cp} * (T11 - T12) \quad (30)$$

$$\dot{Q}_{Rejection} = 6.309x10^{-5} * \mathrm{FL16} * \rho * \mathrm{Cp} * (T12 - T11) \quad (31)$$

where:

FL16: Is the water-propylene glycol solution flow rate in the ground loop (gal/min)

T11: The temperature of water/propylene glycol entering the GSHP (˚C)

T12: The temperature of water/propylene glycol leaving the GSHP (˚C)

C_p: The specific heat of the ground loop water/propylene glycol solution (kJ/kg.K)

4.6 Water and Propylene Glycol (PG) solution

The earth loop of the GSHP uses 30% propylene glycol (PG) and 70% water. The density of the 30% PG solution as a function of temperature is obtained and plotted in Figure A 2 in Appendix A (Curme & Johnston, 1952). This function is given in Equation 32. According to the same study by Curme and Johnston, the specific heat of PG is fairly constant ranging from 3.891 – 3.974 kJ/kg.K between 0˚C and 40˚C. Thus, a constant specific heat of 3.915 kJ/kg.K based on 15.55˚C is used for the equation[VI].

$$\rho = -7x10^{-5}(T^3) - 0.0008(T)^2 - 0.4561\,(T) + 1032.1 \quad (32)$$

4.7 Heat supplied from the desuperheater

Similar to the heating/cooling output, and the heat extraction/rejection of the ground loop, the desuperheater supplied heat to the preheat tank can be obtained as follows:

$$\dot{Q}_{Desuperheater} = 6.309x10^{-5} * \mathrm{FL15} * \rho * 4.187 * (T19 - T18) \quad (33)$$

Where:

FL15: Is the water flow rate in the desuperheater loop (gal/min)

T19: The temperature of water entering the preheat tank (˚C)

T18: The temperature of water entering the GSHP (˚C)

ρ: The density of desuperheater water (kg/m^3)

[VI] Retrieved from http://www.engineeringtoolbox.com/propylene-glycol-d_363.html

Chapter 5

Data Analysis

Summer 2010

The summer data collection was originally scheduled to start at the beginning of August 2010 and continue until the end of August. However, because of some issues with dysfunctional sensors associated with the two heat pumps, the summer data collection commenced on August 23 through September 14th. During this test period, the ambient temperature range was between 15˚C and 34˚C and provided a good temperature range to analyze the performance of the equipment. Due to simultaneous data collection of the air source and the ground source heat pumps, a direct comparison of thermal performance was made.

5.1 Air Source Heat Pump

In investigating the thermal performance of the ASHP, the electricity consumption of the compressor and outdoor fan was only considered. Further investigation of the entire HVAC system in House A was later analyzed using TRNSYS. Figure 5 represents the relationship between power draw of the air source heat pump (Compressor + Outdoor Fan) and the outdoor temperature. As expected, the electricity draw from the compressor and outdoor fan increases with a rise in ambient temperature. This relationship suggests that the compressor work increases to provide sufficient cooling to the zone in higher ambient temperatures. Figure 6 illustrates the relationship between the ASHP cooling output and the outdoor temperature. The curve illustrates a decrease in cooling output with increasing ambient temperature. Combining the two Figures 5 and 6, the relationship of the coefficient of performance with outdoor temperature can be obtained as shown in Figure 7.

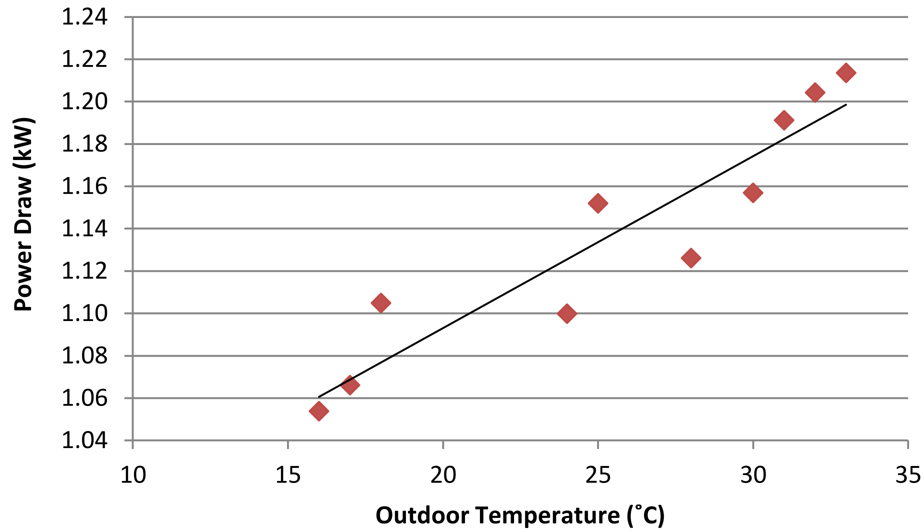

Figure 5 ASHP Power Draw

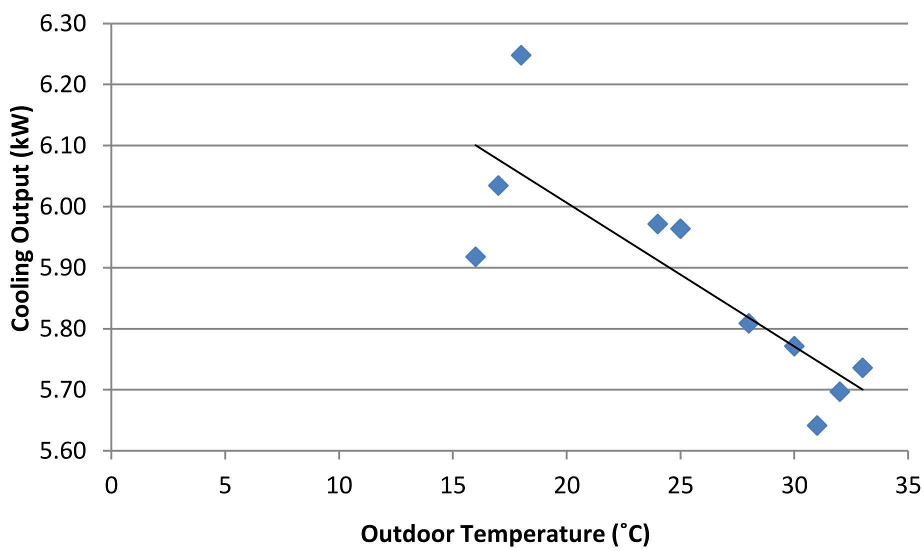

Figure 6 ASHP Cooling Output

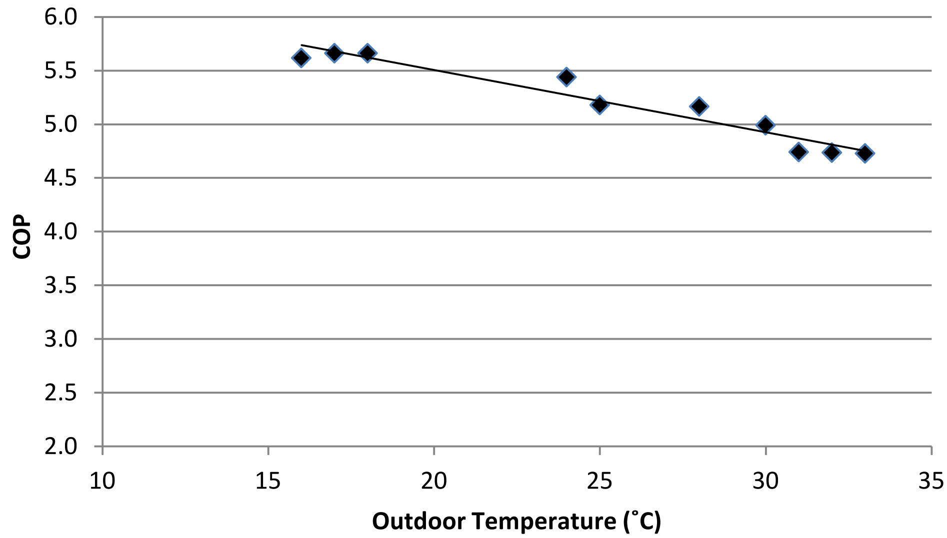

Figure 7 ASHP Cooling COP

During this 23-day test period the power draw from the heat pump ranged from 1.05 to 1.25 kW and the output cooling ranged from 5.6 to 6.3 kW. The coefficient of performance of the ASHP ranged from 4.7 to 5.7. As evident from the COP, the heat pump is very efficient in cooling mode with an output cooling of about 5 times the electricity draw. It should be noted that the values of COP do not include the indoor AHU fan power because the performance of the heat pumps alone are investigated in this section.

5.2 ASHP Part Load Performance

As mentioned earlier in the literature review, the part load characteristics of heat pumps have an impact on the overall coefficient of performance. Larger capacity heat pumps designed for extreme conditions often will have a greater frequency of on-off operation to meet lower thermal demands. This on-off cyclic operation causes a degradation of performance leading to inefficient heat pump operation. Commonly, heat pumps operate at lower capacities than design conditions, and as a result, part load effects play a significant role. The variable speed compressor heat pump is designed to operate for longer periods at lower speeds to meet the part loads. Figures 8 and 9 depict this characteristic of the variable speed compressor heat pump. Figure 8 illustrates the duration of compressor operation starting on August 23 (Day 1) through to September 14 (Day 23). Figure 9 illustrates the number of on-off cycles of the compressor in order to meet the thermal demand. From these two plots, it is clear that the maximum cycles per day is one, with long operating times ranging from 3 hours – 11 hours per day. The figures also illustrate days where cooling to the house was not required.

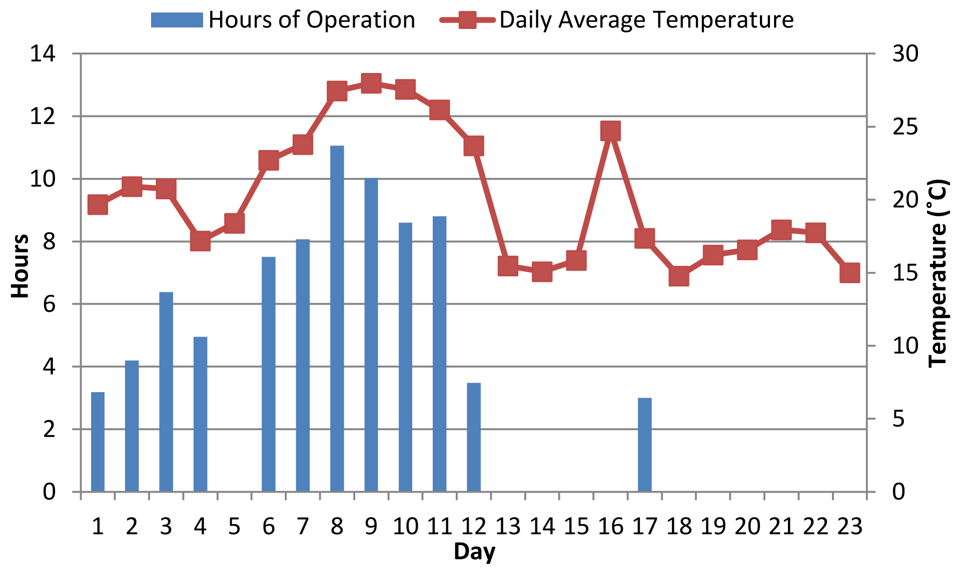

Figure 8 ASHP Duration of Compressor Operation (Aug 23 - Sept 14, 2010)

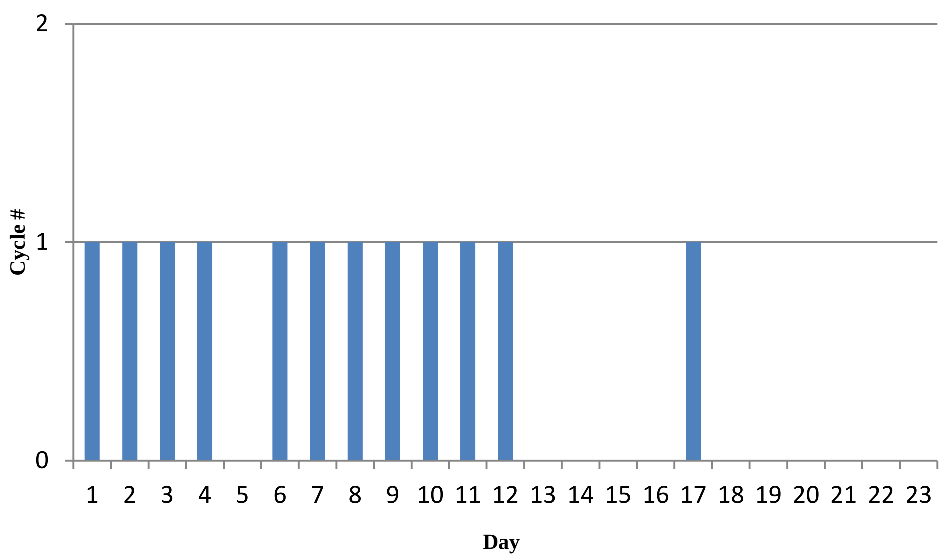

Figure 9 ASHP Compressor Cycling Frequency (Aug 23 - Sept 14, 2010)

Using the data gathered from the sensors, along with the manufacturers rated conditions, the part load performance of the ASHP was investigated. Methods seen in a study on a variable-speed ground-source heat pump were used to investigate the part load performance

(Kavanaugh, Falls, & Parker, 1994). Figure 10 illustrates the part load performance of the ASHP both through data collection and the manufacturer's specifications, where the relationship of COP ratio and input ratio with respect to capacity ratio is given. The COP ratio is defined as the instantaneous COP at a certain heat pump capacity divided by the rated COP at the respective outdoor temperature. The input ratio is defined as the instantaneous heat pump input power at a certain heat pump capacity over the rated input power at the respective outdoor temperature. During the test period, the ASHP capacity ratio ranged from about 52% to 57%. As a result, the experimental part load performance of the heat pump only exists in this region. The experimental COP ratio and the input ratio obtained from the data were plotted on the manufactures part load performance curve to depict the similarities between the two. The experimental COP (COP Expr.) ratio curve in Figure 10 illustrates that at 55% of the rated capacity the heat pump COP is 25% higher than the rated capacity, while the experimental input (Input Expr.) ratio curve in Figure 10 suggest that at 55% of the rated capacity, the ASHP will only require 45% of the rated power. If a single-speed air source heat pump system was used, the compressor would often cycle on and off to meet the required load because only 52%-57% of the full capacity was required. When comparing the experimental data points with the manufacturer's specifications, it can be seen that the experimental data falls near the manufacturer's part load performance curve (COP Manu., Input Manu.)

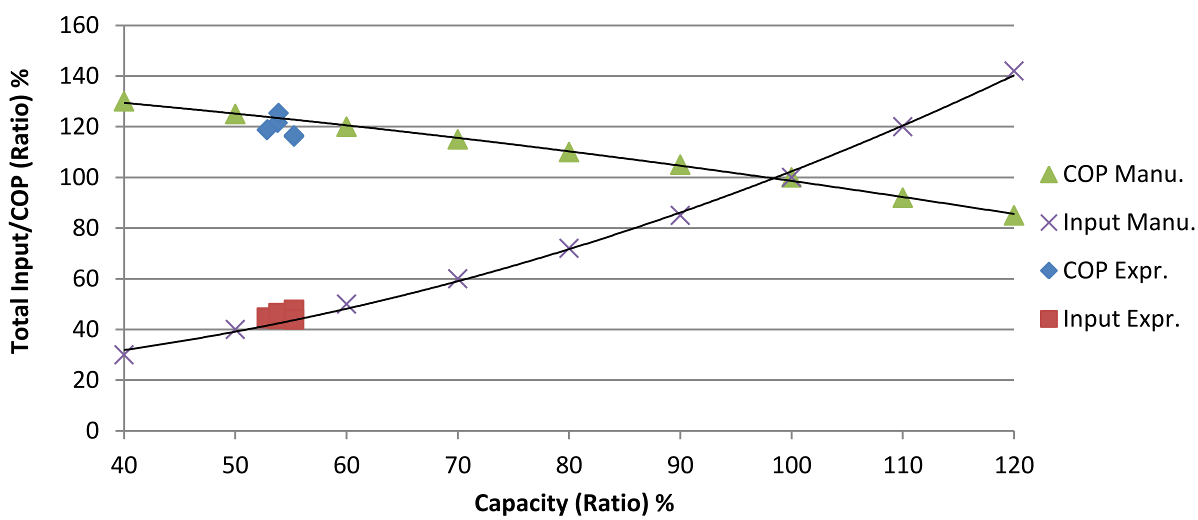

Figure 10 ASHP Part Load Experimental and Manufacturer Cooling Performance

5.3 Air Source Heat Pump Daily Cooling/Electricity Consumption

The daily cooling and electricity consumption of the ASHP during this 23-day period was investigated, as shown in Figure 11. This figure illustrates a peak daily cooling and electricity consumption of 58 kWh and 13 kWh respectively. The daily peak cooling output and electricity consumption took place on the warmest day of the test period at an outdoor average daily temperature of 28˚C. Figure 12 depicts the cumulative cooling and electricity consumption of the ASHP within this 23-day period. The total electricity consumption of the ASHP during this test period turned out to be 92 kWh and the total cooling was 414 kWh which gives a test period COP of 4.5. The relationship between the daily cooling output and the electricity consumption with respect to the average daily outdoor temperature is also shown in Figure 13. This curve is later utilized to extrapolate the summer ASHP performance.

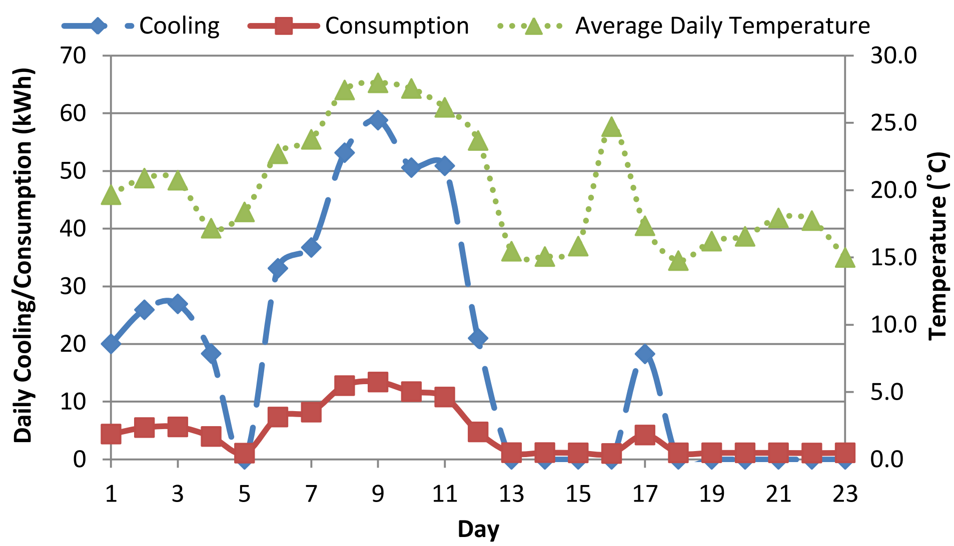

Figure 11 Daily Cooling/Consumption (Aug 23 – Sept 13, 2010)

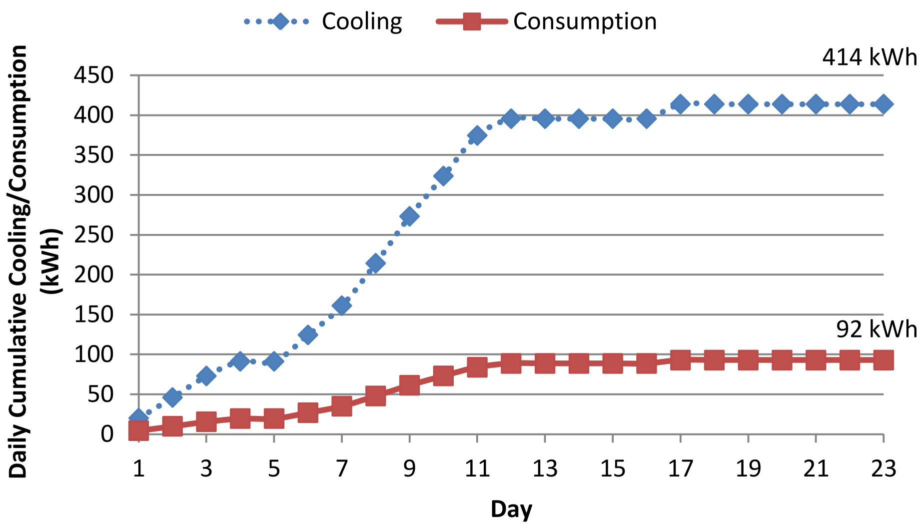

Figure 12 Daily Cumulative Cooling/Consumption (Aug 23 - Sept 13, 2010)

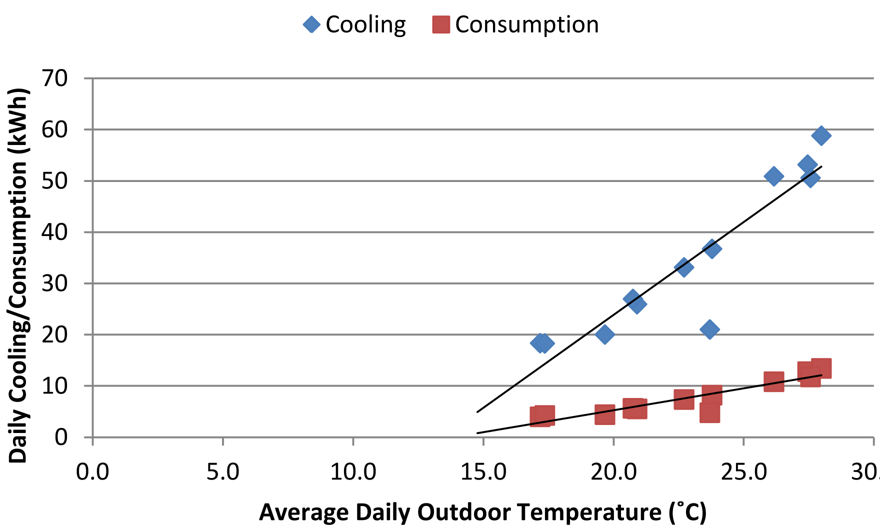

Figure 13 Daily Cooling/Consumption Vs Average Outdoor Temperature (Aug 23 - Sept 13, 2010)

5.4 Ground Source Heat Pump: (Cooling to In-Law Suite)

Similar to the analysis of the ASHP system, the performance of the GSHP is analyzed only considering the compressor and ground loop pump consumptions. The entire system including the buffer tank and AHU will be investigated later on. During this test period of August 23 – September 14th, 2010, the GSHP also supplied chilled water to the In-Law Suite via a cooling coil in a separate AHU system. Consequently the cooling delivered to the In-Law was taken away from the total cooling delivered by the GSHP to obtain the House B cooling requirement. The COP of the GSHP system was investigated with respect to the outdoor temperature as shown in Figure 14. It was noticed that there is minimal change in COP with outdoor temperature as evident from the data points in the figure. The reason for this is because the GSHP system uses the ground loop fluid to condensate the GSHP refrigerant and not the ambient temperature. As a result, the ground loop return fluid temperature plays a much more significant role in the performance of the GSHP system. As expected, because the rated capacity of the GSHP system is larger than the ASHP, the power draw of the compressor and ground loop pump is higher as shown in Figure 15. Having similar characteristic behaviour to the ASHP system, the power draw increases with an increasing sink temperature. The output cooling of the GSHP is also greatly affected by the return ground loop fluid temperature as seen in Figure 16. During this test period, the cooling output from the GSHP system ranged from 10.5 to 13.5 kW. Combining the results of Figures 15 and 16, result in a COP curve at varying ground loop return temperatures. As seen from Figure 17, the COP of the GSHP varies from 2 – 5.3 depending on the ground loop return fluid temperature. The purpose of the ground loop within the overall system in cooling mode is to act as a heat sink. Thus, the heat rejected to the ground from the horizontal loop was also monitored. As seen in Figure 18, the daily heat rejected to the ground is given during the 23-day test period. This curve demonstrates the importance of the ground loop in cooling mode, where much of the heat is transferred from the zone and rejected into the ground. The daily heat rejection to the ground ranges from 15 to 105 kWh. The entering load temperature which is the return temperature from the buffer tank to the GSHP also plays an important role in the performance of the system. Similar to the return temperature from the ground loop, the entering load temperature can affect the system performance. The performance of the GSHP system is commonly shown based on source and load temperatures. As a result, Figure 19 was created to illustrate the COP of the GSHP at varying entering load and entering source temperatures in degrees Celsius. This curve is a good indicator of how a GSHP performs and is later used in the TRNSYS GSHP energy model. From Figure 19, it is evident that the greater the change in temperature between the entering load and source temperature, the lower the COP.

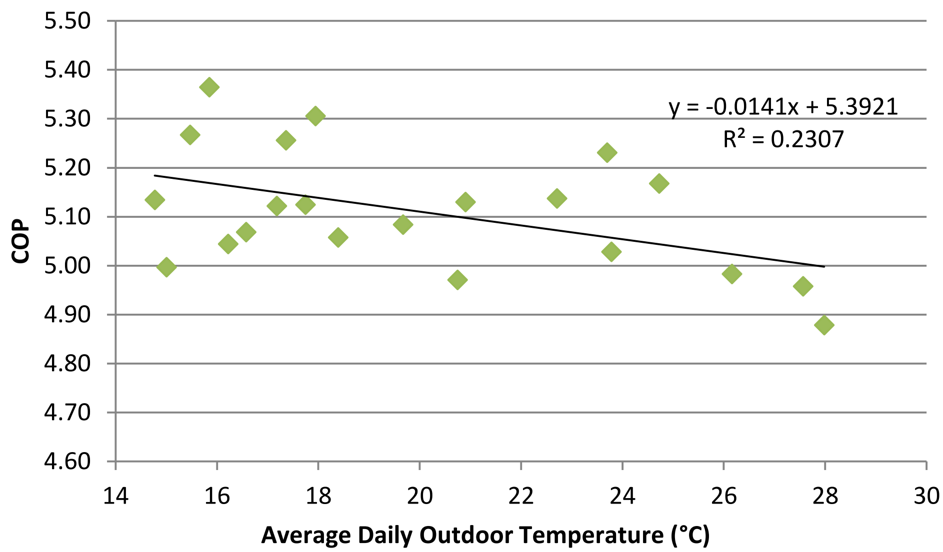

Figure 14 GSHP Cooling COP Vs. Average Daily Outdoor Temperature (Aug 23 - Sept 14, 2010)

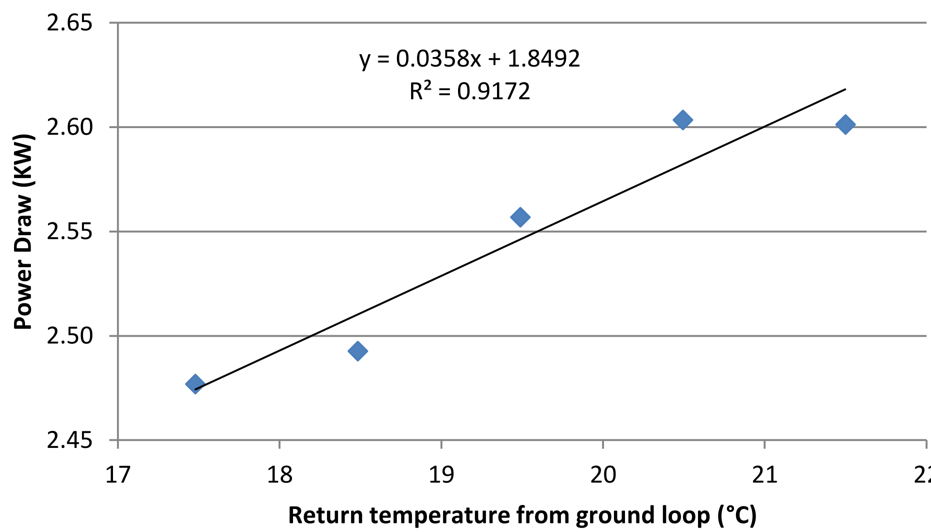

Figure 15 GSHP Daily Power Draw (Aug 23 - Sept 14, 2010)

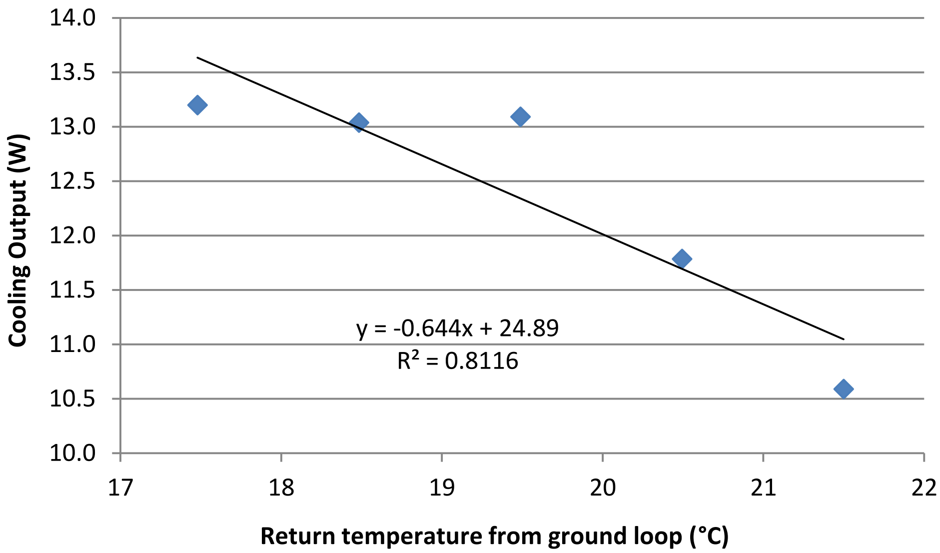

Figure 16 GSHP Cooling output (Aug 23 - Sept 14, 2010)

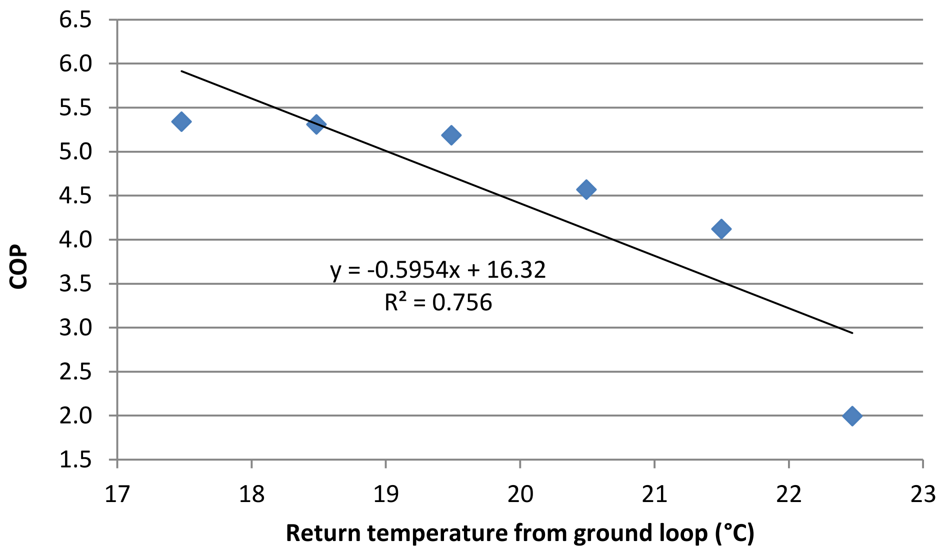

Figure 17 GSHP Cooling COP (Aug 23 - Sept 14, 2010)

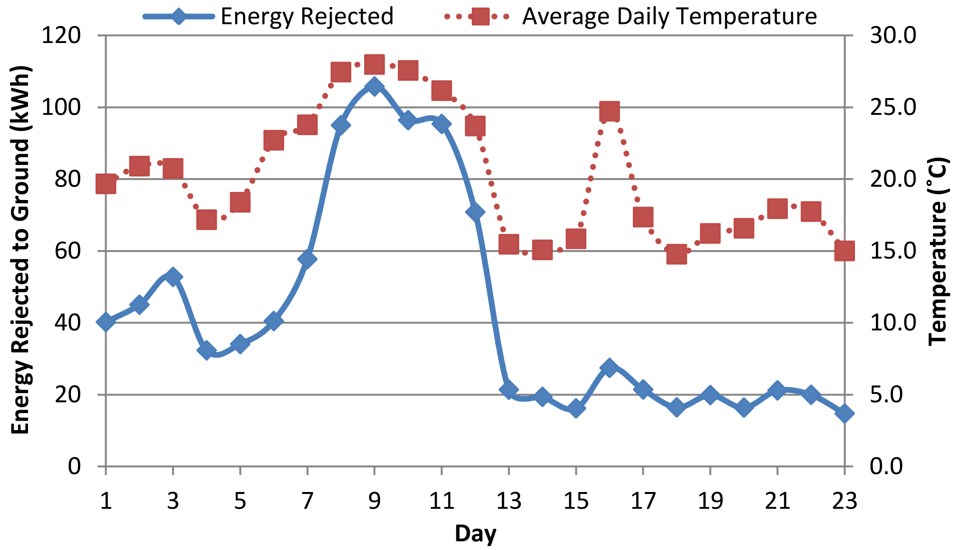

Figure 18 Heat Rejected to Ground (Aug 23 - Sept 14, 2010)

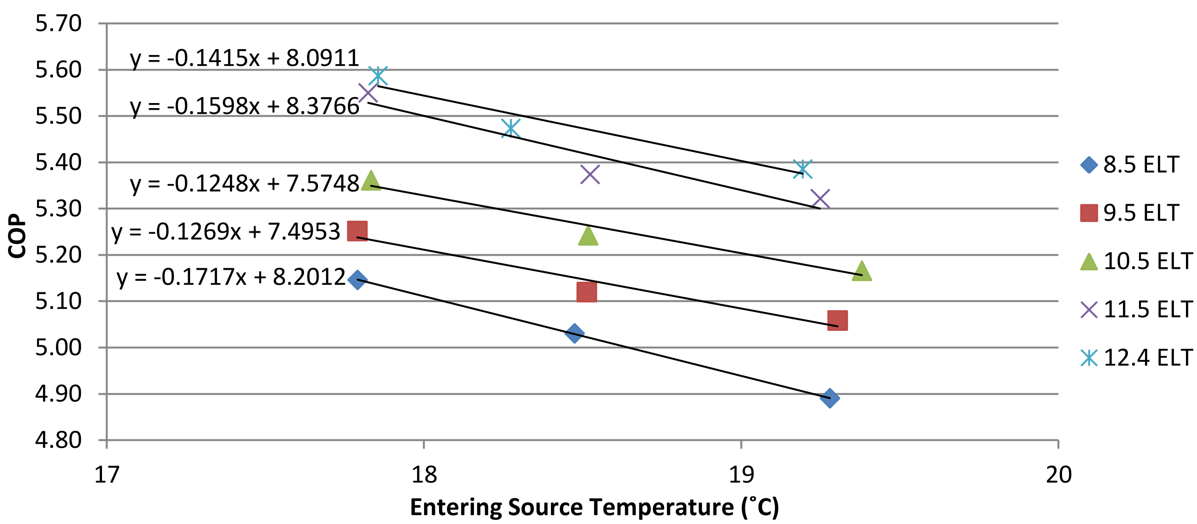

Figure 19 GSHP COP (Aug 23 – Sept 14, 2010)

5.5 Ground Source Heat Pump Daily Cooling/Electricity Consumption

The daily cooling output and electricity consumption of the GSHP during this 23-day period was analyzed as shown in Figures 20-22. As mentioned earlier, during the cooling season, chilled water was also delivered to the In-law suite from the GSHP. Figures 20-22 display the results with the GSHP supplying chilled water to both In-law suite and House B. The peak cooling delivered from the GSHP was 83 kWh at an electricity consumption of 15 kWh. Figure 21 illustrates the cumulative cooling output and electricity consumption. The total cooling delivered at the end of the test period was 773 kWh and the total electricity consumption was 151 kWh, resulting in a test period COP of 5.1. The relationship of daily cooling output and electricity consumption with respect to average daily outdoor temperature is also given in Figure 22. Separate curves were developed to illustrate the cooling delivered to House B (excluding the In-law suite). These curves are shown in Figures 23-25. Since the electricity consumption is based on the compressor and ground loop pump, to estimate the electricity consumption of House B alone, the average daily COP (from the earlier case) was used along with the cooling delivered to House B alone to predict the daily electricity consumption. Figure 23 illustrates the daily cooling and electricity consumption delivered to House B with a peak cooling output of 67 kWh and a peak electricity consumption of 13.8 kWh. Figure 24 illustrates the cumulative cooling output and electricity consumption at the end of the test period. The total cooling was 551 kWh and the total electricity consumption was 112 kWh, resulting in a test period COP of 4.91. Figure 25 illustrates the relationship between the daily cooling output and electricity consumption at various average outdoor temperatures. This Figure is later used for calibrating the House B energy model developed in TRNSYS.

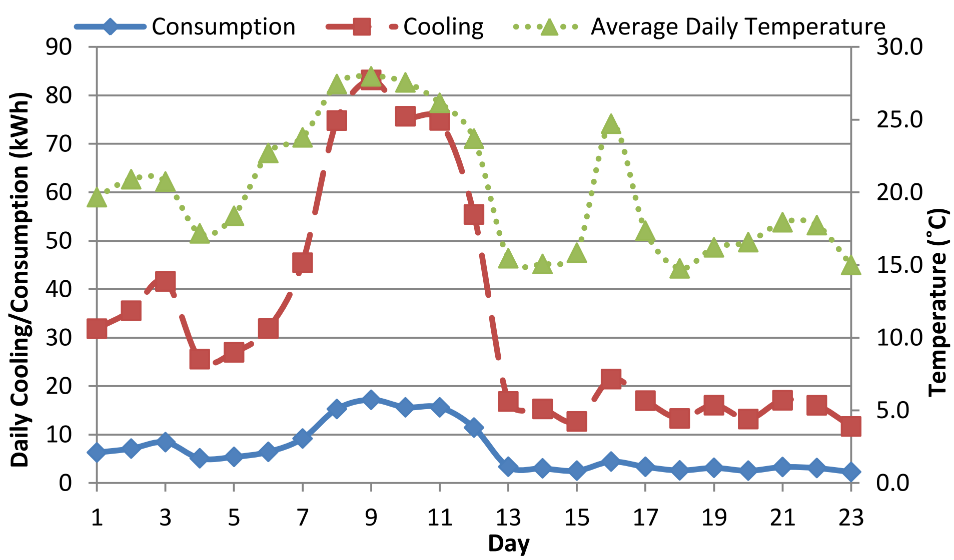

Figure 20 GSHP Daily Cooling/Consumption to House B & In-Law Suite (Aug 23 – Sept 14, 2010)

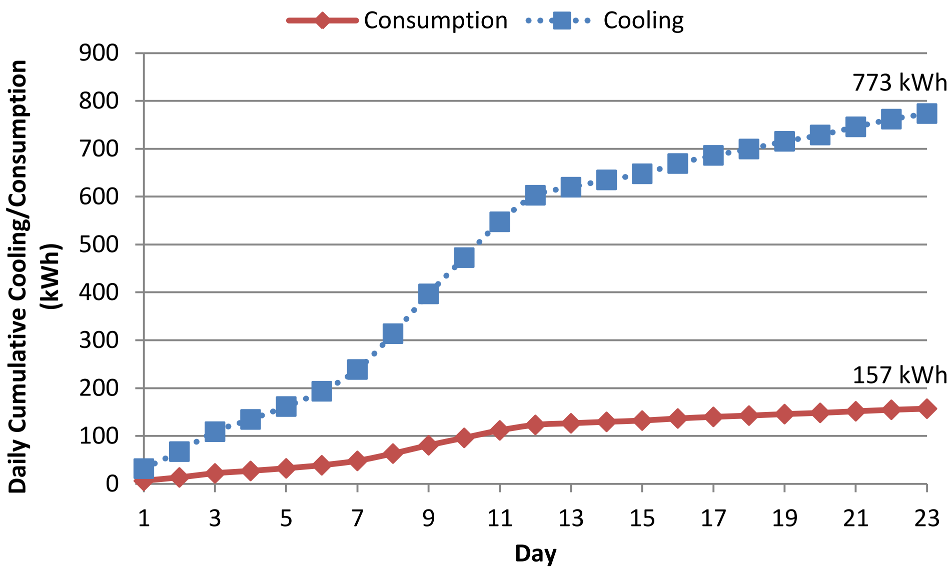

Figure 21 GSHP Daily Cumulative Cooling/Consumption to House B & In-Law Suite (Aug 23 – Sept 14, 2010)

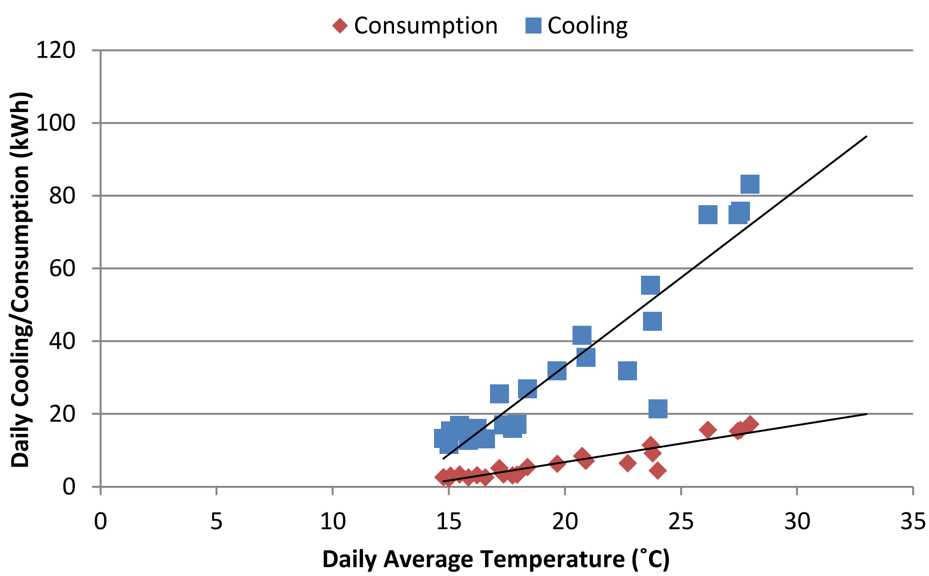

Figure 22 Daily Cooling/Electricity Consumption to House B & In-Law Suite vs. Average Outdoor Temperature

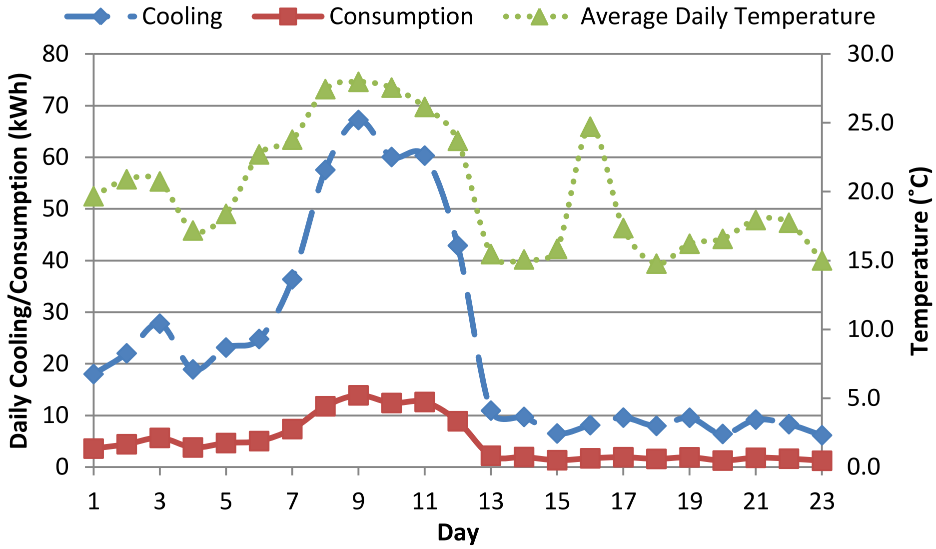

Figure 23 Daily House B Cooling/Consumption (Aug 23 – Sept 14, 2010)

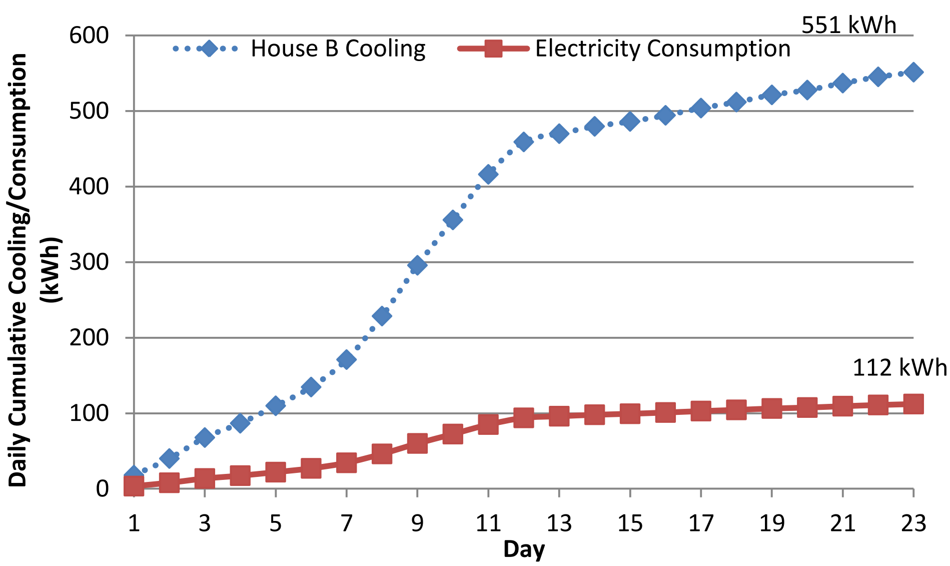

Figure 24 Daily House B Cumulative Cooling/Consumption (Aug 23 – Sept 14, 2010)

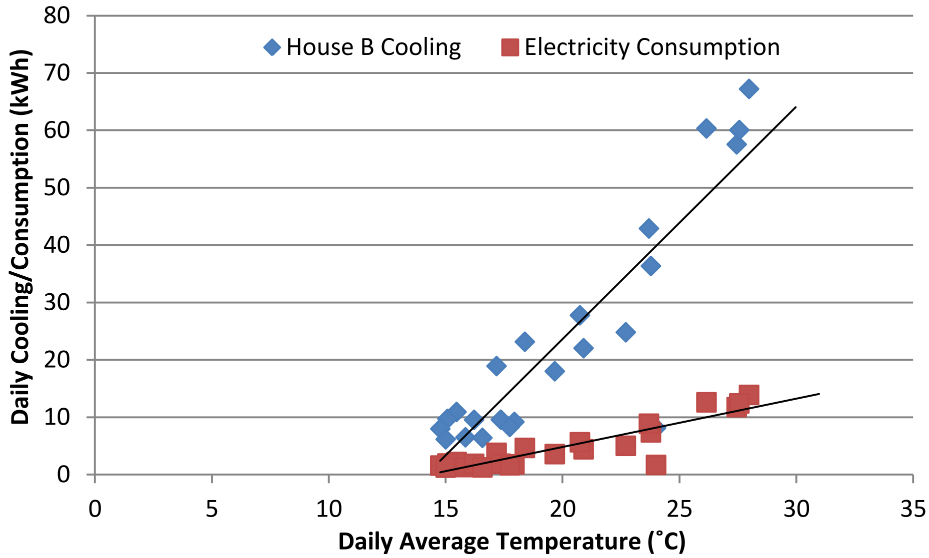

Figure 25 Daily House B Cooling/Consumption Vs. Average Outdoor Temperature

5.6 System Cycling

The GSHP system was investigated for operating time and system cycling. The daily operating time of the GSHP is shown in Figure 26 and the cyclic frequency is illustrated in Figure 27. Based on collected data, day 9 (August 31) had the longest operating time of 6.5 hours and day 13 (September 4) had the shortest operating time of 1 hour. In terms of cyclic frequency, the GSHP had a peak cyclic frequency of 25 cycles in one day. This is an indication of an oversized system that is only capable of operating at a constant output.

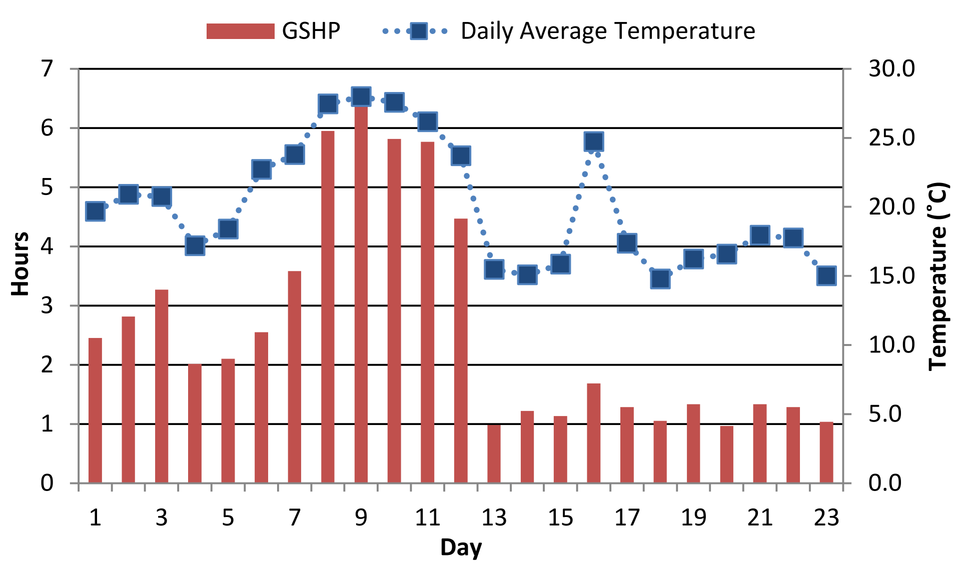

Figure 26 Operating Time of GSHP Compressor (Aug 23 - Sept 14, 2010)

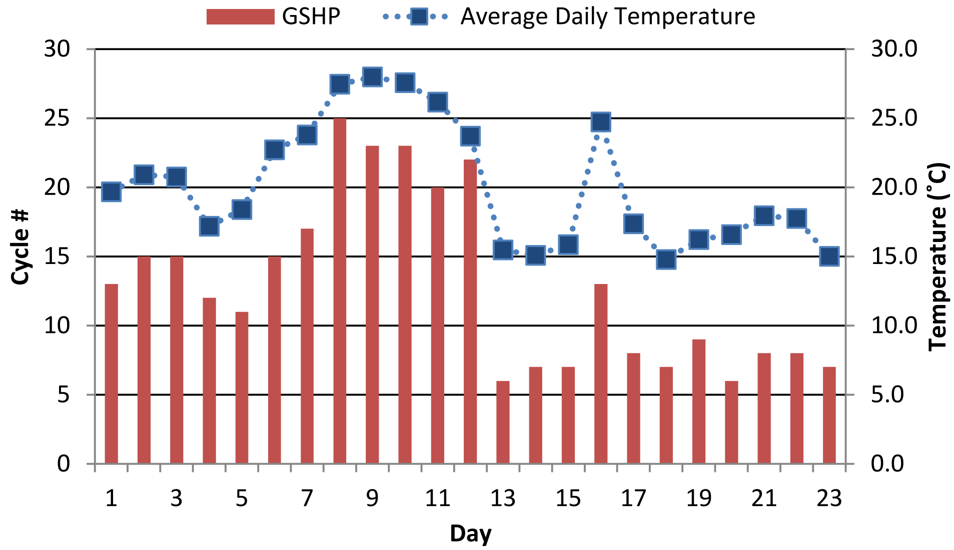

Figure 27 GSHP Cycling Frequency (Aug 23 - Sept 14, 2010)

5.7 Summary of Cooling Test Period

The summary of the cooling test period is given in Table 15. The ASHP and GSHP were tested from August 23 to September 14, 2010. During this test period, the GSHP delivered cooling to the In-law suite. As a result, two cases were shown for the GSHP: 1) Cooling to both the In-law suite and House B, 2) Cooling only to House B. For this study, the cooling to House B is only required. The ASHP delivered 414 kWh of cooling and consumed 92 kWh of electricity, resulting in a test period COP of 4.5. The GSHP delivered 551 kWh of cooling to House B, and consumed 112 kWh, resulting in a test period COP of 4.91.

Table 15 Cooling test period summary

System	Date Tested	Cooling Output (kWh)	Electricity Consumption (kWh)	COP
ASHP	Aug 23 – Sept 14, 2010	414	92	4.50
GSHP	Aug 23 – Sept 14, 2010	551	112	4.91

5.8 ASHP Extrapolated Summer Seasonal Performance

In this section, data extrapolation was used to predict the seasonal performance. The performance of the heat pumps with respect to the daily average outdoor temperature was used to develop an electricity consumption and cooling output curve for the test period of August 23 –September 14, 2010. Using these curves along with the daily average temperature data of metropolitan Toronto obtained from TRNSYS 16, the typical seasonal performance of the ASHP was extrapolated. TRNSYS 16 uses the Meteonorm V5 weather file which incorporates meteorological data and calculation procedures for solar applications and system design at any desired location in the world from 1961-1990 and 1994-2005 (Meteotest, 2010). The extrapolated daily electricity consumption (compressor and outdoor fan) and daily cooling output of the ASHP are shown below in Figure 28. The typical cooling season was assumed to begin on May 22 and end on September 30. According to the metropolitan Toronto weather file from Meteotest, a peak daily average temperature of 26.9˚C occurs on July 20. The typical cooling season average daily temperatures are shown in Figure 28. From Figure 28, it is evident that the ASHP has a peak electricity consumption and cooling output on this particular day. Figure 29 depicts the cumulative electricity consumption and cooling output of the ASHP for the summer season. The ASHP total electricity consumption at the end of the summer was obtained to be 509 kWh while the total cooling output turned out to be 2354 kWh suggesting a seasonal COP of 4.63.

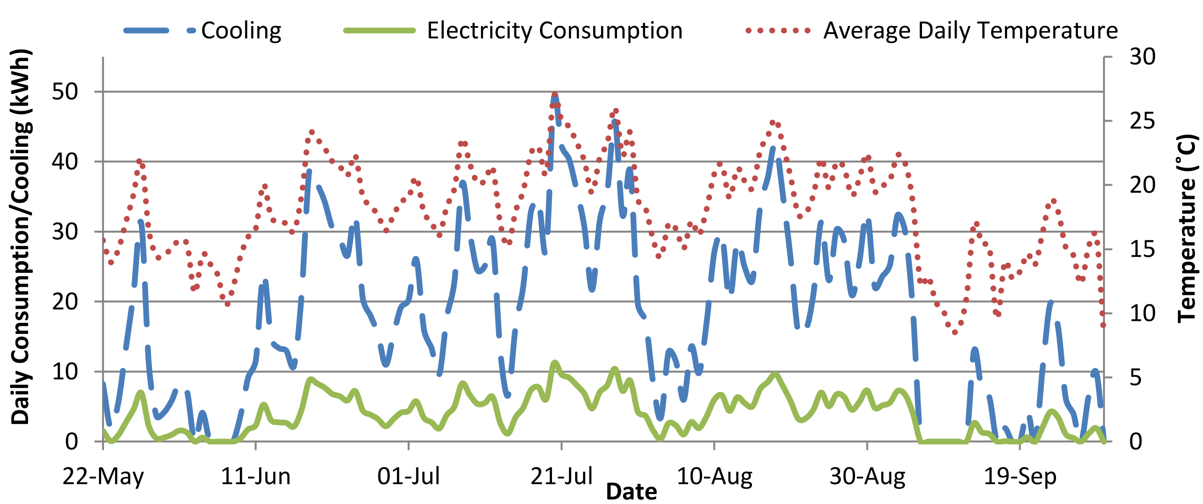

Figure 28 ASHP Daily Consumption/Cooling Extrapolation

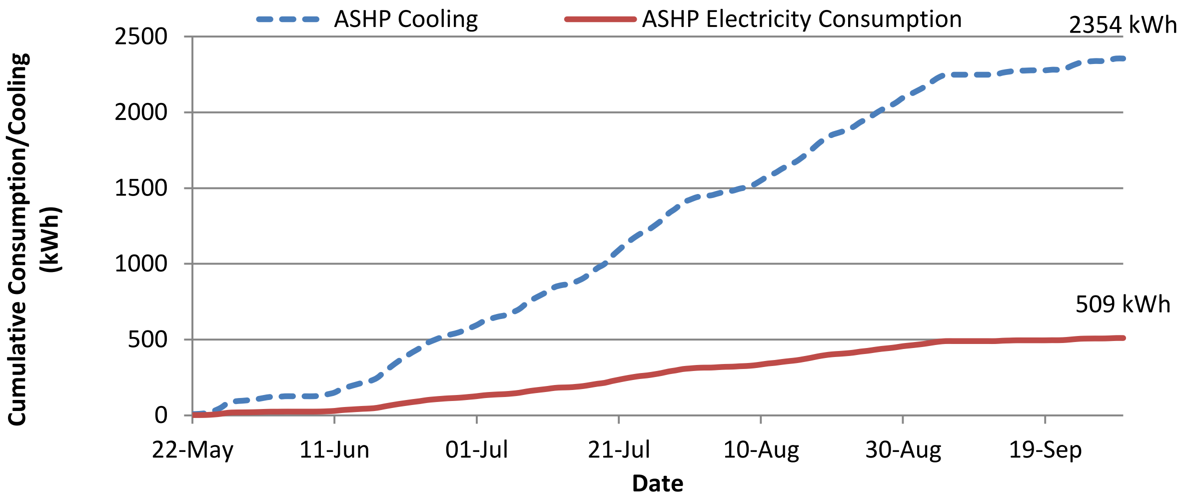

Figure 29 ASHP Daily Cumulative Consumption/Cooling Extrapolation

It is important to note that the ASHP COP value only consider the electricity consumption of the compressor and outdoor unit. The seasonal COP of the total system will be analyzed in the later section.

5.9 ASHP Overall System Analysis

Further analysis is undertaken in this section to investigate the seasonal performance of the ASHP to include the entire system. The electricity consumption of the entire ASHP system is from the compressor, the outdoor fan, and the AHU fan. The AHU was installed such that the fan is constantly operating regardless of the operation of the compressor. This constant electricity draw from the AHU causes a high daily consumption for the system thus decreasing the seasonal COP. The AHU fan power draw ranged from 100 W– 500 W. In this section, the ASHP system performance is further investigated by extrapolating the performance of the entire system as installed, and the entire system is optimized. The optimized system operates such that the AHU fan only operates when the thermostat calls for cooling, in other words only when the compressor is operating. Figure 30 depicts the extrapolated daily consumption and cooling of the entire ASHP system as installed. Figure 31 illustrates the extrapolated cumulative electricity consumption and cooling at the end of the cooling season. The total electricity consumption of the system as installed during the cooling season was obtained as 1044 kWh while the total cooling was 2354 kWh suggesting a seasonal COP of 2.25.

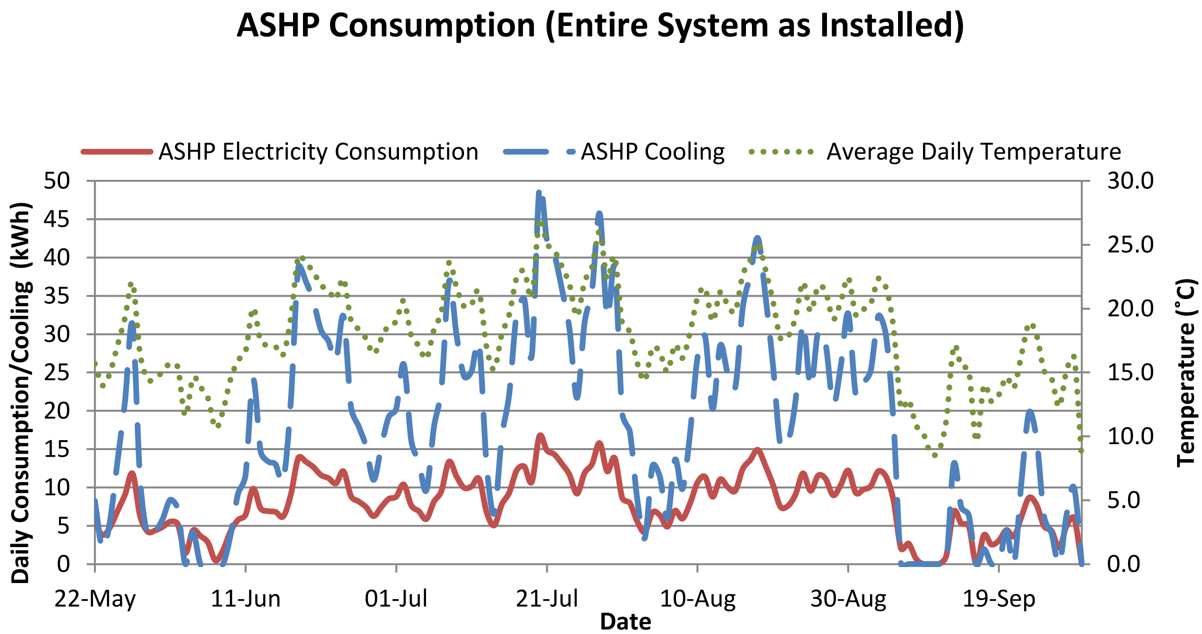

Figure 30 ASHP Daily Consumption/Cooling Extrapolation (Entire System as Installed)

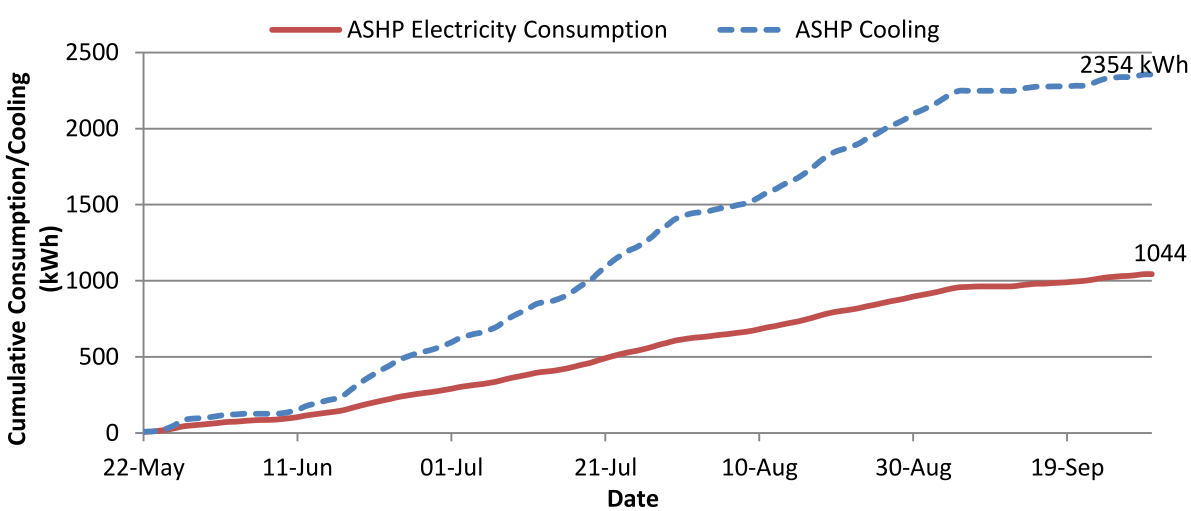

Figure 31 ASHP Daily Cumulative Consumption/Cooling Extrapolation (Entire System as Installed)

ASHP Consumption (Entire System Optimized)

In this section the performance of the optimized ASHP is extrapolated where the AHU fan operates only when required. Figure 32 illustrates the daily consumption and cooling of the optimized ASHP system. Figure 33 represents the cumulative consumption and cooling of the optimized ASHP system. The total electricity consumption of this system turned out to be 665 kWh, and the total cooling was 2354 kWh indicating a seasonal COP of 3.54. As evident from the cumulative consumption of the two operational methods, by having the AHU fan operate with the ASHP compressor, the total seasonal electricity consumption decreases by almost 37%.

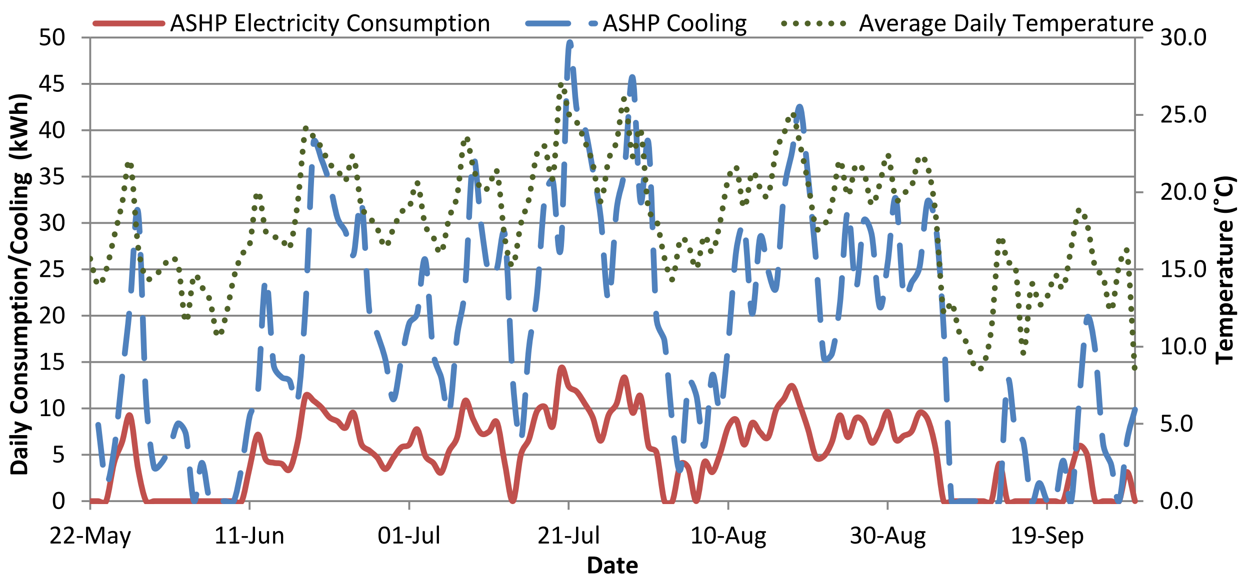

Figure 32 ASHP Daily Consumption/Cooling Extrapolation (Entire System with AHU Operating with Compressor)

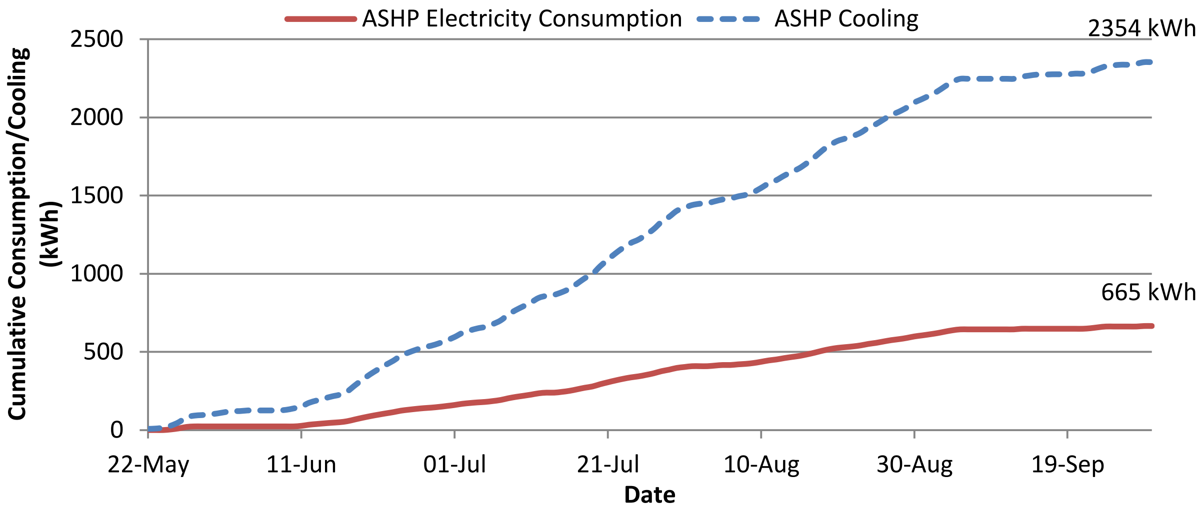

Figure 33 ASHP Daily Cumulative Consumption/Cooling Extrapolation (Entire System with AHU Operating with Compressor)

Table 16 illustrates the seasonal COP of each ASHP operational method. The seasonal COP of the currently installed system turned out to be 2.25, while the seasonal COP of the optimized system having the AHU fan operate with the compressor was 3.54. From these analyses, the importance of a proper control system is evident. Having the AHU fan operate with the compressor can significantly lower the overall electricity consumption of the HVAC system.

Table 16 Extrapolated Seasonal COP of ASHP System Configurations

	Seasonal Electricity Consumption	Seasonal Cooling Output	Seasonal COP
Air Source Heat Pump (Compressor & Outdoor Fan)	**509 kWh**	**2354 kWh**	**4.63**
Air Source Heat Pump Entire System (As Installed)	**1044 kWh**	**2354 kWh**	**2.25**
Air Source Heat Pump Entire System (AHU Operating with Compressor)	**665 kWh**	**2354 kWh**	**3.54**

5.10 GSHP Extrapolated Summer Seasonal Performance (Including In-Law Suite)

The daily electricity consumption (compressor and ground loop circulation pump) and the daily cooling output of the GSHP is shown below in Figure 34. The method of extrapolation was similar to that of the ASHP. During the summer GSHP test period, chilled water was also delivered to the In-Law suite. As a result, the extrapolation also includes cooling to both House

B and the In-Law suite. The typical cooling season was assumed to begin on May 22 and end on September 30. Figure 35 depicts the cumulative electricity consumption and cooling output of the GSHP for the summer season. The GSHP total electricity consumption at the end of the summer was obtained to be 666 kWh while the total cooling output turned out to be 3419 kWh suggesting a seasonal COP of 5.13.

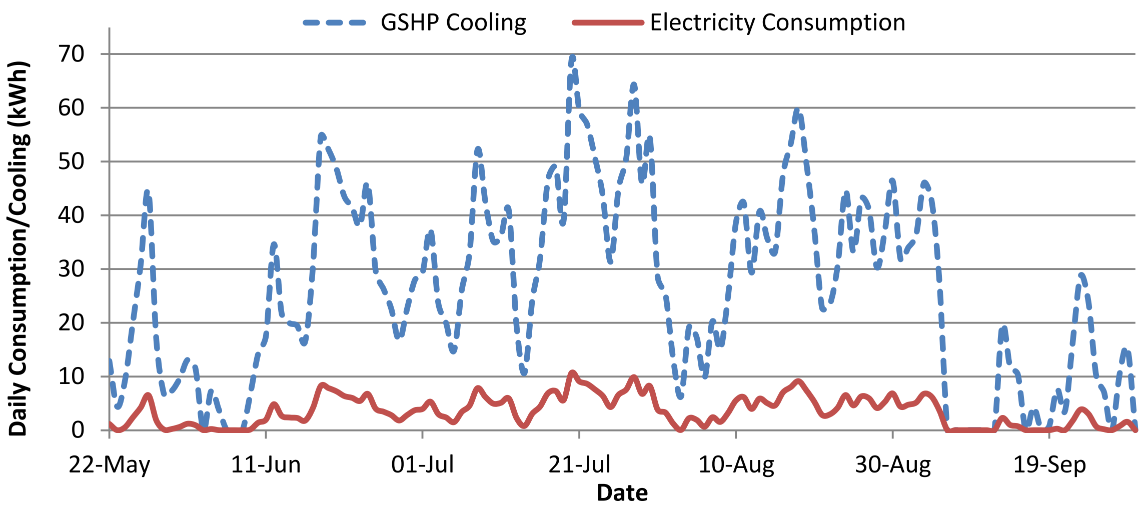

Figure 34 GSHP Daily Consumption/Cooling Extrapolation (Cooling to In-Law)

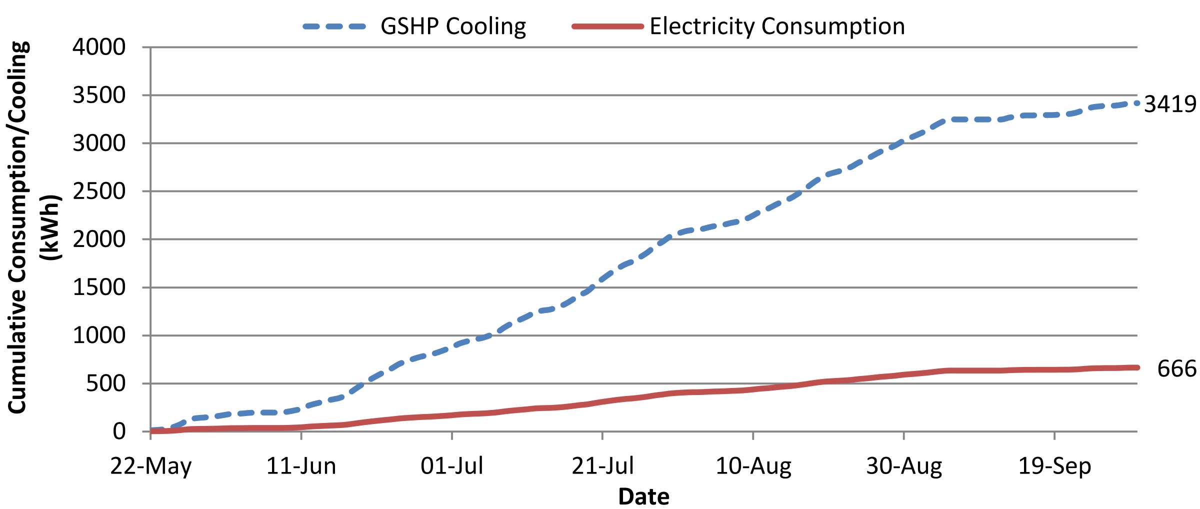

Figure 35 GSHP Daily Cumulative Consumption/Cooling Extrapolation (Cooling to In-Law)

5.11 GSHP Extrapolated Summer Seasonal Performance (Considering only House B)

The extrapolated daily electricity consumption and the daily cooling output delivered to House B is shown in Figure 36. In this case, the chilled water delivered to the In-Law suite was taken away from the total cooling delivered by the GSHP. From Figure 36, it can be seen that the peak cooling was reduced from 68.8 kWh to 54.3 kWh. Figure 37 depicts the GSHP cumulative electricity consumption and cooling output to the House. The GSHP total electricity consumption at the end of the summer was obtained to be 485 kWh while the total cooling output turned out to be 2396 kWh suggesting a seasonal COP of 4.94.

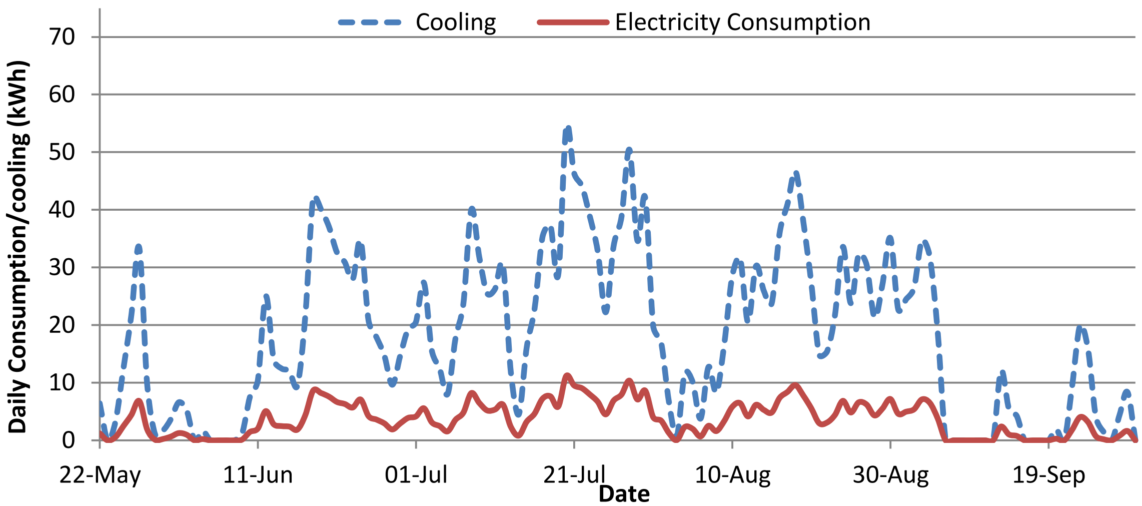

Figure 36 GSHP Daily Consumption/Cooling Extrapolation (Cooling only to House B)

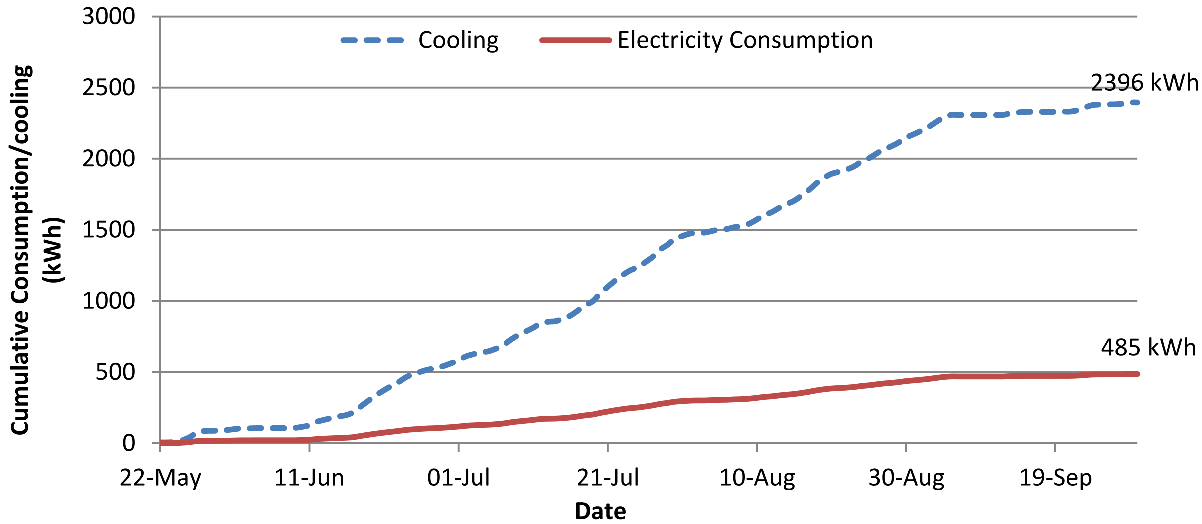

Figure 37 GSHP Daily Cumulative Consumption/Cooling Extrapolation (Cooling only to House B)

5.12 GSHP Overall System Analysis (Including In-Law Suite)

Further analysis is done in this section to investigate the seasonal performance of the GSHP to include the entire system. The purpose of this section is to investigate the effects the system components and control strategies have on the overall performance of the heat pump. A schematic of the full system is shown in Figure 38, where the electricity consumption of the entire system includes the compressor, the ground loop circulation pump, the pump from the GSHP to the buffer tank, the pump from the buffer tank to the AHU, and the AHU fan. The approximate power draw of each component is given in Table 17. This particular GSHP system was installed such that the pump from the GSHP to the buffer tank will often operate to circulate the water in the buffer tank to and from the heat pump to check the water temperature. If the set point temperature is not satisfied, the compressor will begin to operate. Also, the pump from the buffer tank to the AHU is constantly circulating water into and out of the AHU regardless of the AHU fan operation. The electricity consumption associated with the improper control system for the two pumps result in a significant decrease in the overall coefficient of performance. The seasonal cooling performance of four scenarios was investigated in this section. These four scenarios include 1) the performance of the entire GSHP system as currently installed, 2) the performance of the GSHP only including the compressor, ground loop pump, and pump from GSHP to buffer tank, 3) the performance of the GSHP only including the compressor, ground loop pump, and the pump from GSHP to buffer tank controlled by the compressor, and finally 4) the performance of the entire system optimized by having the pump from GSHP to buffer tank and the pump from the buffer tank to the AHU operating only when needed.

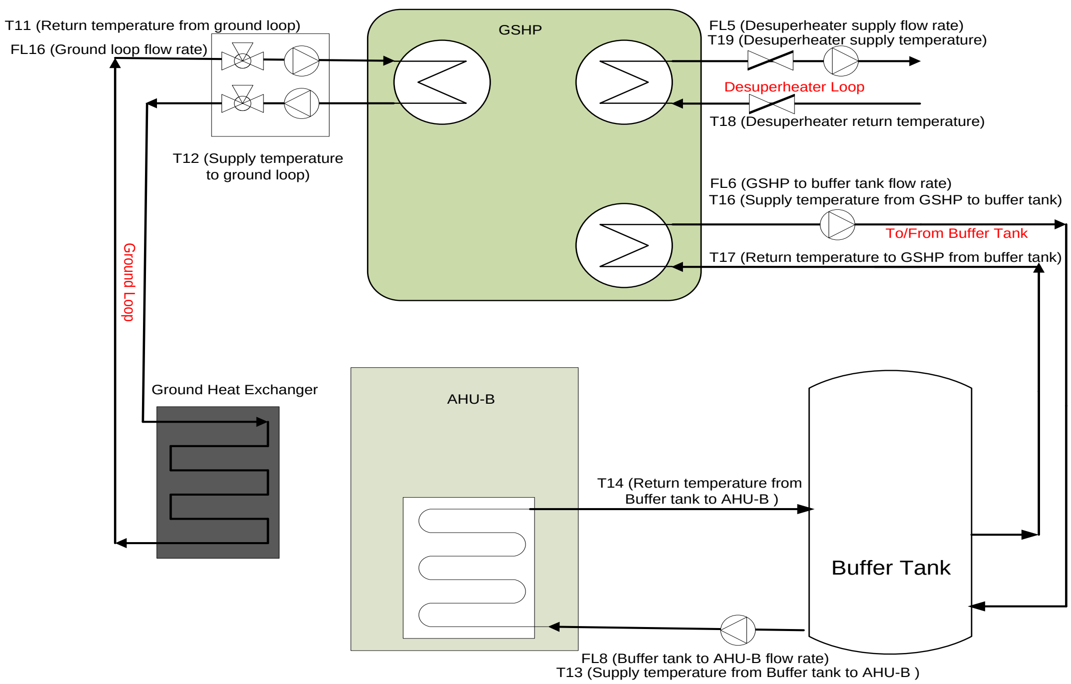

Figure 38 GSHP Entire System Schematic

Table 17 Equipment Power Draw

Equipment	**Power Draw (W)**
GSHP to Buffer Tank Circulation Pump	180
Ground Loop Circulation Pump	670
Buffer Tank to AHU-B Circulation Pump	185
Desuperheater Pump	50
AHU-B Fan	180 – 600

GSHP Consumption Entire System as Installed

(Compressor + Ground Loop Pump + Pump to Buffer Tank + Pump to AHU + AHU)

The performance of the entire GSHP system as currently installed is shown below in Figures 39 and 40. Figure 39 illustrates the extrapolated daily electricity consumption, and Figure 40 illustrates the extrapolated cumulative electricity consumption at the end of a typical summer season. The final consumption of the as-installed system turned out to be 1294 kWh. The seasonal cooling COP of the entire GSHP system as installed is 2.64.

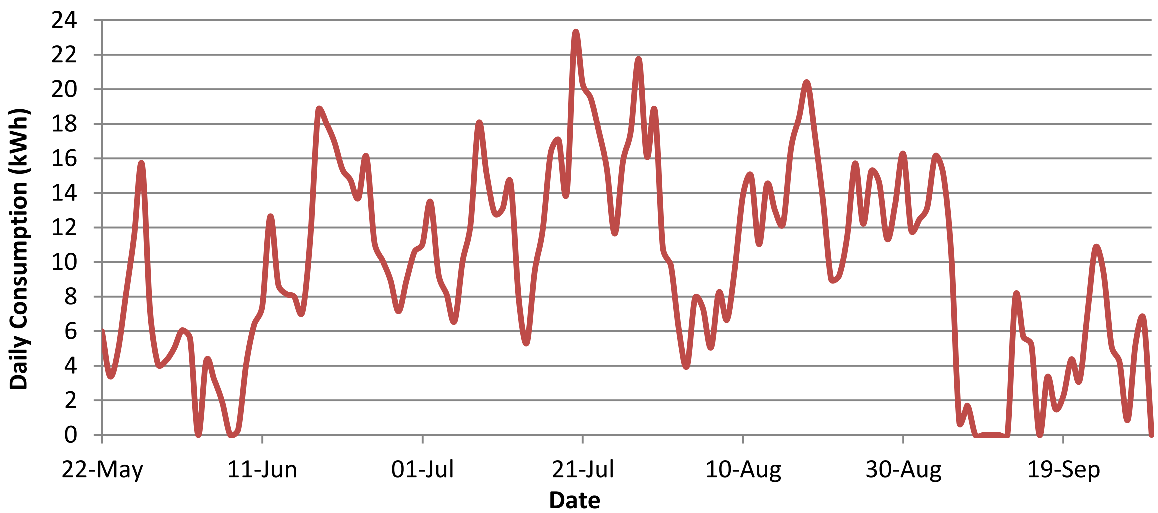

Figure 39 GSHP Extrapolated Daily Electricity Consumption (Entire System as Installed)

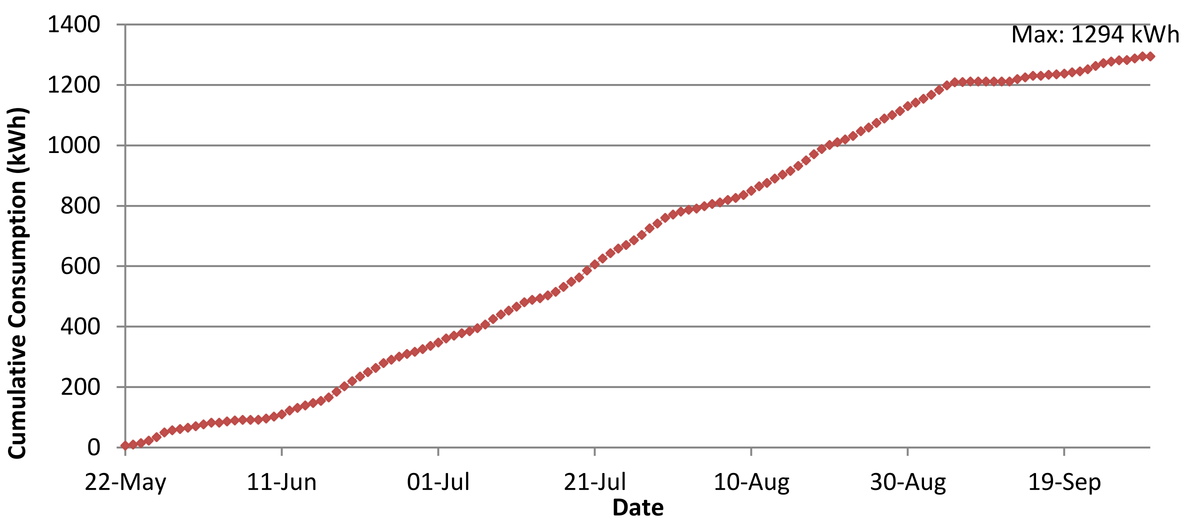

Figure 40 GSHP Extrapolated Cumulative Electricity Consumption (Entire System as Installed)

GSHP Consumption (Excluding Pump to AHU and AHU Fan)

(Compressor + Ground Loop Pump + Pump to Buffer Tank as Installed)

The performance of the GSHP system only including the compressor, ground loop pump, and pump from GSHP to buffer tank as installed is given below in Figures 41 and 42. In this analysis, the consumption of the AHU fan and the pump circulating water to the AHU was not included. The aim here is to point out the effect of using an improper temperature control system on the cumulative electricity consumption. Figure 41 depicts the extrapolated daily electricity consumption and Figure 42 illustrates the extrapolated cumulative electricity consumption at the end of a typical summer season. The final electricity consumption of the compressor plus ground loop pump and pump to buffer tank as installed turned out to be 858 kWh.

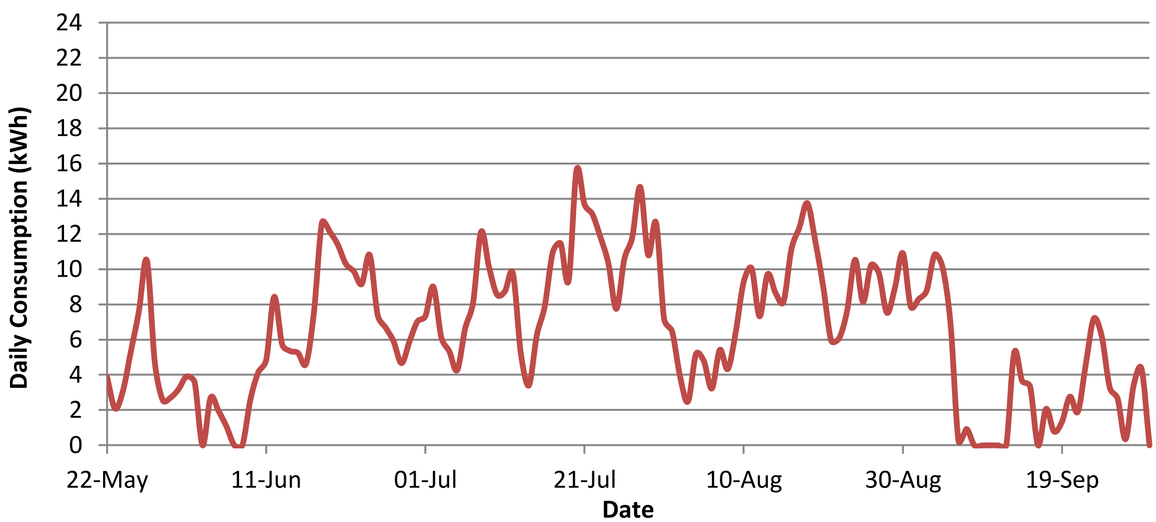

Figure 41 GSHP Extrapolated Daily Electricity Consumption
(Compressor + Ground Loop Pump + Pump from GSHP to Buffer Tank as Installed)

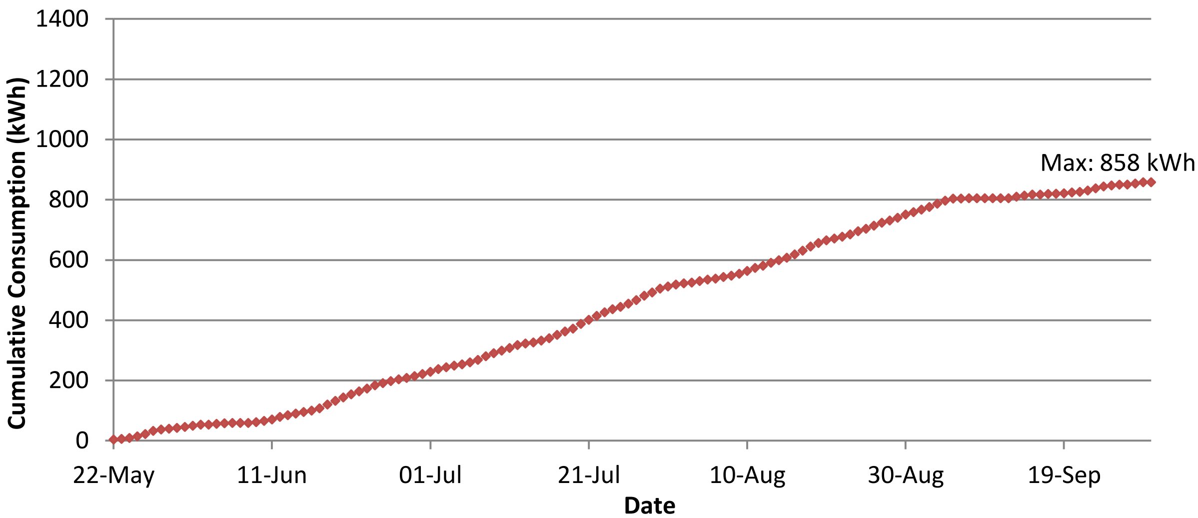

Figure 42 GSHP Extrapolated Cumulative Electricity Consumption
(Compressor + Ground Loop Pump + Pump from GSHP to Buffer Tank as Installed)

GSHP Consumption (Excluding Pump to AHU, AHU Fan, with Pump to Buffer Tank Controlled by Compressor)

(Compressor + Ground Loop Pump + Pump to Buffer Tank controlled by compressor)

Similar to the previous case, the performance of the GSHP system only including the compressor, ground loop pump, and pump from GSHP is investigated. The only difference here is a modified temperature control scheme where the pump delivering chilled water to the buffer tank from the GSHP only operates with the compressor. The results are given in Figures 43 and 44. Comparing these two figures with that of Figures 41 and 42 will provide a good understanding of the effects of proper temperature control system. In this analysis, the pump from the GSHP to the buffer tank only operates when the compressor is operating. Assuming a separate thermostat in the buffer tank controls the compressor, there is no need for constant water circulation from the buffer tank to the GSHP to check the tank temperature. Figure 43 depicts the extrapolated daily electricity consumption and Figure 44 shows the extrapolated cumulative electricity consumption at the end of a typical summer season. The seasonal electricity consumption of this system is obtained as 712.9 kWh. Comparing this value with the system above where the pump was not being controlled, energy savings of 16.9 % can be utilized over the summer season.

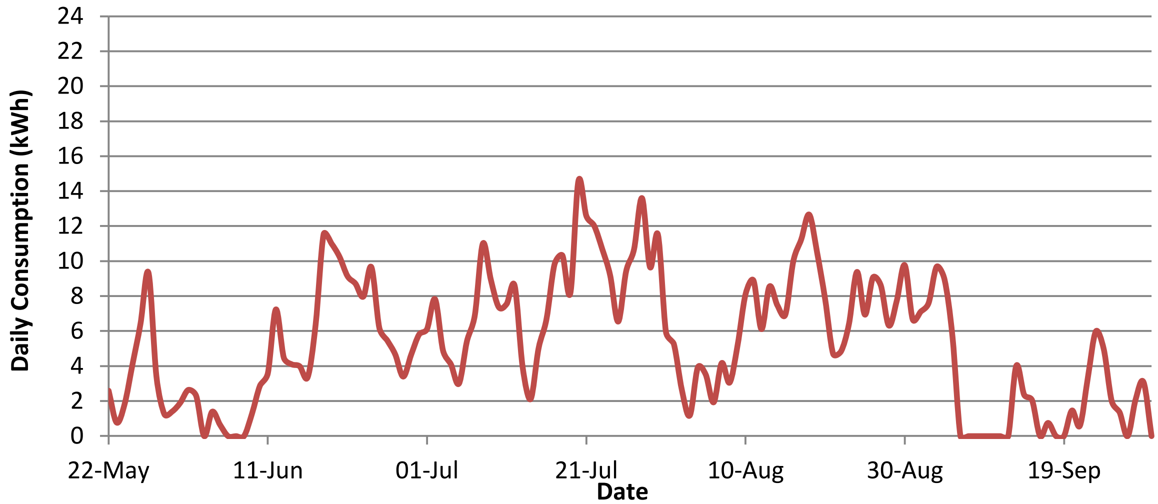

Figure 43 GSHP Extrapolated Daily Electricity Consumption
(Compressor + Ground Loop Pump + Pump to Buffer Tank Controlled by Compressor)

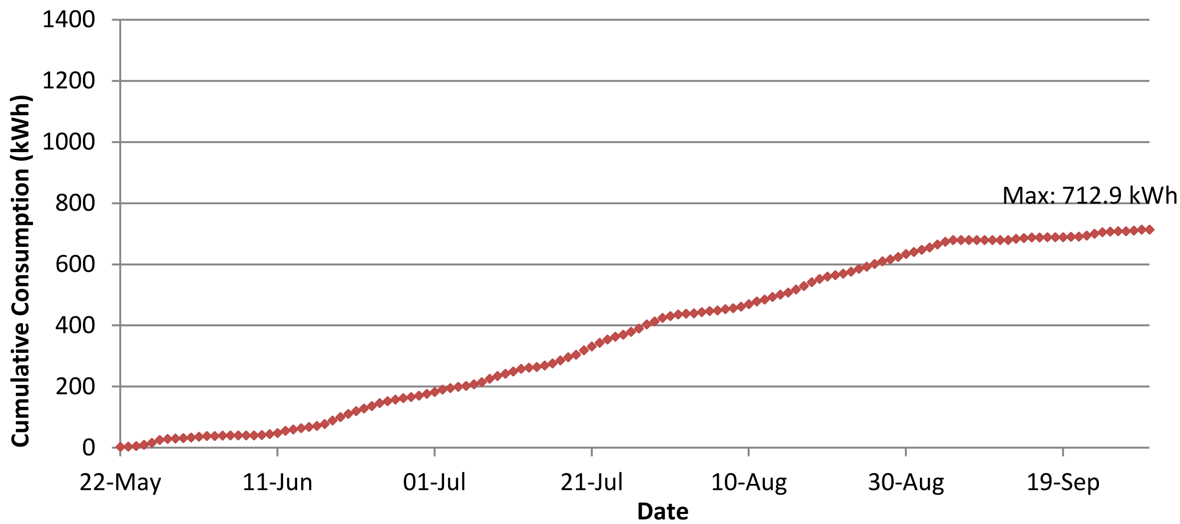

Figure 44 GSHP Extrapolated Cumulative Electricity Consumption
(Compressor + Ground Loop Pump + Pump to Buffer Tank Pump to Buffer Tank Controlled by Compressor)

GSHP Consumption (Entire System Optimized)

This section investigates the performance of the entire GSHP system optimized. The optimized system is similar to the currently installed system except that the pump from the GSHP to the buffer tank and the pump from the buffer tank to the AHU unit are utilized only when needed. Ideally, this scenario represents the type of system that should have been followed. Figure 45 depicts the extrapolated daily electricity consumption of the entire system while Figure 46 illustrates the extrapolated cumulative electricity consumption at the end of a typical summer season. The final electricity consumption of the entire system optimized was obtained to be 929.61 kWh. Comparing this value to that of the entire system as installed, energy savings of 28% is noticed. The seasonal cooling COP of the entire optimized GSHP system is 3.68. A summary of the performance of all GSHP scenarios mentioned earlier is given in Table 18.

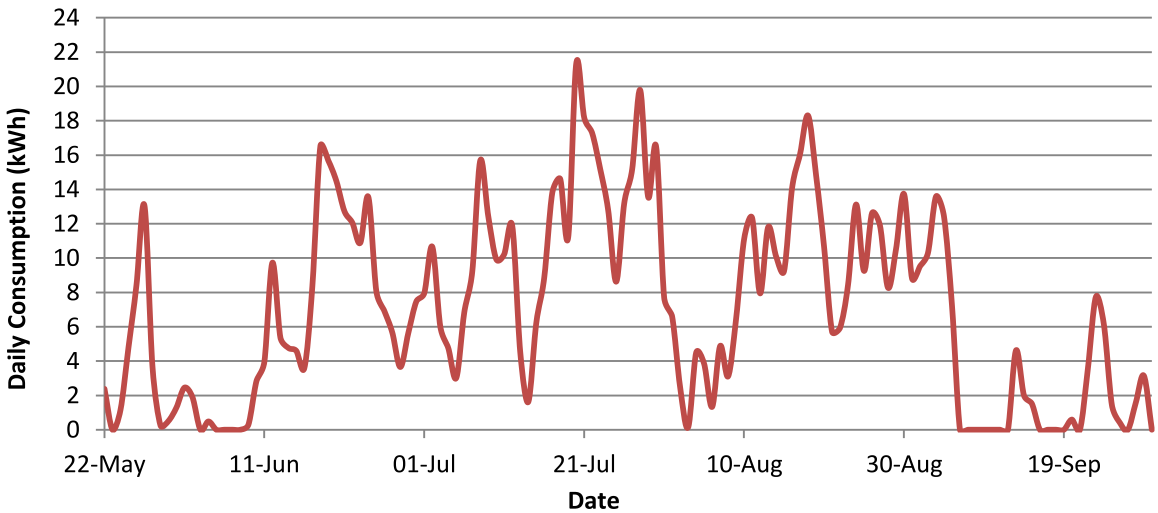

Figure 45 GSHP Extrapolated Daily Electricity Consumption (Entire System Optimized)

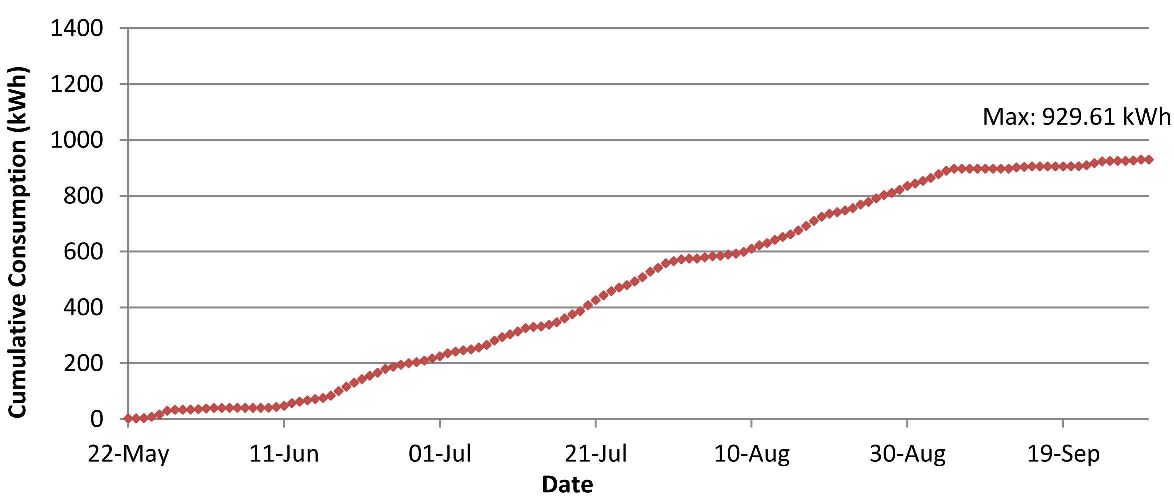

Figure 46 GSHP Extrapolated Cumulative Electricity Consumption (Entire System Optimized)

The as built system shows a lower performance than expected, with a seasonal COP of 2.64. With an improvement in the overall control system of the GSHP, this seasonal performance can be increased to 3.68. It was noted that the pump from the GSHP and the buffer tank often circulates the water into and from the buffer tank to check the water temperature. This frequent circulation causes the overall electricity consumption of the system to increase. A better solution to check the water temperature in the buffer tank would be to have a separate thermostat at the tank so the pump would not have to circulate the water to check the temperature. In this regard, the pump would only operate when the compressor operated. It was also noticed that the pump from the buffer tank to the AHU constantly circulated water to and from the AHU. This constant power draw from the pump played a major role in reducing the efficiency of the overall system. This pump is only required when the AHU is in operation. With these two issues solved, the optimized extrapolated analysis showed an improvement in overall system efficiency having a seasonal COP of 3.68.

Table 18 Extrapolated Seasonal COP of GSHP System Configurations

	Seasonal Electricity Consumption (kWh)	Seasonal Cooling Output (kWh)	Seasonal COP
GSHP (Compressor & Ground Loop Pump)	666	3419	5.13
GSHP – Cooling to House B Only (Compressor & Ground Loop Pump)	485	2396	4.94
GSHP (Entire System as Installed)	1294	3419	2.64
GSHP (Compressor, Ground Loop Pump, Pump from GSHP to Buffer Tank as Installed)	858	3419	3.98
GSHP (Compressor, Ground Loop Pump, Pump from GSHP to Buffer Tank Controlled by Compressor)	712	3419	4.79
GSHP (Entire System Optimized)	929	3419	3.68

Winter 2010/2011

The winter data collection began on December 1, 2010 and continued until February 9, 2011. During this test period, the ambient temperature ranged between 9˚C to -19˚C and provided a good temperature range to analyze the performance of the two pieces of equipment. Similar to the cooling analyses, a direct comparison of thermal performance between the ASHP and GSHP was made.

5.13 Air Source Heat Pump

Similar to the summer performance analyses, when investigating the thermal performance of the ASHP, the electricity consumption of the compressor and outdoor fan was only considered. Figure 47 represents the relationship between the power draw from the air source heat pump and the outdoor temperature. From the curve, it is evident that the first-stage compressor electricity draw increases with a lower ambient temperature. This relationship suggests that the compressor work increases to provide sufficient heating to the zone in colder ambient temperatures. It is also noticed that the second-stage compressor operates when ambient temperatures are lower than -15˚C. The power draw rapidly increases from 2.5 kW to 5 kW indicating that the heat pump is operating in the second stage. The ASHP requires the second-stage compressor to operate in higher heating demands. Figure 48 illustrates the relationship between the ASHP heating output and the outdoor temperature. The curve suggests that in first stage compressor operation, the heating output decreases with decreasing ambient temperature. Once the second-stage operation begins, the heating output rises from about 6 kW to 10 kW. When combining Figures 47 and 48, the relationship of the coefficient of performance with outdoor temperature is obtained as shown in Figure 49. The heating COP curve illustrates a linear relationship with ambient temperature. The lowest temperature the ASHP was tested during the monitoring period was -19˚C. At this temperature, the COP turned out to be around 1.79. It is also noted that according to the best fit line of Figure 49, below -24˚C, the outdoor temperature is below the evaporator heat exchange temperature and no heat transfer will occur.

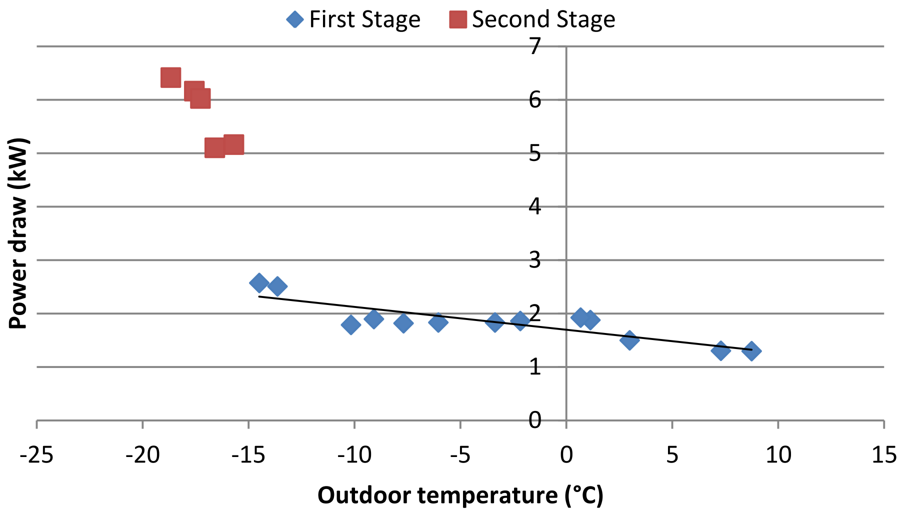

Figure 47 ASHP Heating Power Draw (Dec 1, 2010 – Feb 9, 2011)

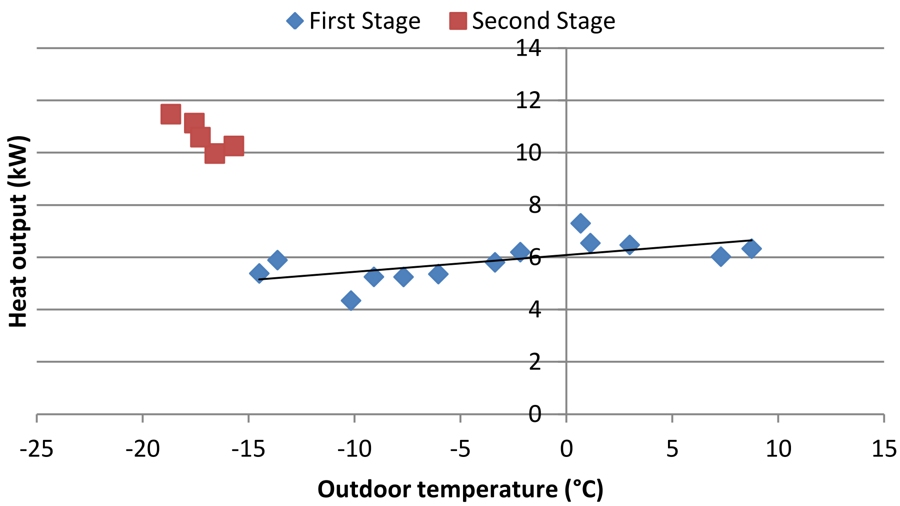

Figure 48 ASHP Heating Output (Dec 1, 2010 – Feb 9, 2011)

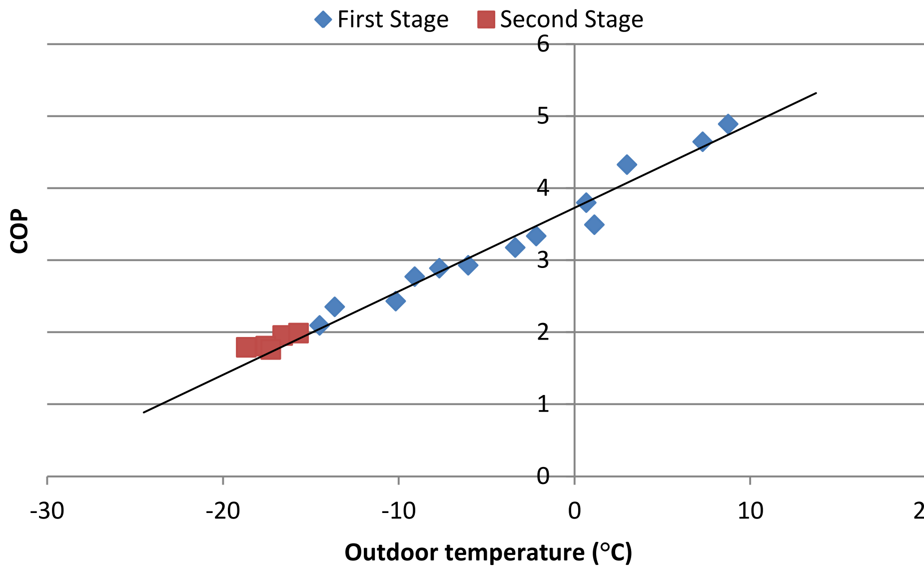

Figure 49 ASHP Heating COP (Dec 1, 2010 – Feb 9, 2011)

5.14 Air Source Heat Pump Daily Heating/Electricity Consumption

The daily heating output and electricity consumption of the ASHP were measured from test period December 24th to January 12, 2011. Figure 50 illustrates this relationship, suggesting that a peak daily heating output of 125 kWh and a peak electricity consumption of 50.3 kWh occurs on day 18th (January 10th, 2011). The cumulative heating output and electricity consumption are also given in Figure 51. Figure 51 illustrates that at the end of the 20 day test period, the heating output and electricity consumptions were 1832 kWh and 645 kWh respectively. This results in a test period COP of 2.84.

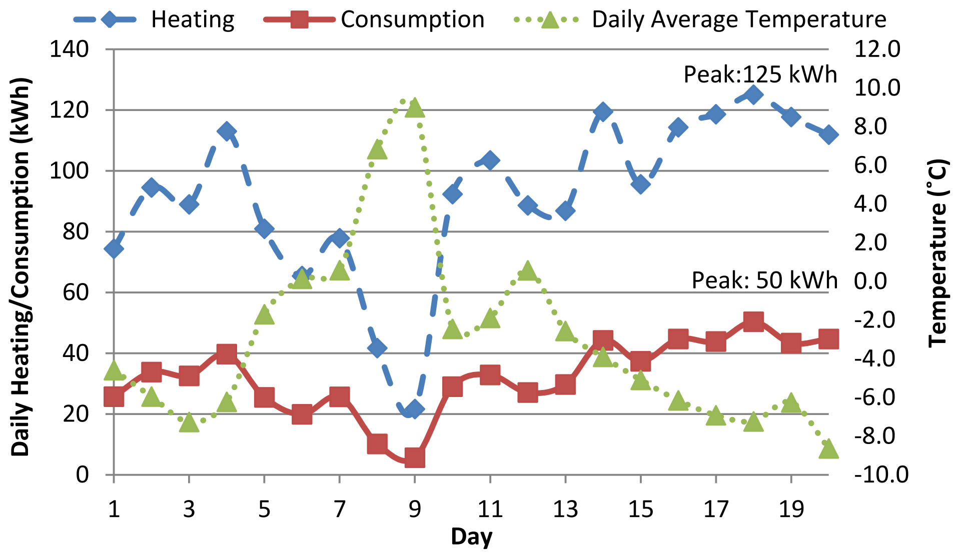

Figure 50 Daily Heating/Consumption (Dec 24 – Jan 12, 2011)

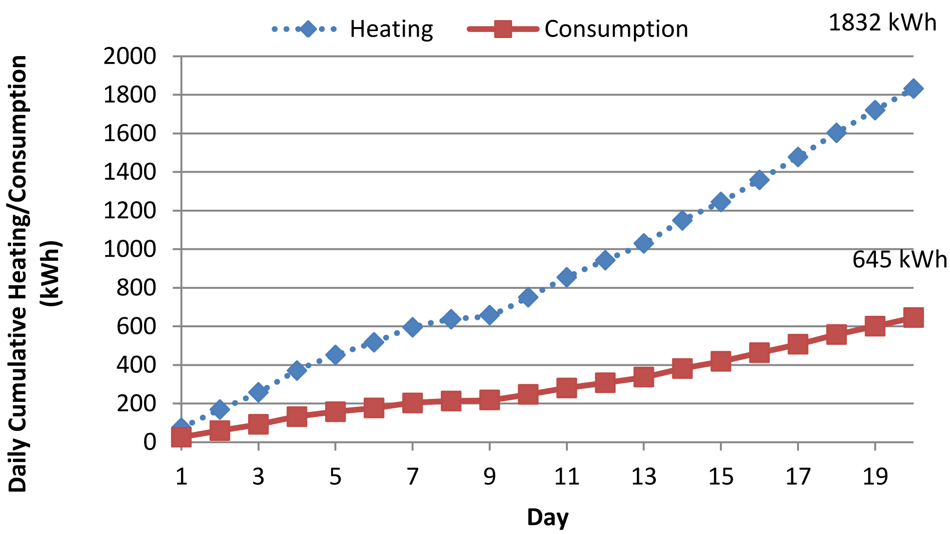

Figure 51 Daily Cumulative Heating/Consumption (Dec 24 - Jan 12, 2011)

Figure 52 illustrates the relationship between the daily heating output/electricity consumption with respect to the average daily outdoor temperature. As expected, both heating output and electricity consumption rise as the average ambient temperature drop. This heating curve is later used to validate the House A model created in TRNSYS as well as to extrapolate the seasonal performance of the heat pump.

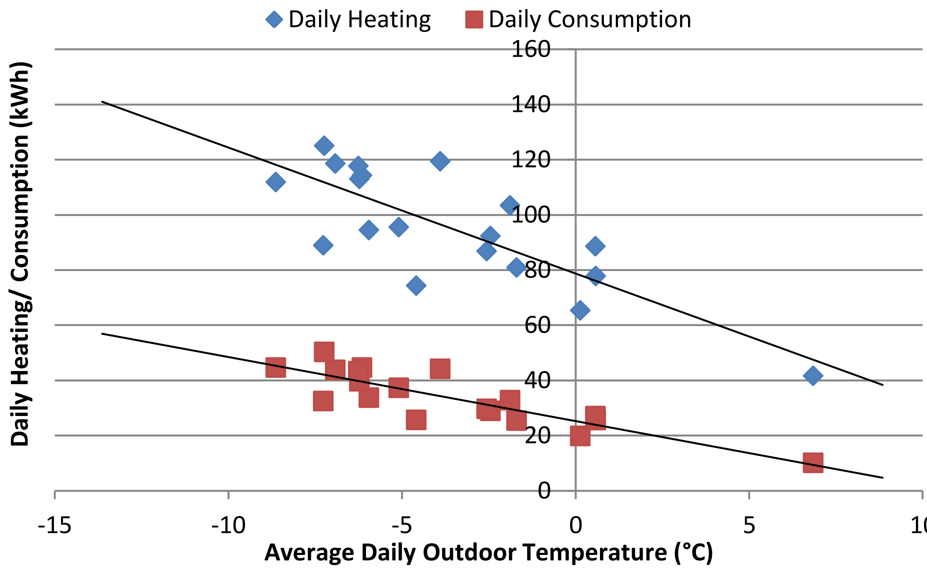

Figure 52 Daily Electricity Consumption Vs Average Daily Outdoor Temperature (Dec 24 – Jan 12, 2011)

5.15 ASHP Part Load Performance

A heating part load curve was developed using the same principles as for the cooling part load curve. Unlike the cooling season, the heat pump utilized both the first stage and the second stage compressor in sustaining the indoor set-point temperature. This variation in heating capacity allowed for a better understanding of the experimental part load performance. Figure 53 illustrates the heating part load performance of the ASHP. Unlike in cooling mode where the capacity only ranged from 52 % to 57 % of the rated capacity, in heating mode the capacity ranged from 54% to 103 % of the rated capacity. This figure clearly illustrates the change from single compression operation to two-stage operation. During the test period, the single compressor operation was from 52% to 66 % capacity ratio. During the second stage, the capacity ratio ranged from 92% to 103%. In this case, the heat pump did not operate between the two stages at 67% – 91 % of the rated capacity.

The experimental COP ratio curve in Figure 53 illustrates that at 54% of the rated capacity, the heat pump COP is 40% higher than the rated capacity, while the experimental input ratio curve in Figure 53 suggests that at 54% of the rated capacity the ASHP will only require 40% of the rated power. Similarly at 103 % of the rated capacity, the heat pump COP ratio and input ratio are close to that of the rated capacity.

If a single speed air source heat pump system was used instead, the compressor would often cycle on and off to meet the part loads when the heat pump was operating at the single stage. Unlike the cooling part load curve, a manufacturer curve was not provided to compare with the experimental results.

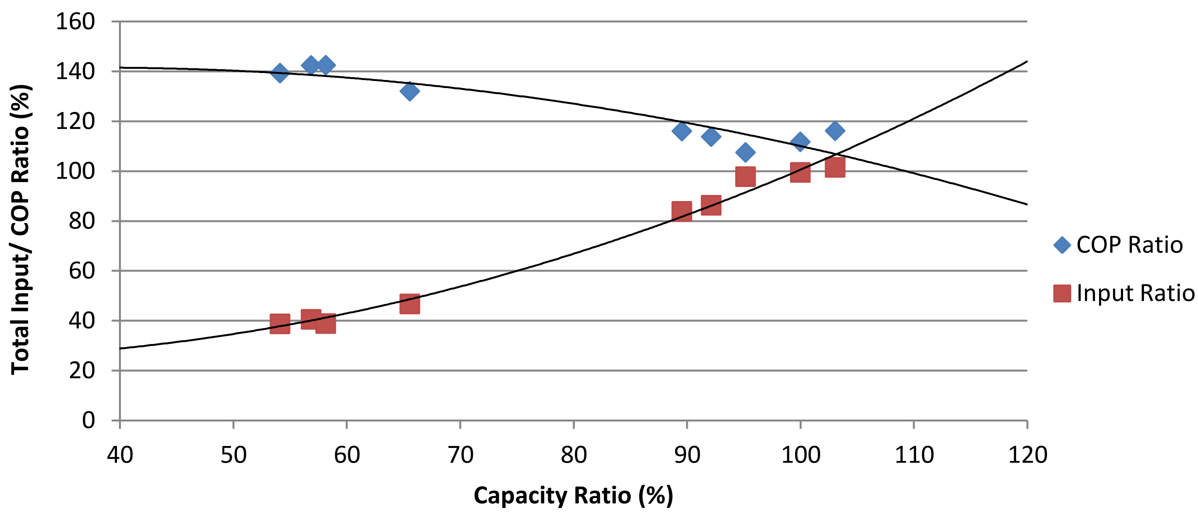

Figure 53 ASHP Experimental Part Load Heating Performance

5.16 Ground Source Heat Pump with Desuperheater (Dec 1 – Dec 19, 2010)

The performance of the GSHP was investigated with the desuperheater system in operation. The test period took place from December 1 to December 19, 2010. In heating mode, the desuperheater draws a portion of the hot water produced from the heat pump and delivers it to the domestic hot water tank. The GSHP heating output, electricity draw, and COP with respect to entering ground loop temperature is illustrated in Figures 54, 55, and 56 respectively. The heating output includes both the heating for space heating and domestic hot water heating through the desuperheater. Similarly, the electricity consumption includes the ground loop pump and compressor, along with the desuperheater pump used to deliver hot water to the domestic hot water tank. During the test period, the ground loop return temperature ranged from around 2˚C to 5˚C. The heating output shown in Figure 54 ranged from 13.5 to 14.25 kW. Figure 55 illustrates the electricity draw ranging from 4.30 to 4.37 kW. The COP curve is shown in Figure 56, ranging from 3.1 to 3.31.

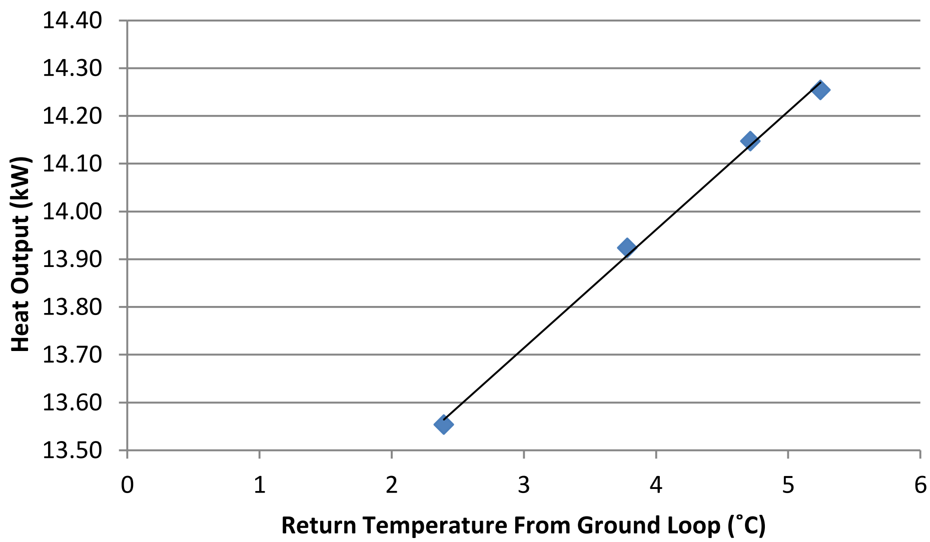

Figure 54 GSHP with Desuperheater heating output (Dec 1 - Dec 19, 2010)

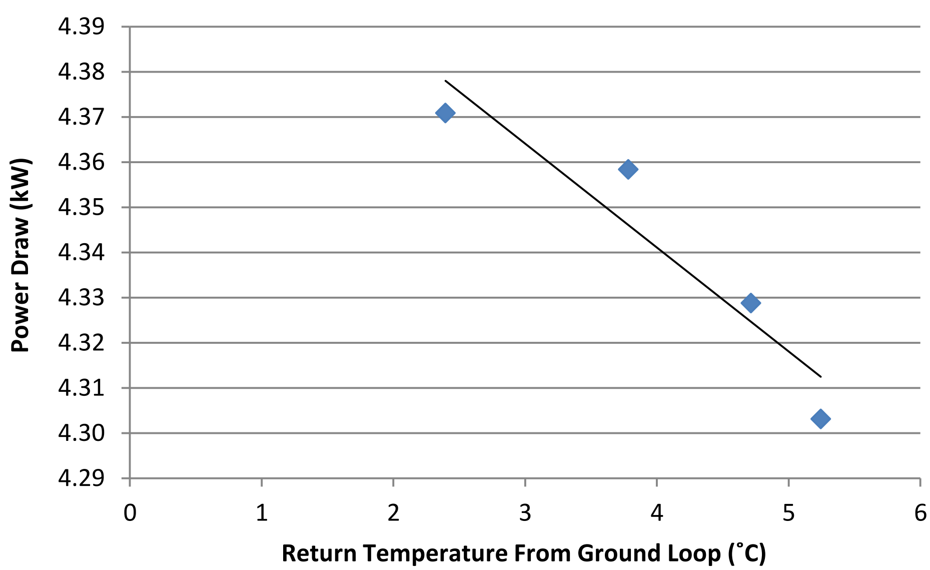

Figure 55 GSHP with Desuperheater Power Draw (Dec 1 - Dec 19, 2010)

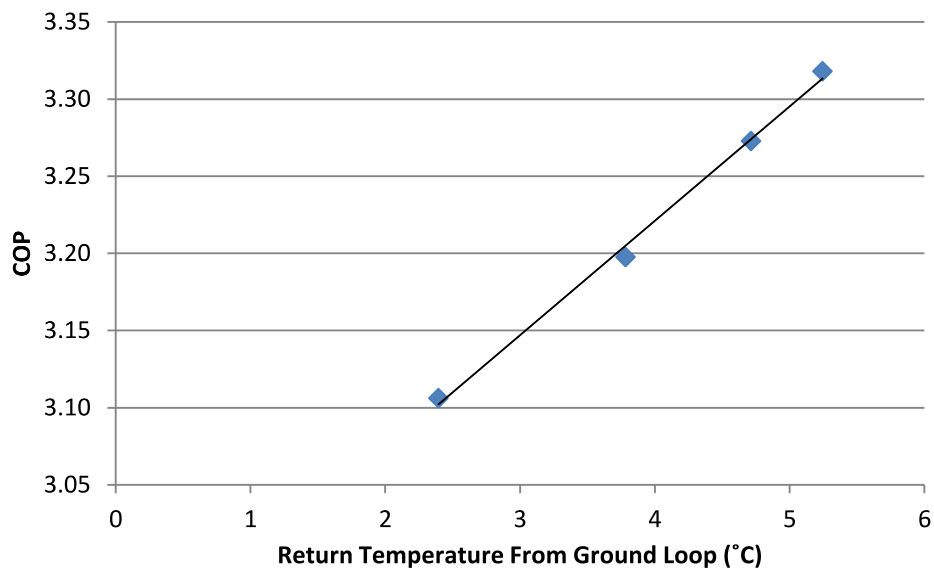

Figure 56 GSHP with Desuperheater COP (Dec 1- Dec 19, 2010)

A better indication of heat pump performance is the graph shown in Figure 57, depicting the COP at various entering source and load temperatures. The GSHP COP is affected by both the entering source temperature (temperature entering the heat pump from the ground loop) and also the entering load temperature (temperature of the fluid entering the heat pump from the buffer tank). Figure 57 illustrates that as the entering load temperature decreases and the entering source temperature increases, the COP increases. As expected, the lower the difference between source and load temperature, the higher the COP.

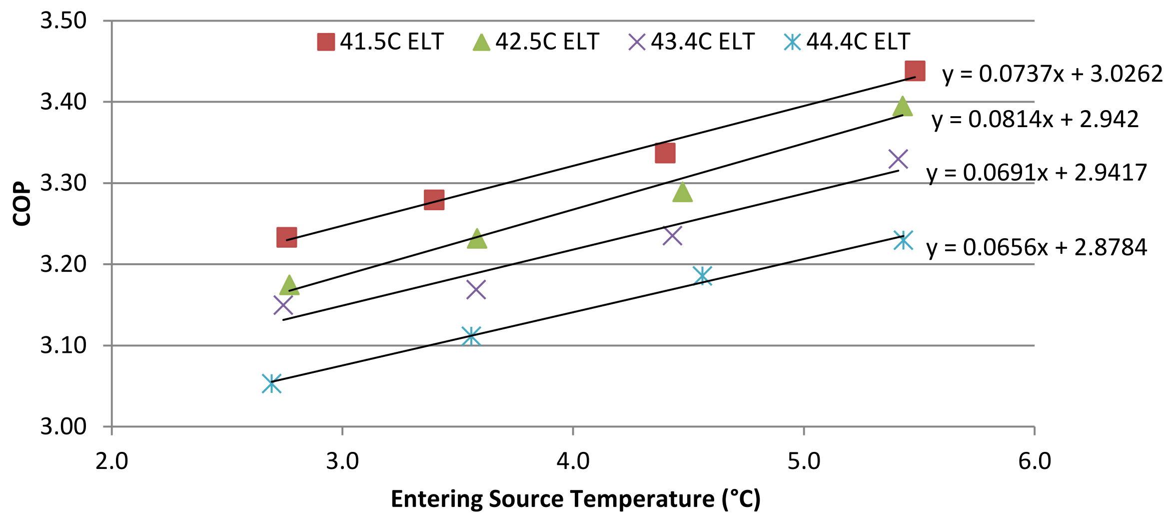

Figure 57 GSHP COP with desuperheater (Dec 1 - Dec 19, 2010)

5.17 Ground Source Heat Pump Daily Heating/Electricity Consumption

The daily heating output and daily electricity consumption during the 19 day test period is shown in Figure 58. The amount of heating for both space heating and domestic hot water is also shown in this figure. The daily space heating ranged from a minimum of 70.9 kWh to a maximum of 148.8 kWh, while the daily desuperheater heating ranged from a minimum of 8.2 kWh to a maximum of 12.4 kWh. Figure 59 illustrates the daily cumulative space heating, electricity consumption, and desuperheater heating. At the end of the test period, the total space heating, electricity consumption, and desuperheater heating were 2069 kWh, 732 kWh, and 194 kWh respectively. During the test period, the portion of total heating transferred for domestic hot water is 8.6 %. To obtain the overall COP during the test period, the total heating (space heating + desuperheater heating) is divided by the total electricity consumption (compressor + ground loop pump + desuperheater pump). The test period COP therefore turned out to be 3.09.

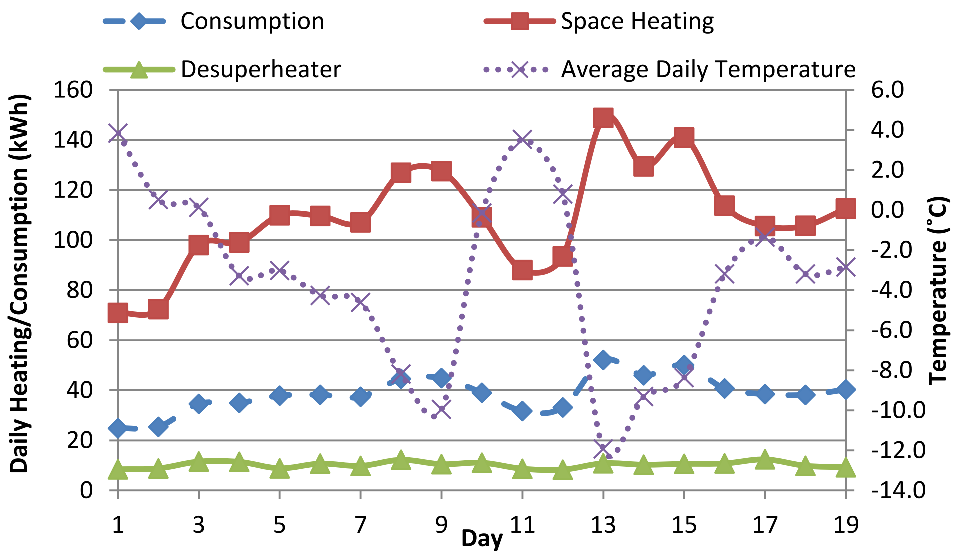

Figure 58 GSHP Daily Heating/Consumption with Desuperheater (Dec 1- Dec 19, 2010)

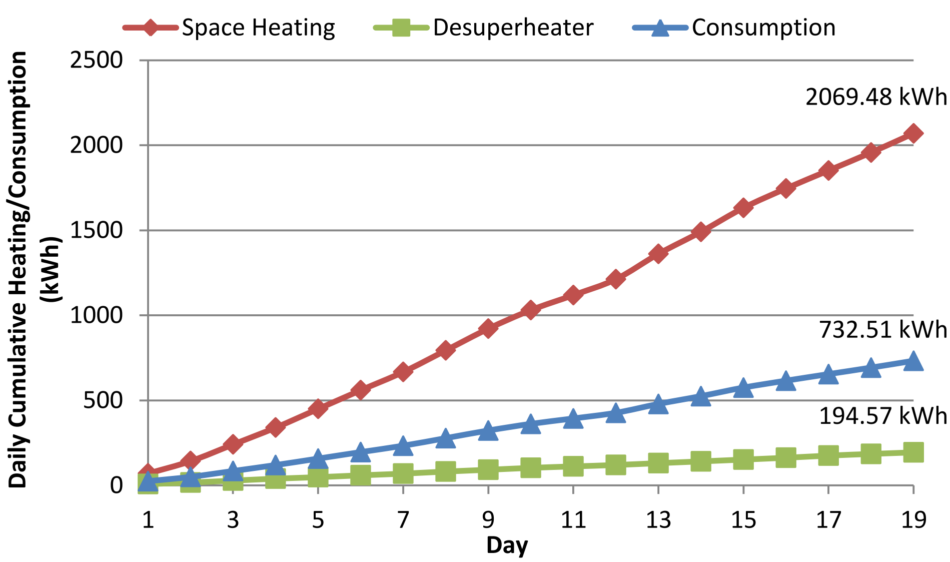

Figure 59 GSHP Daily Cumulative heating/Consumption with Desuperheater (Dec 1 -Dec 19, 2010)

The daily heating and electricity consumption of the GSHP (including the desuperheater) with respect to the average daily outdoor temperature is given in Figure 60. The daily energy extraction from the ground is given in Figure 61 depicting the amount of heat taken out during the test period of Dec 1 – Dec 19, 2010. The daily heat extraction ranged from 53 kWh – 106 kWh.

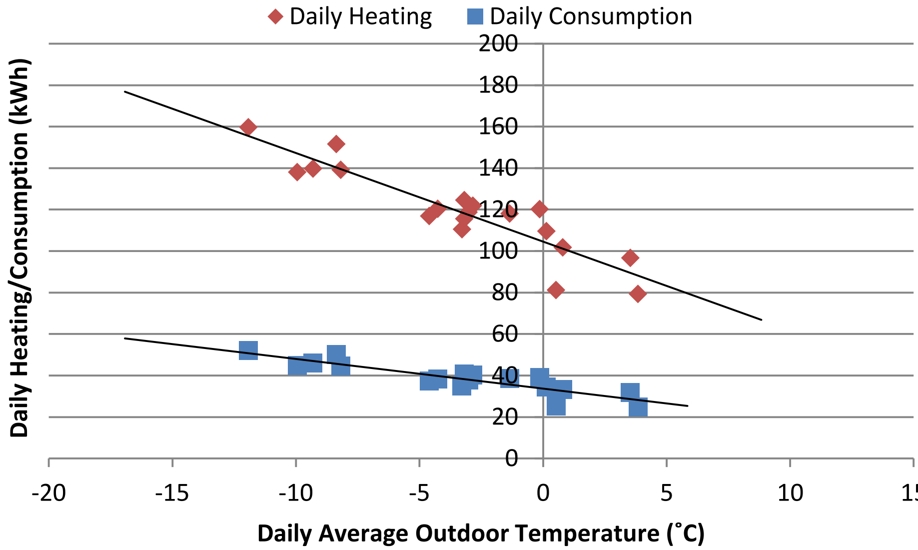

Figure 60 GSHP Daily Space Heating/Consumption vs Daily Average Outdoor Temperature (Dec 1 - Dec 19, 2010)

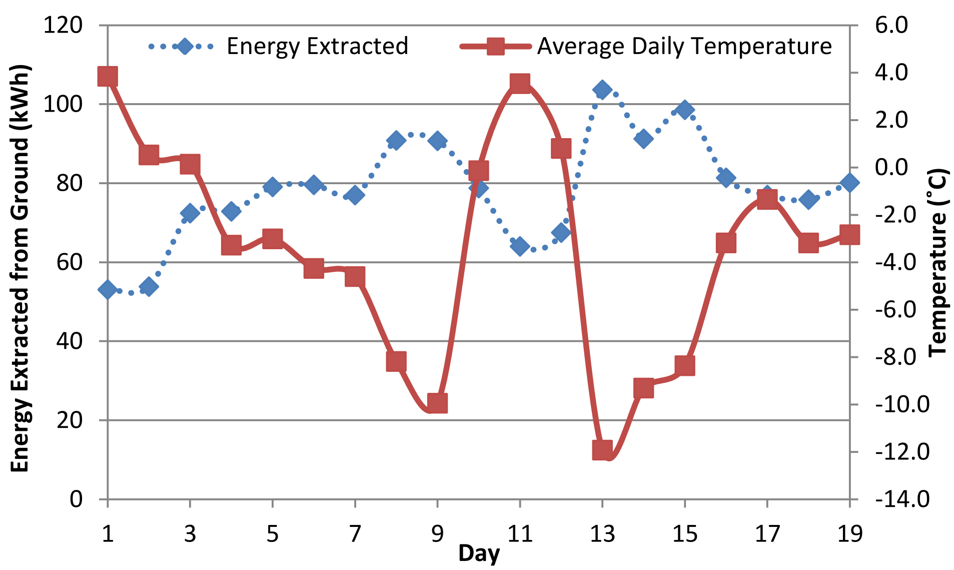

Figure 61 Energy Extraction from Ground (Dec 1 - Dec 19, 2010)

5.18 Ground Source Heat Pump without Desuperheater: (Jan 27 – Feb 17, 2011)

The performance of the GSHP was investigated without the desuperheater from the test period of January 27 – February 17, 2011. The GSHP heating output, electricity draw, and COP with respect to entering ground loop temperature is illustrated in Figures 62, 63, and 64, respectively. During the test period, the desuperheater was not in operation, thus all heating output was delivered for space heating. Consequently, the electricity consumption includes the ground loop pump and compressor only. During the test period, the ground loop return temperature ranged from -3˚C to 0˚C. The heating output shown in Figure 62 ranged from 12.52 kW to 12.62 kW. Figure 63 illustrates the electricity draw ranging from 4.15 kW to 4.35 kW. The resulting COP curve is shown in Figure 64, ranging from 2.9 to 3.01

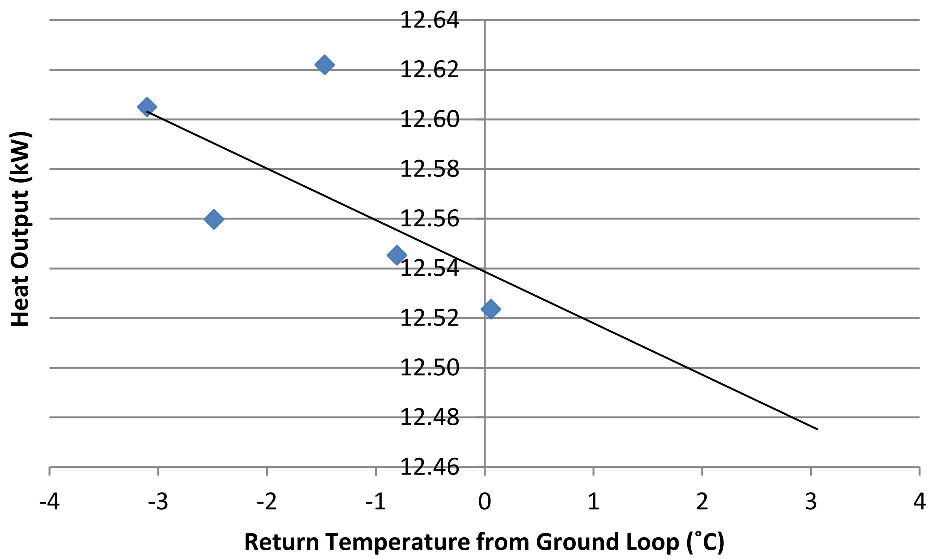

Figure 62 GSHP without desuperheater heating output (Jan 27 – Feb 17, 2011)

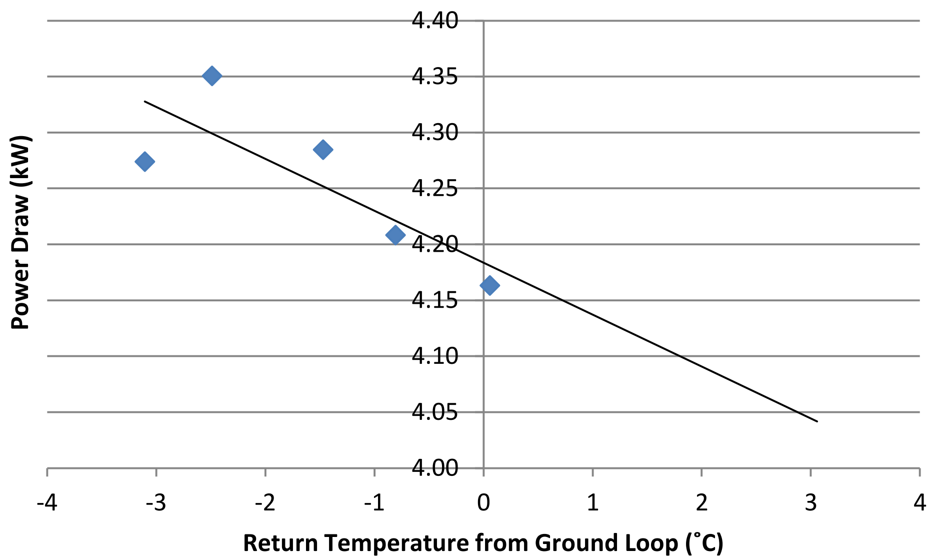

Figure 63 GSHP without desuperheater power draw (Jan 27 – Feb 17, 2011)

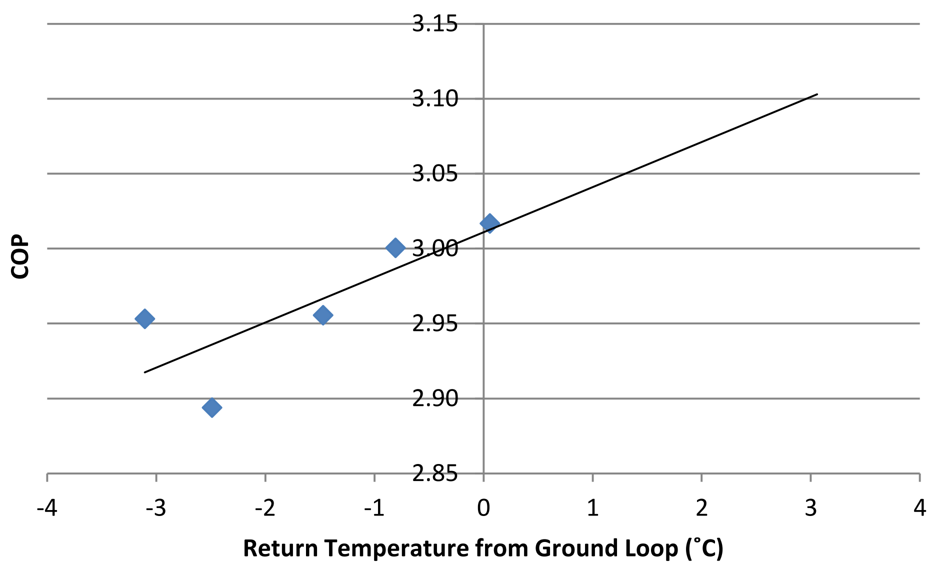

Figure 64 GSHP without desuperheater COP (Jan 27 - Feb 17, 2011)

The detailed heat pump performance is shown in Figure 65, depicting the COP at various entering source and load temperatures. Similar to the test done with the desuperheater, this figure illustrates that as the entering load temperature decreases and the entering source temperature increases, the COP increases. As expected, the smaller the difference between source and load temperature, the higher the COP. Figure 65 is later used for a TRNSYS GSHP performance curve.

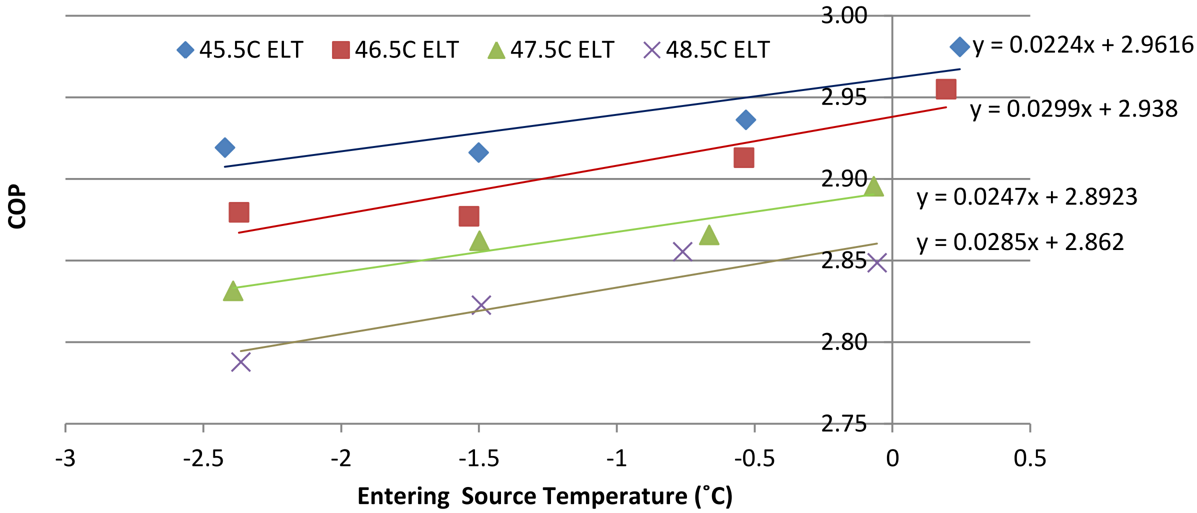

Figure 65 COP without Desuperheater (Jan 27 – Feb 17, 2011)

5.19 Ground Source Heat Pump Daily Heating/Electricity Consumption

The daily heating output and electricity consumption during the test period is shown below in Figures 66 and 67. The daily space heating ranges from a minimum of 59 kWh to a maximum of 179 kWh while the electricity consumption ranges from minimum of 21.2 kWh to a maximum 59.46 kWh. Figure 67 illustrates the daily cumulative space heating and electricity consumption. At the end of the test period, the total space heating and electricity consumption were 2767 kWh and 951 kWh respectively. The test period COP was therefore calculated to be 2.9.

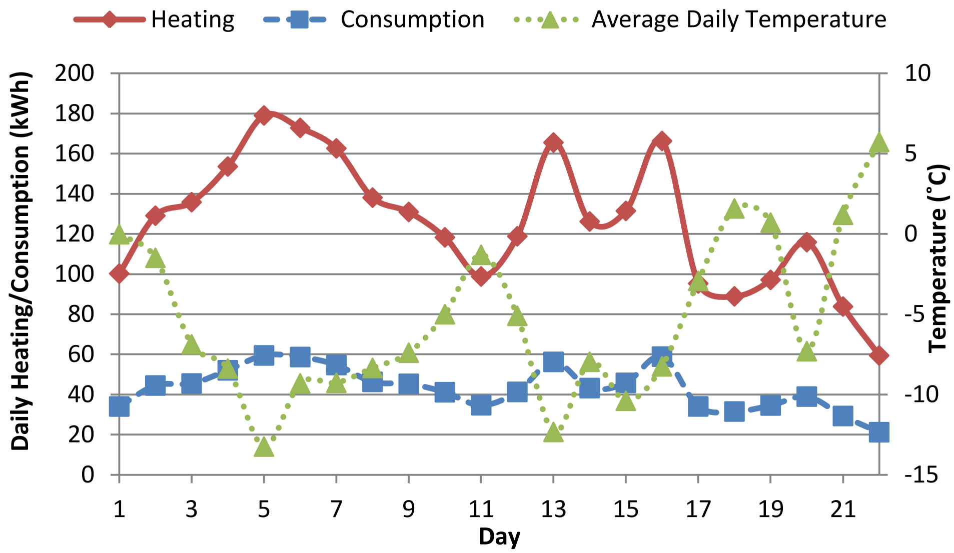

Figure 66 GSHP Daily Heating/Consumption without Desuperheater (Jan 27- Feb 17, 2011)

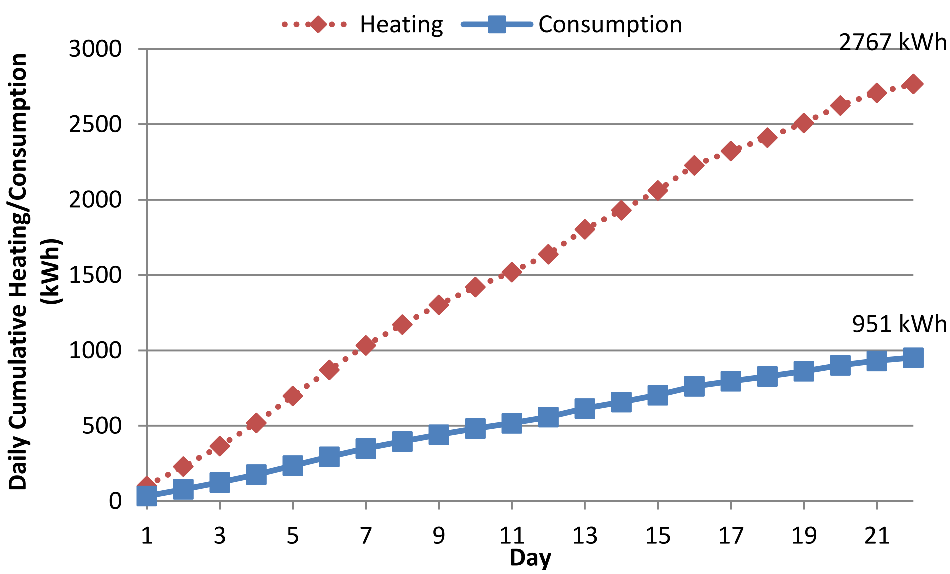

Figure 67 GSHP Daily Cumulative Heating/Consumption without Desuperheater (Jan 27 – Feb 17, 2011)

The daily heating and electricity consumption with respect to the average daily outdoor temperature is given in Figure 68. This Figure is later used to validate the House B model created in TRNSYS 16. The daily energy extraction from the ground is given in Figure 69 depicting the amount of heat taken out during the test period of Jan 27 – Feb 17, 2011. The daily heat extraction ranged from 38 kWh to 103.2 kWh.

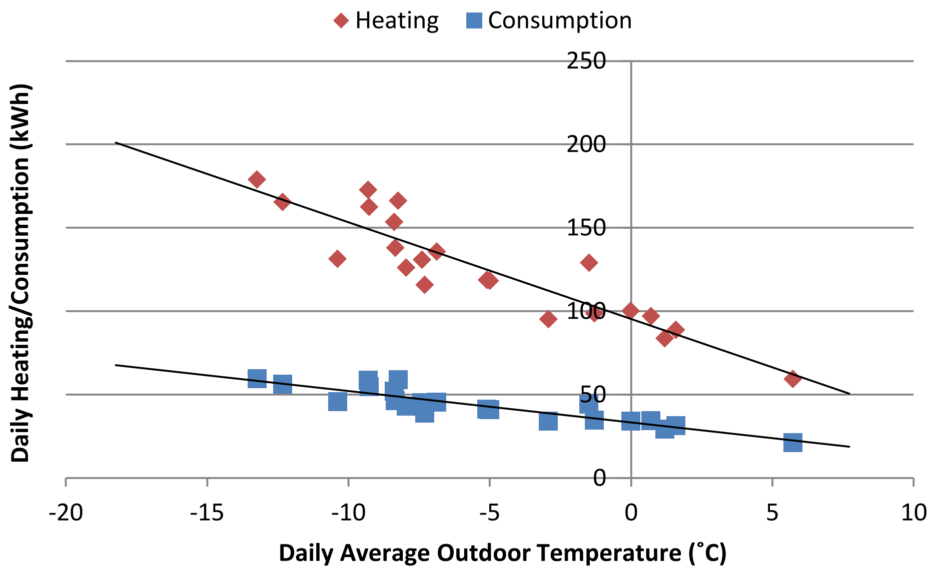

Figure 68 GSHP Daily Space Heating/Consumption vs Daily Average Outdoor Temperature

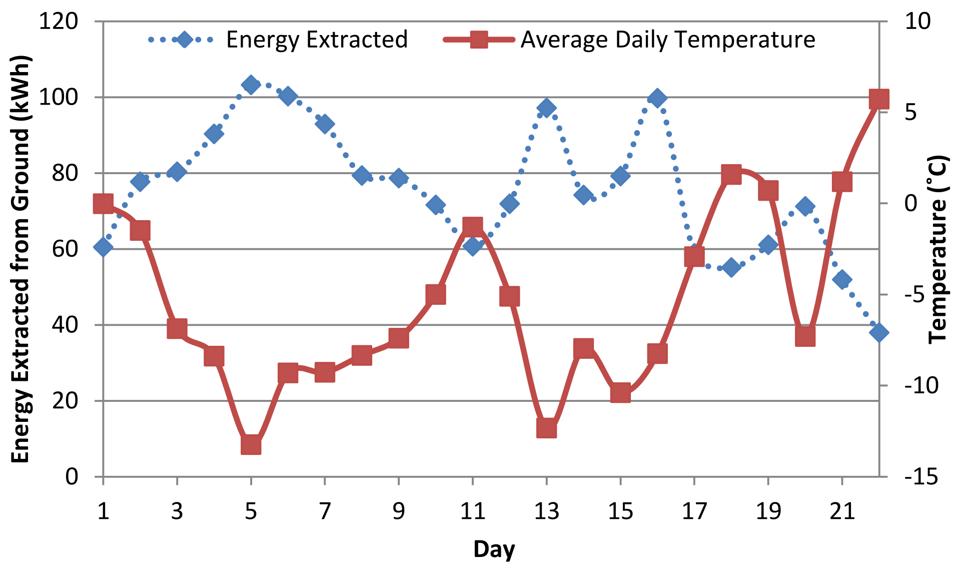

Figure 69 Energy Extraction from ground (Jan 27 - Feb 17, 2011)

5.20 Summary of Heating Test Period

The summary of the heating test period is given in Table 19. The three systems tested were the ASHP, the GSHP with the desuperheater, and the GSHP without the desuperheater. The ASHP was tested on December 24 – Jan 12, 2011, the GSHP with desuperheater was tested on December 1 – December 19, 2010, and the GSHP without desuperheater was tested on January

27 – Feb 17, 2011. The ASHP performance during this test period suggested that the heat pump was able to meet the temperature set-point in an efficient manner having a minimum COP of 1.79 at -19˚C. The variable capacity was clearly demonstrated having an output between 54 and 103 % rated capacity. As well, the performance indicated efficient heat pump operation having a test period COP of 2.84, slightly lower than the GSHP COP's. However it is also noted that below -24˚C, supplementary heating should be considered because the COP would drop below 1. The GSHP was first tested with the desuperheater in operation. It was expected that the desuperheater would not alter the performance of the heat pump, however will take away some heat to the domestic hot water tank. During the test period, the return temperature from the ground loop ranged from 2 to 5˚C and the COP ranged from 3.05 to 3.44 based on entering load temperature. It was noted that over the duration of the test period, the desuperheater delivered 8.6 % of the total heating to the domestic hot water tank. The performance of the heat pump was slightly better than the ASHP, having a test period COP of 3.09. It was also noted that the heat pump extracted between 53kWh and 103 kWh of heat per day from the ground. The GSHP was also tested without the desuperheater. The test period began nearly 2 months after the first GSHP test. It was clearly noted that the return temperature from the ground was significantly lower than the first test period. The return temperature from the ground loop ranged from -3 to 0˚C and as a result the COP was lower than the first GSHP test with the desuperheater. The COP ranged from 2.78 to 2.98. The test period COP was slightly lower than the GSHP with the desuperheater at 2.9. It can be concluded that the ground temperature around the loop was higher during the first test period in December than the second test period during the later winter months. This reduction in ground temperature after several months of heat pump operation lowers the GSHP efficiency. As a result, studies have looked at combining solar collectors with GSHP's to recharge the ground loop during the winter months. It can be expected that the ground loop temperature would further reduce as the end of the heating season approaches.

Table 19 Heating Test Period Summary

System	Date Tested	Heating Output (kWh)	Electricity Consumption (kWh)	COP
ASHP	Dec 24 – Jan 12, 2011	1832	645	2.84
GSHP with Desup.	Dec 1 – Dec 19, 2010	2264	732	3.09
GSHP without Desup.	Jan 27 – Feb 17, 2011	2767	951	2.90

5.21 Extrapolated Winter Seasonal Performance

The heating output and electricity consumption with respect to the daily average temperature was used to extrapolate the performance of the heat pumps. Using these curves along with the daily average temperature data of metropolitan Toronto obtained from TRNSYS 16, the typical seasonal performance was obtained. The extrapolation includes the total electricity consumption of the heat pump (compressor + outdoor unit) and the total heating delivered by the heat pump over the entire heating season. The heating season was assumed to begin on October 1st and end on May 21st. In the heating season, the temperature profile of metropolitan Toronto has a daily average minimum temperature of -17˚C on January 12.

5.22 ASHP Heating Extrapolation

The ASHP extrapolated daily electricity consumption and heating output with respect to the daily average outdoor temperature is shown in Figure 70. The maximum daily electricity consumption and heating output occurred on January 12, having a daily electricity consumption of 66.5 kWh and a daily heating output of 160 kWh. Figure 71 illustrates the daily cumulative electricity consumption and heating output of the heat pump with respect to the daily average outdoor temperature. At the end of the heating season the total electricity consumption turned out to be 5325 kWh and the total heating output was 16251 kWh, leading to a seasonal COP of 3.05.

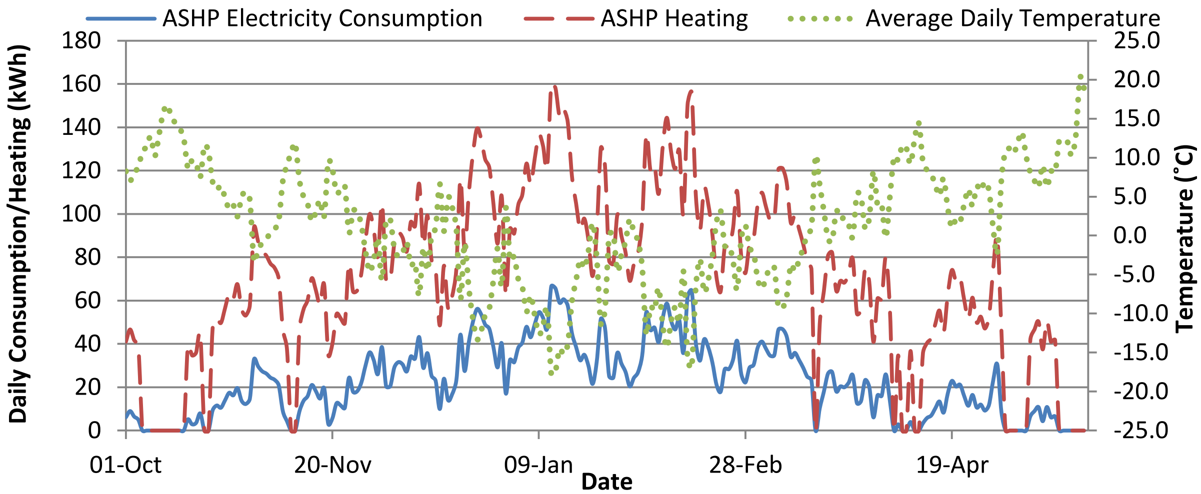

Figure 70 ASHP Daily Consumption/Heating Extrapolation

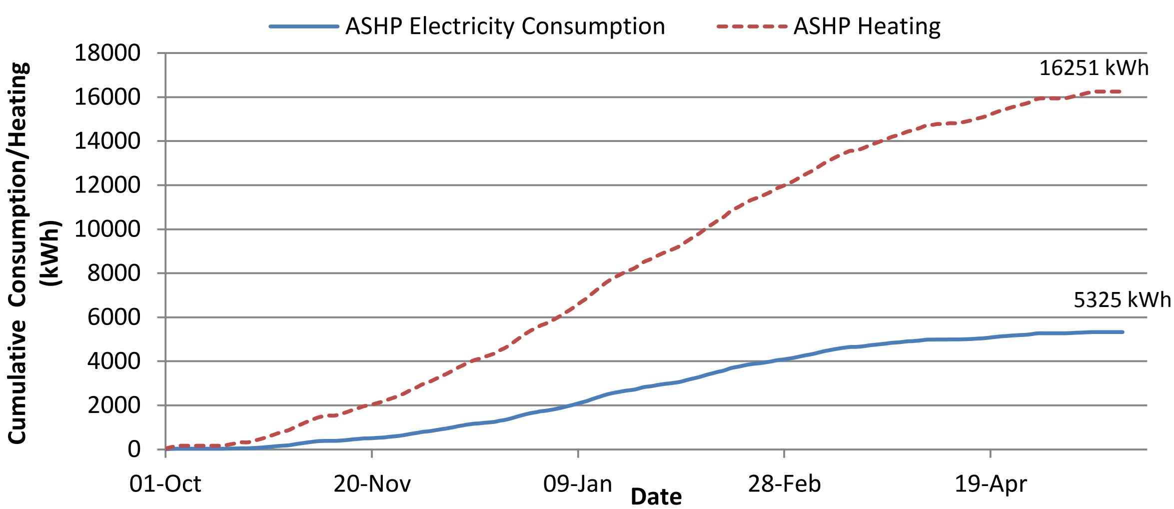

Figure 71 ASHP Daily Cumulative Consumption/Heating Extrapolation

5.23 GSHP with Desuperheater Heating Extrapolation

The GSHP with desuperheater extrapolated results are shown in Figures 72 and 73. Figure 72 illustrates the daily electricity consumption and heating output with respect to the daily average outdoor temperature. In the extrapolation, the maximum daily electricity consumption and heating output occurred on January 12, with a daily electricity consumption of 59.1 kWh and a daily output heating of 180.57 kWh. Figure 73 illustrates the daily cumulative electricity consumption and heating output of the heat pump with respect to the daily average outdoor temperature. At the end of the heating season, the total electricity consumption turned out to be 6879 kWh and the total heating output was 21351 kWh, resulting in a seasonal COP of 3.1.

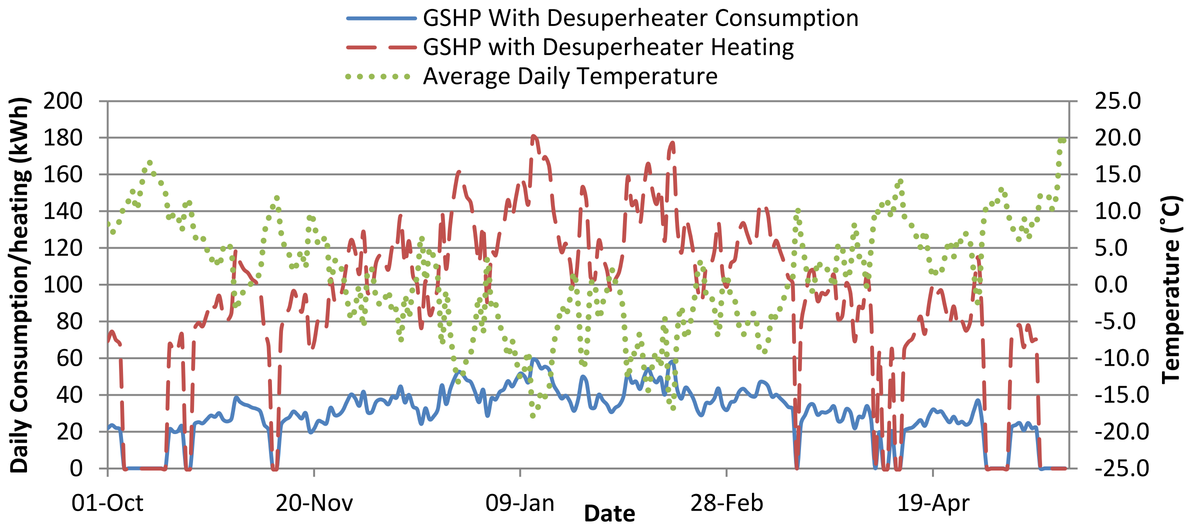

Figure 72 GSHP with Desuperheater Daily Consumption/Heating Extrapolation

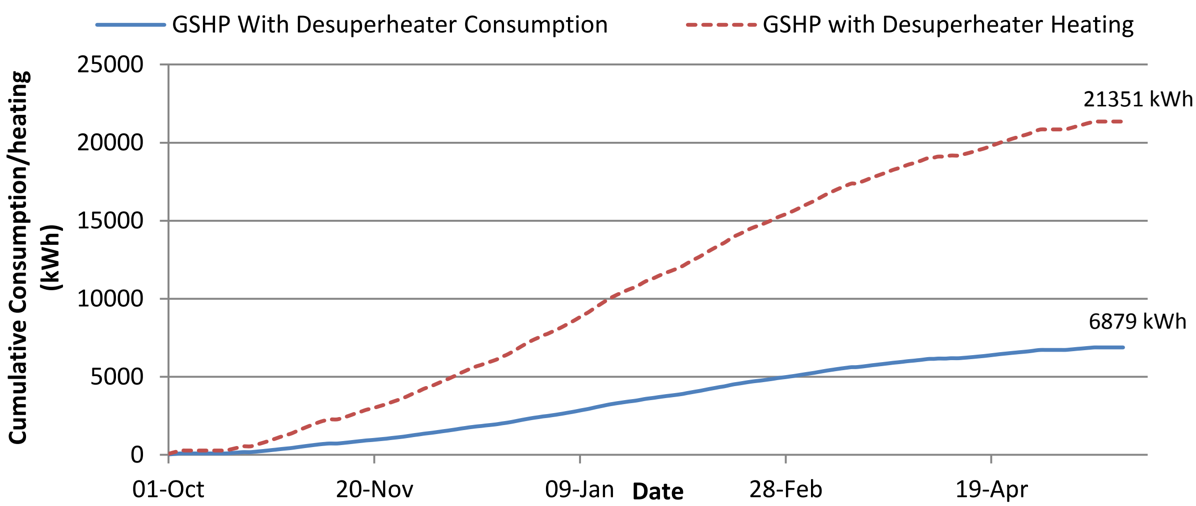

Figure 73 GSHP with Desuperheater Daily Cumulative Consumption/Heating Extrapolation

5.24 GSHP without Desuperheater Heating Extrapolation

The GSHP without desuperheater extrapolated results are shown in Figures 74 and 75. Figure 74 illustrates the daily electricity consumption and heating output with respect to the daily average outdoor temperature. Similar to both the ASHP and the GSHP with desuperheater, the maximum daily electricity consumption and heating output occurred on January 12. On this day, the daily electricity consumption of the heat pump turned out to be 66 kWh and the daily output heating was 198 kWh. Figure 75 illustrates the daily cumulative electricity consumption and heating output of the heat pump with respect to the daily average outdoor temperature. At the end of the heating season the total electricity consumption turned out to be 6875 kWh and the total heating output was 19704 kWh, resulting in a seasonal COP of 2.86.

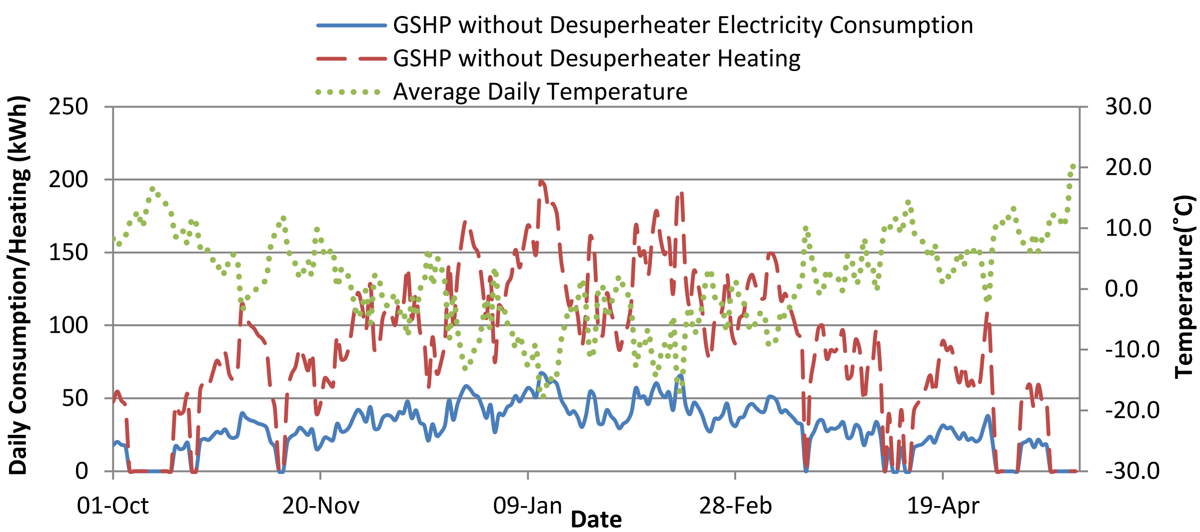

Figure 74 GSHP without Desuperheater Daily Consumption/Heating Extrapolation

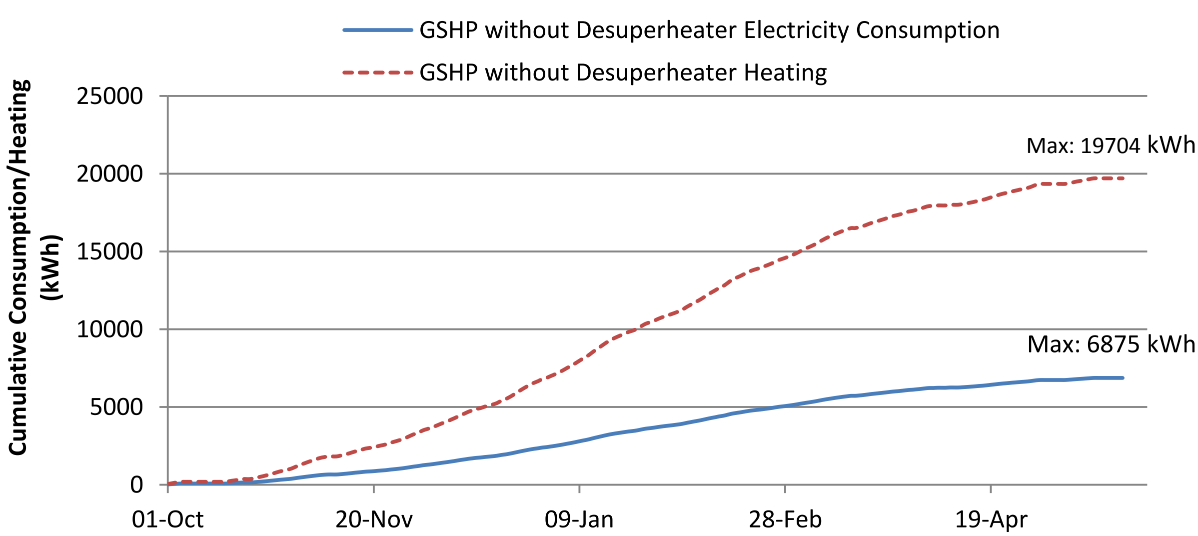

Figure 75 GSHP without Desuperheater Daily Cumulative Consumption/Heating Extrapolation

The summary of the heating season extrapolation is given in Table 20. Over the duration of the heating season, the ASHP performed efficiently with a seasonal electricity consumption of 5325 kWh and a seasonal heating output of 16251 kWh resulting in a COP of 3.05. The GSHP with the desuperheater had a seasonal electricity consumption of 6879 kWh and a seasonal heating output of 21351 kWh. The seasonal COP turned out to be 3.10. The GSHP without the desuperheater had a seasonal electricity consumption of 6875 kWh and a seasonal heating output of 19704 kWh, resulting in a seasonal COP of 2.86. As expected the GSHP with the desuperheater had the largest heating output because the system supplied hot water for both space heating and domestic hot water heating. However the seasonal COP of the GSHP's were lower than expected. Since the GSHP system performance is dependent on the entering source and load temperatures, extrapolating the GSHP performance using the average outdoor temperature is not as accurate as using energy modeling which incorporates source and load temperatures.

Table 20 Summary of Heating Season Extrapolation

	Seasonal Electricity Consumption (kWh)	Seasonal Heating Output (kWh)	Seasonal COP
Air Source Heat Pump	**5325**	**16251**	**3.05**
Ground Source Heat Pump with Desuperheater	**6879**	**21351**	**3.10**
Ground Source Heat Pump without Desuperheater	**6875**	**19704**	**2.86**

Chapter 6

TRNSYS Simulation

TRNSYS is a transient system energy modeling software designed to solve complex energy system problems. The software uses individual components referred as types connected to each other with each representing one part of the overall system. For instance, a house model is one component which can be connected to the ASHP or heat pump component that calculates the amount of heating and cooling provided to the building. Within each component there are inputs, parameters, and outputs that can be linked with the other components. The building model was created using provided information from the twin houses, and the HVAC systems were modeled based on the actual data collected. According to a study on various energy modeling programs (Crarley, Hand, Kummert, & Griffith, 2005), TRNSYS is reasonably powerful in terms of HVAC system modeling. As a result, the program allowed the modeling of specific HVAC system performance.

6.1 House A – Model Validation

The House A model was created using TRNBuild with known building envelope characteristics. The model was then validated with the data collected from monitoring the ASHP. From the results of the data collection, a curve was developed illustrating the daily cooling and heating output of the ASHP with respect to the daily average outdoor temperature. This curve was used to validate the TRNSYS house model by matching the TRNSYS daily cooling and heating demand of House A at various daily average outdoor temperatures with the developed curve from the data. The heating and cooling demand of the TRNSYS House A model was slightly adjusted by altering the shading devices on the house. With a proper shading schedule, the model was validated by matching the cooling and heating output of the ASHP. Figure 76 demonstrates the House A cooling validation where the TRNSYS daily cooling demand of the house at different daily average outdoor temperatures are matched with the daily ASHP cooling output at different daily average outdoor temperatures. Similarly, Figure 77 demonstrates the House A heating validation where the TRNSYS daily heating demand of the house at different daily average outdoor temperatures are matched with the daily ASHP heating output at different daily average outdoor temperatures.

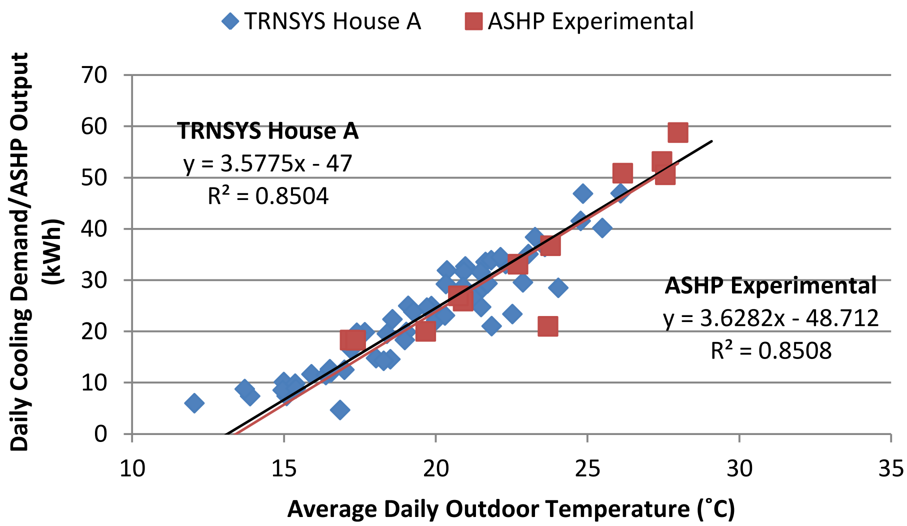

Figure 76 TRNSYS House A Cooling Validation

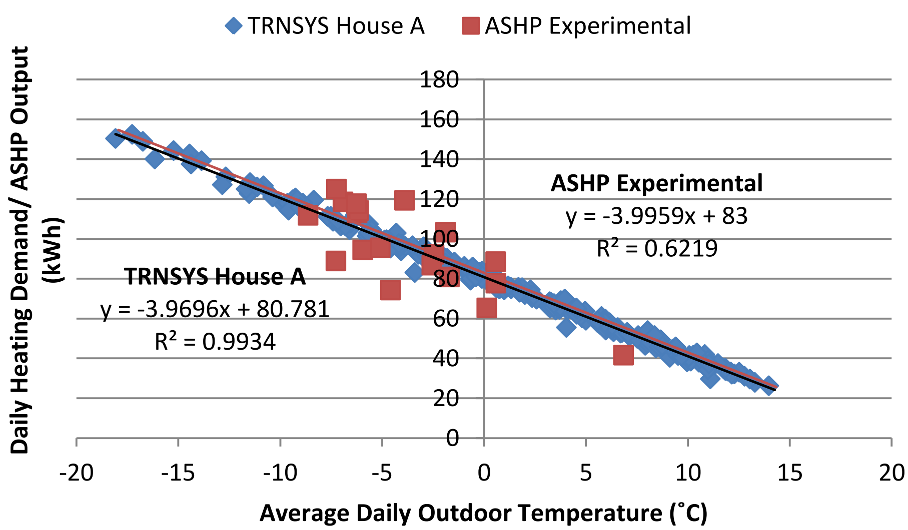

Figure 77 TRNSYS House A Heating Validation

6.2 House A Thermal Demand

The validated House A model was simulated over the yearly period to obtain the annual heating/cooling and peak demand. The weather file used to simulate the thermal demand is the metropolitan Toronto weather given in the TRNSYS library. The cooling season was assumed to begin on May 22 (3408 hour) and end on September 30th (6575 hour) with an indoor set point temperature of 23˚C. The heating season was assumed to begin October 1st (6576 hour) to May 21 (3407 hour) with an indoor set-point temperature of 21˚C. The indoor temperature set points were matched with the data collection experiment. Figure 78 illustrates the TRNSYS cooling/heating demand of House A where the peak heating demand is 6.76 kW and the peak cooling demand is 5.08 kW. Figure 79 demonstrates the cumulative cooling/heating demand of House A where the total cooling demand at the end of the cooling season is 2313 kWh, and the total heating demand at the end of the heating season is 17557 kWh. Figure 80 illustrates the annual outdoor temperature profile of Metropolitan Toronto. The maximum hourly temperature turned out to be 33.9˚C, and the minimum hourly temperature was -22.11˚C. The peak cooling and heating loads were obtained at these maximum and minimum temperatures respectively.

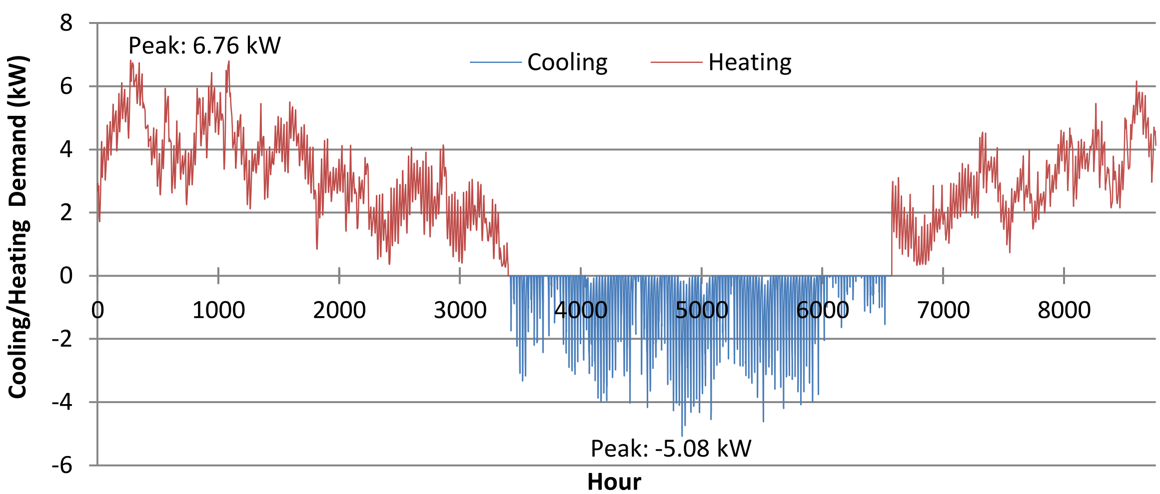

Figure 78 House A Cooling/Heating Demand

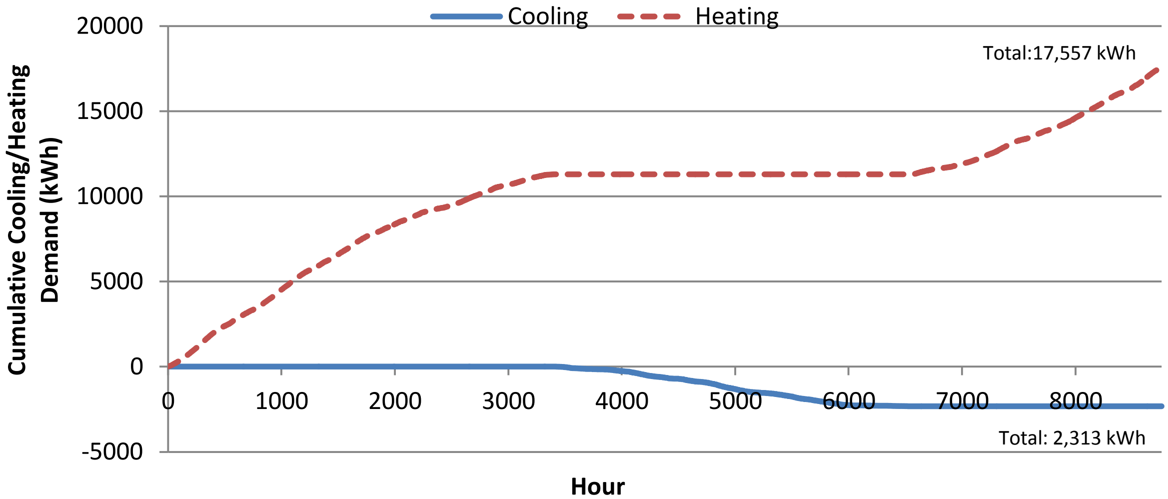

Figure 79 House A Cumulative Cooling/Heating Demand

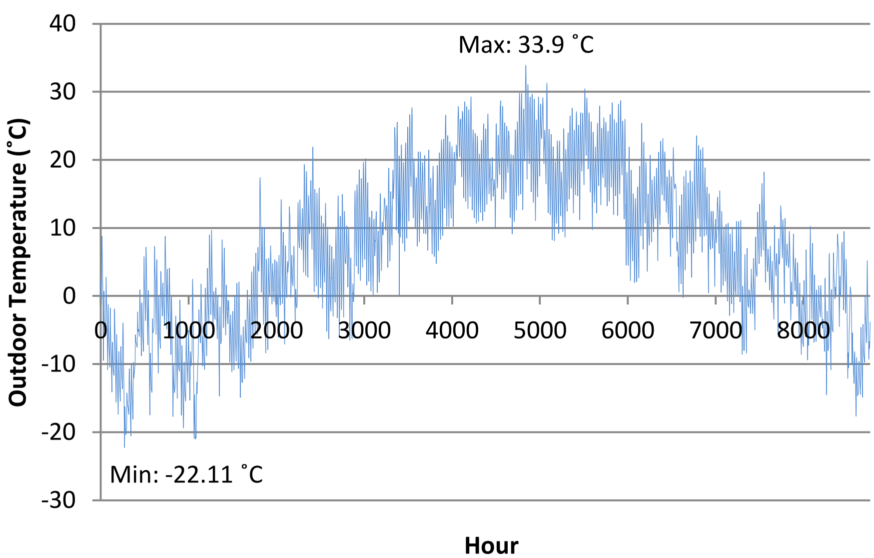

Figure 80 Metropolitan Toronto Outdoor Temperature Profile

6.3 Air Source Heat Pump Model

The ASHP Type 665 module in TRNSYS (Klein, Beckman, Mitchell, Duffie, Duffie, & Freeman, 2006) uses manufacturer's performance data to model a split system heat pump. This model was used with a developed heating and cooling performance curve from the results of the data collection. The heating and cooling was delivered through a direct expansion air handling unit which supplied conditioned air to all floors of the house. Using a schedule, the heating and cooling season was differentiated. Depending on the season, the appropriate performance curve was called up by the ASHP module to determine the thermal output and electricity consumptions at various outdoor temperatures. An optional auxiliary heater can be used with the model in heating mode, however for this model, no supplementary heating was added. The ASHP module is controlled by a room thermostat with a set-point dead band of 1.5˚C which is located on the main floor. For a more accurate simulation, a one minute time step was used. The results of the simulation are given in Figures 81 and 82. Figure 81 illustrates the annual heating and cooling output of the ASHP. During the heating season, the ASHP mainly operated in the single-stage mode providing approximately 6 kW of thermal heating. The ASHP operated in the second-stage at limited periods with a peak thermal heating of 13.17 kW. In cooling mode, the ASHP only operated at the single stage with a peak cooling output of 5.76 kW. Figure 82 illustrates the annual heating and cooling input of the ASHP. In heating mode, the peak electricity draw took place during second stage operation when the outdoor temperature was -22.11˚C. The peak heating electricity draw was 8.30 kW which translates to a COP of 1.58. In cooling mode, the peak electricity draw was 1.05 kW at an outdoor temperature of 33.9˚C. This translates to a COP of 5.48.

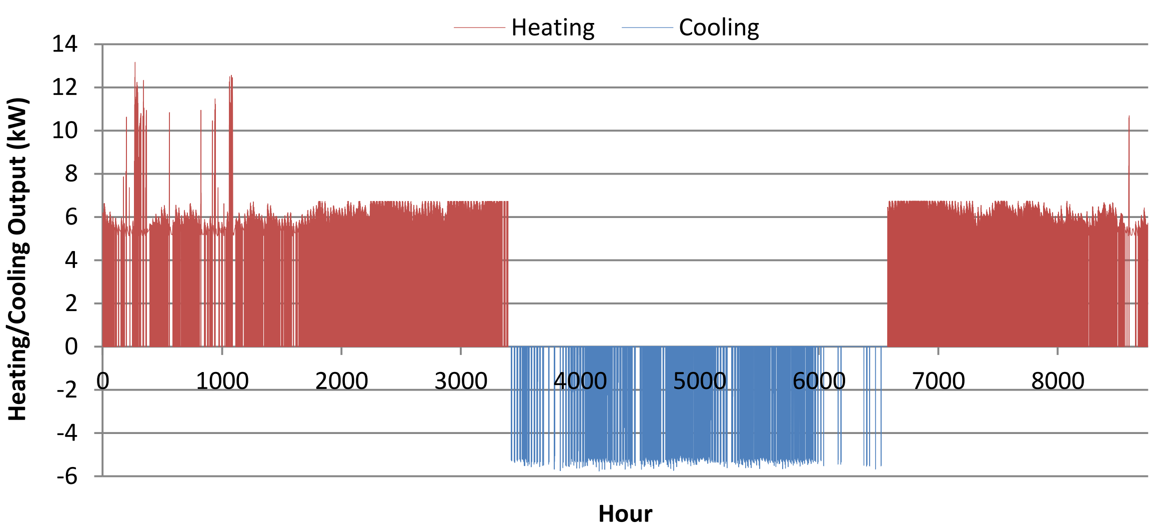

Figure 81 ASHP TRNSYS Heating/Cooling Output

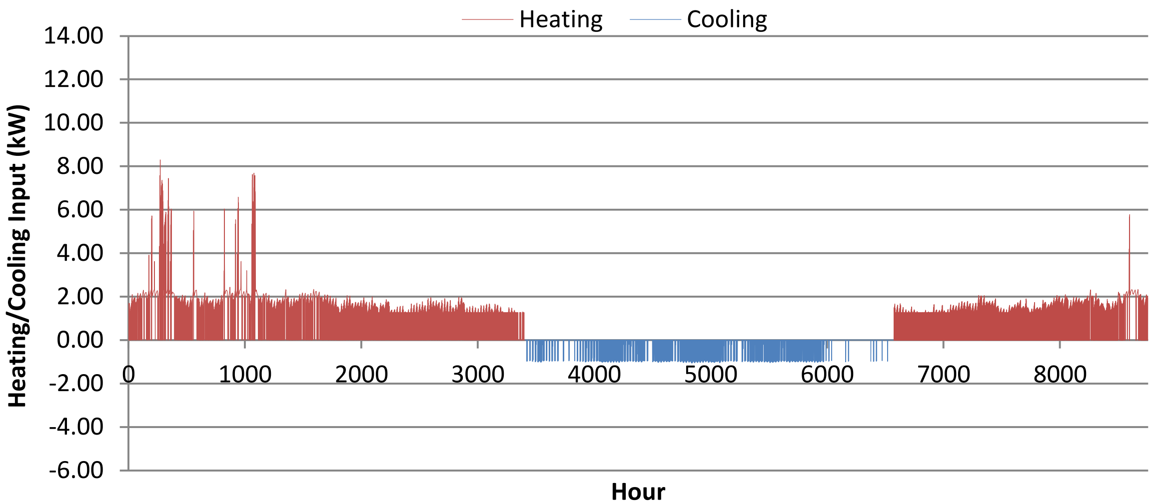

Figure 82 ASHP TRNSYS Heating/Cooling Input

The overall results of the ASHP simulation are given in Table 21. During the heating season, the total heating output was 17,579 kWh, and the total electricity consumption was 5,442 kWh. The heating seasonal COP therefore turned out to be 3.23. In the cooling season, the ASHP provided 2289 kWh of cooling while consuming 434 kWh of electricity. The seasonal cooling COP turned out to be 5.27. When including the indoor fan electricity consumption (without control issues), the resulting seasonal heating and cooling COP's turned out to be 2.1 and 3.5 respectively.

Table 21 ASHP Simulation Results

	Seasonal Output (kWh)	Seasonal Electricity Consumption (kWh)	AHU Fan (kWh)	Seasonal COP (Not Including AHU Fan)	Seasonal COP (Including AHU Fan)
Heating	17,579	5,442	2,753	3.23	2.1
Cooling	2,289	434	219	5.27	3.5

6.4 House B – Model Validation

Similar to House A, the House B TRNSYS model was validated using the output cooling and heating of the GSHP at daily average outdoor temperatures. Figure 83 demonstrates the House B cooling validation where the TRNSYS daily cooling demand of the house at different daily average outdoor temperatures are matched with the experimental daily GSHP cooling output at different daily average outdoor temperatures. Similarly Figure 84 depicts the House B heating validation where the TRNSYS daily heating demand at different daily average outdoor temperatures is matched with the experimental daily GSHP heating output at different outdoor temperatures.

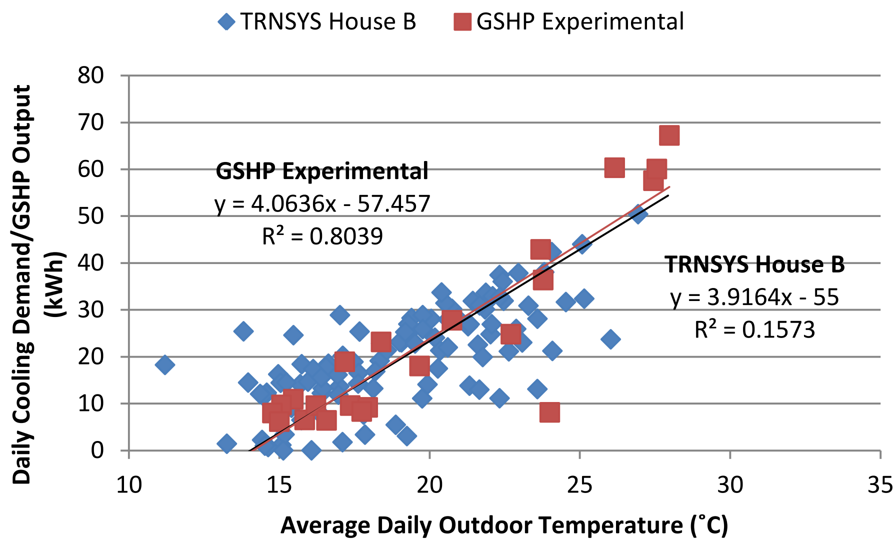

Figure 83 TRNSYS House B Cooling Validation

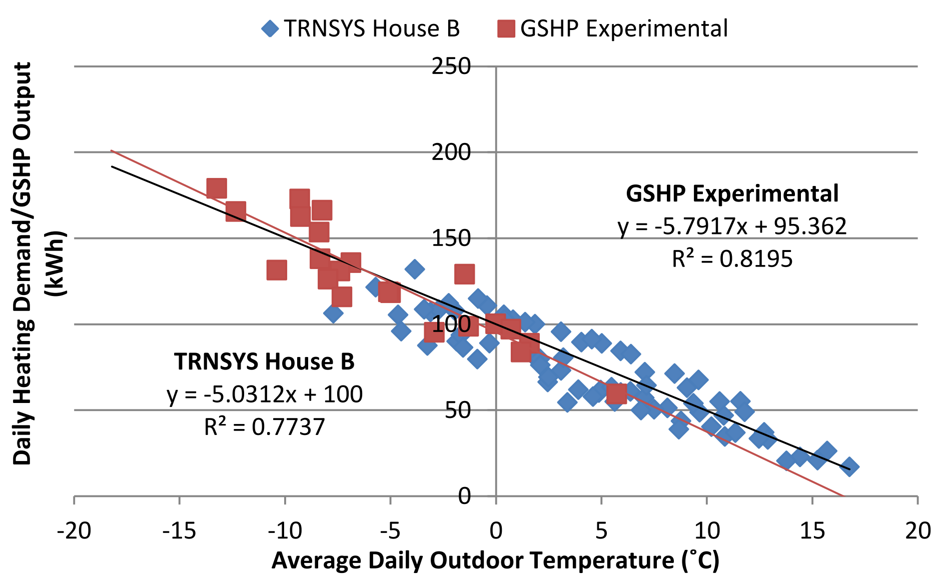

Figure 84 TRNSYS House B Heating Validation

6.5 House B Thermal Demand

The validated House B model was simulated over the entire year to obtain the annual heating/cooling and peak demand. Similar to the ASHP simulation, the weather file used in the energy model is the metropolitan Toronto given in the TRNSYS library. For consistency with the ASHP model, the cooling season was assumed to begin on May 22 (3408 hour) and end on September 30th (6575 hour) with an indoor set-point temperature of 23˚C. The Heating season was assumed to begin October 1st (6576 hour) to May 21(3407 hour) with an indoor set-point temperature of 21˚C. Figure 85 below illustrates the TRNSYS cooling/heating demand of House B where the peak heating demand is 8.02 kW and the peak cooling demand is 4.86 kW. Figure 86 demonstrates the cumulative cooling/heating demand of House B where the total cooling demand at the end of the cooling season is 2440 kWh, and the total heating demand at the end of the season is 18,701 kWh.

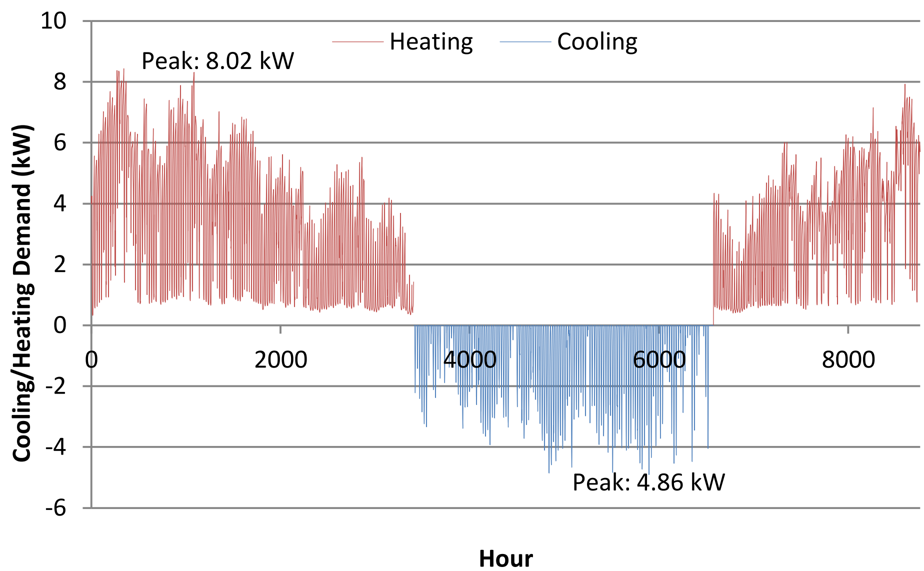

Figure 85 House B Heating/Cooling Demand

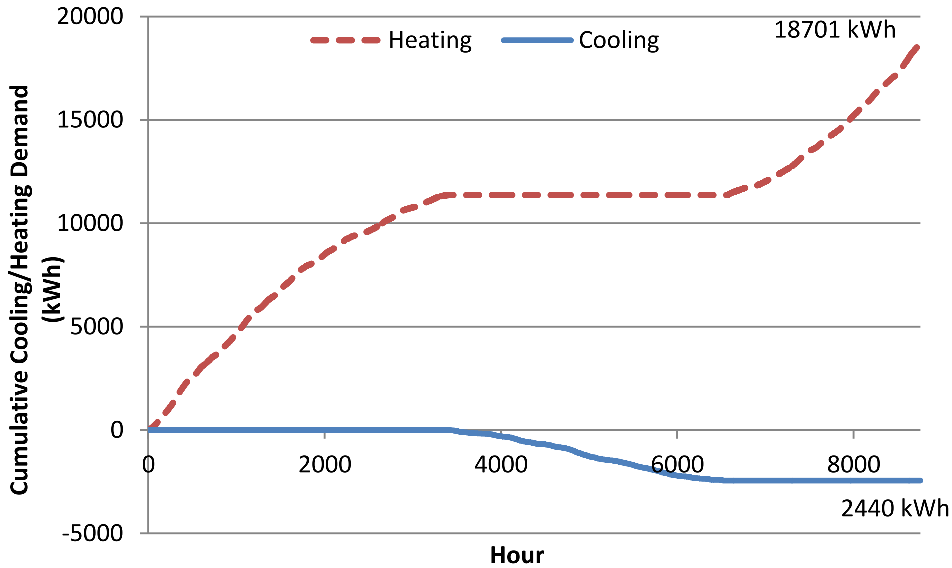

Figure 86 House B Cumulative Heating/Cooling Demand

6.6 Ground Source Heat Pump Model

The GSHP Type 668 module In TRNSYS (Klein, Beckman, Mitchell, Duffie, Duffie, & Freeman, 2006) uses manufacturer's performance data based on entering load and source temperatures. Depending on the season, the program calls up the respective performance curve. The entire system includes a horizontal ground loop heat exchanger, the GSHP, a buffer tank for thermal storage, and either a fan coil AHU or radiant in-floor heating depending on the season. The water temperature in the buffer tank is controlled using a thermostat that is set to call for heating or cooling. The system uses a multi-zone thermostat with a set point dead band of 1.5 ˚C to control the AHU in cooling mode or the in-floor radiant heating system in heating mode. Similar to the ASHP model, the GSHP was simulated using a 1 minute time step. See Appendix D for the GSHP model input parameters. The results of the simulation are given in Figures 87 and 88. Figure 87 illustrates the annual heating and cooling output of the GSHP. During the heating season, the GSHP outputted 12-15 kW of thermal heating depending on the return source temperature. In cooling mode, the system outputted 12-13 kW. Figure 88 illustrates the annual heating and cooling input of the GSHP. In heating mode, the electricity draw was fairly constant around 4.4 kW, and in cooling mode, the electricity consumption was 2.21 to 2.63 kW. The effect of ground temperature can clearly be seen on the output heating and cooling of the heat pump. At the beginning of the heating season (hour 6575) the heating output was 14.65 kW. During mid-winter (hour 0) this heating output decreased to just below 12 kW. This is due to a reduced inlet source temperature from the ground loop. At this point, the ground loop extracts less heat from the soil resulting in a lower heating output. A similar relationship can also be seen during the cooling season. At the beginning of the cooling season, there is a high cooling output and lower electricity consumption. This relationship reverses as the end of the cooling season approaches.

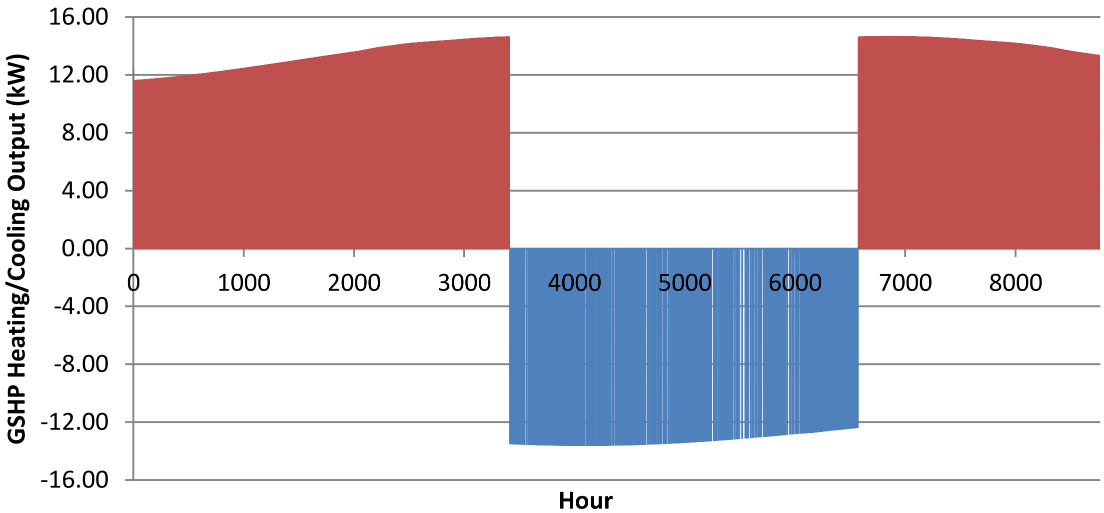

Figure 87 GSHP TRNSYS Heating/Cooling Output

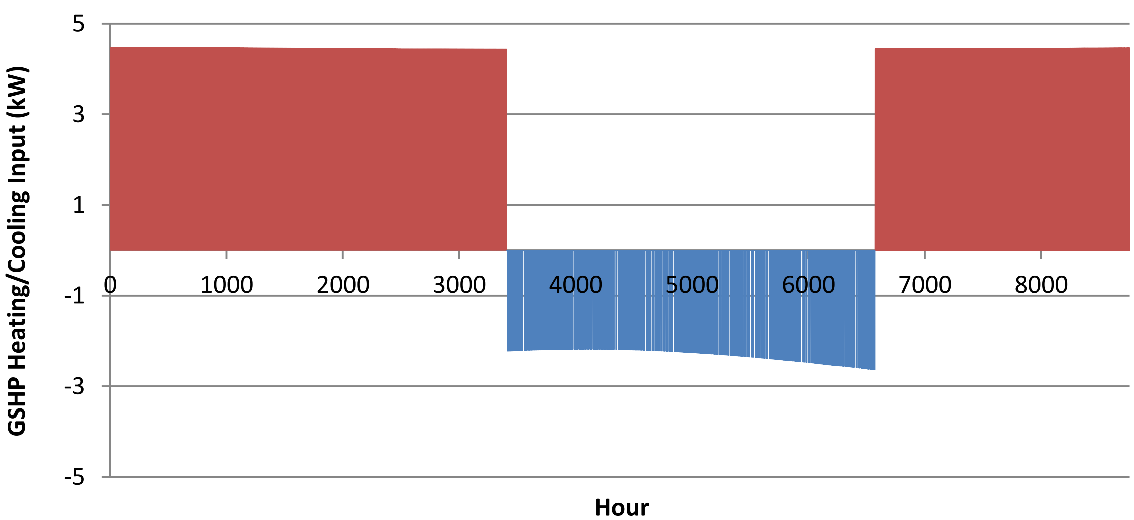

Figure 88 GSHP TRNSYS Heating/Cooling Input

The overall results of the GSHP simulation are given in Table 22. During the heating season, the total heating output was 18,764 kWh, and the total electricity consumption was 5,460 kWh. The heating seasonal COP therefore turned out to be 3.44. In the cooling season, the GSHP provided 2,459 kWh of cooling while consuming 425 kWh of electricity. The seasonal cooling COP turned out to be 5.78. When including the electricity consumption of the pump to buffer tank and pump to in-floor heating, the seasonal heating COP turns out to be 3.14. When including the electricity consumption of the pump to buffer tank, pump to AHU, and the AHU fan, the seasonal cooling COP turns out to be 2.71. In cooling mode, it can be noted that this type of system consumes a significant amount of electricity. The pump to AHU-B is constantly operating due to the multi zone thermostat signal for cooling. This consumption along with the AHU fan consumption significantly lowers the seasonal cooling efficiency. The results of the TRNSYS simulation of both ASHP and GSHP are compared with the results of the ASHP and GSHP data extrapolation in Table 23.

Table 22 GSHP Simulation Results

	Seasonal Output (kWh)	Seasonal Electricity Consumption (kWh) (Compressor & Ground Loop Pump)	Ground Loop Pump (kWh)	Pump to Buffer Tank (kWh)	Pump to Radiant Floors (kWh)	Pump to AHU-B (kWh)	AHU-B (kWh)	Seasonal COP (Not Including Indoor Unit)	Seasonal COP (Including Indoor unit)
Heating	18,764	6,014	844	240	279	-	-	3.12	2.87
Cooling	2,459	425	255	72	-	174	236	5.78	2.71

Table 23 TRNSYS Simulation Vs Data Extrapolation Results

	TRNSYS Heating Output (kWh)	TRNSYS Cooling Output (kWh)	TRNSYS Heating Consumption (kWh)	TRNSYS Cooling Consumption (kWh)	Extrapolated Heating Output (kWh)	Extrapolated Cooling Output (kWh)	Extrapolated Heating Consumption (kWh)	Extrapolated Cooling Consumption (kWh)
ASHP	17,579	2,289	5,442	434	16,251	2,354	5,325	509
GSHP	18,764	2,459	6,014	425	19,704	2,282	6,875	462

6.7 Simulated Heat Pump Performance in Selected Canadian Regions

The developed TRNSYS House models, along with the heat pump model were simulated in four other Canadian regions to obtain the seasonal efficiencies. Along with the metropolitan Toronto weather file used in the initial simulation, the weather files of Halifax, Vancouver, Edmonton, and Montreal were also utilized in the model. For the ASHP simulations, a simple weather file was replaced. The GSHP model however required both a weather file and a ground temperature model that represented the selected regions mentioned above. A good indication of the building heating and cooling demand in a selected region is the heating and cooling degree days (HDD & CDD). The TRNSYS weather files were used to obtain the respective HDD, CDD and maximum/minimum temperatures. The HDD and CDD were calculated using the following equations (ASHRAE, 2009):

$$\boldsymbol{HDD} = \sum_{i=1}^{N}(T_{base} - \overline{T}_{i})^{+} \tag{34}$$

$$\boldsymbol{CDD} = \sum_{i=1}^{N}(\overline{T}_{i} - T_{base})^{+} \tag{35}$$

where:

N: Is the number days in a year
$\overline{\mathbf{T}}_{\mathbf{i}}$ **:** Is the mean daily temperature
$\mathbf{T_{base}}$**:** Is the base temperature (Heating: 18˚C, Cooling: 10˚C)

The resulting HDD and CDD, along with the maximum and minimum hourly average temperatures are given below in Table 24.

Table 24 Yearly Heating and Cooling Degree Days

Location	HDD	CDD	Max Temp (˚C)	Min Temp (˚C)
Metro-Toronto	4122	1114	33.9	-22.2
Halifax	4297	710	28.1	-19.8
Vancouver	3034	785	26.3	-5.7
Edmonton	5514	812	29.4	-30.6
Montreal	4460	1130	32.2	-24.7

6.8 ASHP Selected Regions Results

The results of the ASHP simulation in selected Canadians regions are given in Table 25. It can be seen that the ASHP operates ideally in Vancouver because of a seasonal heating COP of 4.47 and a seasonal cooling COP of 5.73. It was also noted that the ASHP performed poorly in the heating season of Montreal and Edmonton due to such cold temperatures. In fact, it is important to note that the ASHP could not meet the set-point temperature and required back up heating in Edmonton. In Montreal, the indoor temperature was seen to drop a few degrees below the set-point as well. This was expected due to the -30˚C ambient temperature experienced in Edmonton and the -24.7˚C experienced in Montreal. Also, the lowest seasonal cooling COP was witnessed in Toronto with a peak outdoor temperature of 33.9˚C. The results of the selected region analysis conclude that the ASHP performs well in cooling mode given the following above mentioned regions. However in heating mode, regions with really low ambient temperatures will require supplementary heating.

Table 25 ASHP Heating and Cooling Simulation Results for Selected Canadian Regions

Location	Heating Output (kWh)	Cooling Output (kWh)	Heating Consumption (kWh)	Cooling Consumption (kWh)	Heating SCOP	Cooling SCOP
Metro-Toronto	17,579	2,289	5,442	434	3.23	5.27
Halifax	21,689	1,133	6,009	203	3.61	5.58
Vancouver	18,916	1,404	4,236	245	4.47	5.73
Edmonton	26,644	1,830	10,141	337	2.63	5.43
Montreal	23,888	2,934	8,031	540	2.97	5.42

6.9 GSHP Selected Regions Results

The results of the GSHP simulation in selected Canadians regions are given in Table 26. In the GSHP selected region simulations, both the weather file and the ground temperature model were altered. The ground temperature model parameters change from region to region. These parameters include 1) mean surface temperature, 2) amplitude of surface temperature, and 3) the time shift, which is the time difference (in days) between the beginning of the calendar year and the occurrence of the minimum surface temperature. Information on ground temperatures were obtained from Natural Resources Canada RETScreen program (Natural Resources Canada, 2011). Halifax, Toronto, and Vancouver had similar annual mean surface temperatures in the range of 6-8 ˚C, while Edmonton and Montreal had an annual mean surface temperature of 2.6˚C and 5.2˚C respectively. As a result, the seasonal heating COP of Edmonton was the lowest amongst the other regions at 2.83 followed by Montreal at 2.93. Montreal and Toronto had the highest monthly average surface temperature at 20.9˚C and 20.5˚C respectively, followed by Halifax at 19.1˚C, Edmonton at 18.1˚C, and lastly Vancouver at 16.6˚C. Consequently, the GSHP performed slightly better in Vancouver due to a relatively lower summer ground temperatures. Toronto, Halifax, and Edmonton had a cooling COP of 5.77-5.78, while Montreal and Vancouver had a cooling COP of 5.92 and 6.14, respectively. It is worth mentioning that the GSHP did not require any supplementary heating as in the case of the ASHP in Edmonton.

Table 26 GSHP Heating and Cooling Simulation Results for Selected Canadian Regions

Location	Heating Output (kWh)	Cooling Output (kWh)	Heating Consumption (kWh)	Cooling Consumption (kWh)	Heating SCOP	Cooling SCOP
Metro-Toronto	18,764	2,459	6,014	425	3.12	5.78
Halifax	23,188	1,225	7,361	212	3.15	5.77
Vancouver	20,240	1,519	6,445	247	3.14	6.14
Edmonton	28,589	2,023	10,102	350	2.83	5.78
Montreal	25,230	2,503	8,610	422	2.93	5.92

6.10 Cost Analysis

A simple cost analysis was completed on the two systems using software called RETSCREEN to compute an estimate payback period. In this cost analysis it is assumed that existing mechanical systems for a home will be replaced with one of two cases (conventional system or heat pump system). As well, the effect of interest rate on the overall result is neglected. The input parameters were taken from the results of the TRNSYS energy model created for the two houses using the Toronto weather file. The heat pump systems were compared to a conventional system where an electric heater is used during the heating season, and an air-conditioner system is used for the cooling season. The ASHP case is shown in Table 27 and the GSHP case is shown in Table 28.

House A: Air Source Heat Pump vs. Conventional System # 1

Table 27 ASHP Payback Period

Conventional System # 1		**Proposed Case # 1**	
Heating: Electric-Heater		**Heating:** ASHP	**Approximate Cost: $14,500**
Heated Floor Area (m^2)	344	Heated Floor Area (m^2)	344
Fuel Type	Electricity	Fuel Type	Electricity
Seasonal Efficiency	100%	Seasonal Efficiency	323%
Peak Heating (kW)	6.8	Peak Heating (kW)	6.8
Fuel Consumption (kWh)	17,579	Fuel Consumption (kWh)	5442
Fuel Rate ($/kWh)	0.095*	Fuel Rate ($/kWh)	0.095*
Fuel Cost ($)	1670	Fuel Cost ($)	517
Cooling: A/C		**Cooling:** ASHP	
Cooled Floor Area (m^2)	344	Cooled Floor Area (m^2)	344
Fuel Type	Electricity	Fuel Type	Electricity
SCOP	3	SCOP	5.27
Peak Cooling (kW)	5.1	Peak Cooling (kW)	5.1
Fuel Consumption (kWh)	763	Fuel Consumption (KWh)	439
Fuel Rate ($/kWh)	0.095*	Fuel Rate ($/kWh)	0.095*
Fuel Cost ($)	73	Fuel Cost ($)	42
Total Cost ($)	**1743**	**Total Cost ($)**	**559**
		Simple Payback:	**12.2 Years**

* See Table 29 for Electricity price breakdown

House B: Ground Source Heat Pump vs. Conventional System # 1

Table 28 GSHP Payback Period

Conventional System # 1		**Proposed Case # 1**	
			Approximate Cost: $34,500
Heating: Electric Heater		**Heating:** GSHP	(Natural Resources Canada, 2005)
Heated Floor Area (m²)	321	Heated Floor Area (m²)	321
Fuel Type	Electricity	Fuel Type	Electricity
Seasonal Efficiency	100%	Seasonal Efficiency	312%
Peak Heating (kW)	8.02	Peak Heating (kW)	8.02
Fuel Consumption (kWh)	18,701	Fuel Consumption (kWh)	5994
Fuel Rate ($/kWh)	0.095*	Fuel Rate ($/kWh)	0.095*
Fuel Cost ($)	1776	Fuel Cost ($)	569
Cooling: A/C		**Cooling:** ASHP	
Cooled Floor Area (m²)	321	Cooled Floor Area (m²)	321
Fuel Type	Electricity	Fuel Type	Electricity
SCOP	3	SCOP	5.78
Peak Cooling (kW)	4.86	Peak Cooling (kW)	4.86
Fuel Consumption (kWh)	813	Fuel Consumption (KWh)	422
Fuel Rate ($/kWh)	0.095*	Fuel Rate ($/kWh)	0.095*
Fuel Cost ($)	73	Fuel Cost ($)	40
Total Cost ($)	**1849**	**Total Cost ($)**	**609**
		Simple Payback:	**27.8 Years**

* See Table 29 for Electricity price breakdown

The annual cost of energy for the ASHP is $559 while the conventional system energy cost is $1743. With an initial equipment cost of $14,500 the simple payback turned out to be 12.2 years. The annual cost of energy for the GSHP is $609 while the conventional system energy cost is $ 1849. With an initial investment of $34,500 the simple payback turned out to be 27.8 years. It can be concluded that although the GSHP is slightly more efficient in both heating and cooling, the simple payback period suggests the ASHP to be the favourable choice.

Electricity Price Breakdown (Ontario)

Table 29 Electricity Price Breakdown Ontario (Energy Shop, 2011)

Cost of Electricity	**$/kWh**
Distribution Charge	0.0134
Transmission: Network	0.0064
Transmission: Connection	0.0026
Debt Retirement Charge	0.007
Regulated Price Plan	0.079
Total	**0.095**

Chapter 7

Summary & Conclusion

The Archetype Sustainable House project presented the opportunity to study and compare two popular types of efficient residential heating and cooling devices: a two-stage variable capacity air source heat pump and a horizontal loop coupled ground source heat pump. The implementation of a comprehensive monitoring system allowed for detailed performance analyses of these equipment. Data was collected from the monitoring systems every 5 seconds in a test period that was conducted over a 3-6 weeks in both cooling and heating modes. Points of interest for the ASHP were the efficiency of the heat pump at colder outdoor temperatures, efficiency of the heat pump at part loads, and two stage compressor operating characteristics. Points of interest for the GSHP were the efficiency of the heat pump at different load/source temperatures, and the cyclic characteristics of the compressor. Further analysis was done to investigate problems and potential improvements of the equipment control systems. Issues with the as-built system were presented, and methods of system improvements were shown through the use of data extrapolation. Lastly, TRNSYS 16 was utilized to model the twin houses as well as the heat pump systems including all conditioning equipment. The heat pumps were modeled using the performance curves obtained from the data collection. The TRNSYS house model was validated using experimental results, and an annual simulation was completed to obtain yearly heat pump performance. The systems were then simulated in different Canadian regions, and a final payback analysis was investigated using results of the TRNSYS simulation.

7.1 Heat Pump Performance

The ASHP performed very well in the cooling test period with a COP range of 4.7 at 33°C to 5.7 at around 16°C. When analyzing the part load cooling efficiency, it was noted that the heat pump only operated in the first stage at around 52 – 57 % of the rated capacity. It was noticed that the COP at this range was about 20% higher than the rated capacity COP. This suggests an enhancement of efficiency at part loads. Due to the ASHP having much of its operation in the first stage, explains the very high cooling COP. In heating mode, the ASHP performed satisfactorily at milder winter temperature, and poorly at temperatures below -19 ˚C. The ASHP heating COP ranged from 1.79 at -19˚C to 5.0 at around 9˚C. It was noticed that below -24˚C, the outdoor temperature is lower than the evaporator heat exchange temperature and no heat transfer will occur. When analyzing the part load performance, it was noted that the ASHP operated in both single and two-stage operation in the region of 54 – 103% of the rated capacity. At 54% of the rated capacity, the COP was 40% higher than the rated capacity. At 100% of the rated capacity the COP was close to the rated capacity COP. The GSHP also performed very well in the cooling test period with a COP range of 4.9 (at an ELT of 8.5°C and EST of 19.2°C) to 5.6 (at an ELT of 12.4°C and EST of 17.8°C). In heating mode, the GSHP was tested both in early and late winter. During the early heating test period, the GSHP performed well with a COP range of 3.05 (at an ELT of 44.4°C and an EST of 2.7°C) to 3.44 (at an ELT of 41.5°C and an EST of 5.48°C). In the later test period, the performance slightly deteriorated due to a lower ground temperature around the loop. The COP ranged from 2.78 (at an ELT of 48.5°C and an EST of -2.36°C) to 2.98 (at an ELT of 45.5°C and an EST of 0.2°C). Unlike the ASHP, the GSHP showed a constant performance which can be explained by a relatively constant ground temperature as opposed to the air temperature. The two systems were then compared in terms of operation characteristics and compressor cycling during the cooling test period. It was concluded that due to a variable capacity compressor, the ASHP was able to operate for longer periods at lower speeds. This capability of the ASHP not only provides better thermal comfort by closely meeting the temperature set-point, but it also enhances the efficiency as seen in the part load performance curves. The GSHP on the other hand showed high frequency, shorter operating times due to its constant capacity compressor. This is an indication of an oversized system which often causes thermal comfort issues and lower reliability of equipment.

7.2 Control System Issues

With the use of data extrapolation, the as-built ASHP and GSHP systems were analyzed for control issues. An issue was noted in the control system of House A where the AHU fan was constantly operating at a low speed although the compressor was not operating. This simple control issue can significantly affect the overall energy consumption of the system if addressed. Energy savings of 36.3% can be achieved by simply controlling the AHU to operate with the compressor. The GSHP also contained various control system issues. The first notable issue was with the buffer tank temperature control system. Water temperature was controlled by frequently circulating water from the buffer tank into the GSHP system. A separate thermostat should have been installed in the tank to monitor tank temperature so the pump would not need to operate so often. In this regard, the pump would only operate when the compressor operated. As well, the pump from the buffer tank to the AHU constantly circulated water to and from the AHU regardless of the AHU operation. Having solved these two control issues, energy savings of 28.2% was noticed. These simple control issues could have been avoided if commissioning was commenced after the system was built.

7.3 Energy Modeling and Simulation

A TRNSYS House model was developed and validated for House A and B. Also, an ASHP and GSHP model was created and integrated with the house models. Energy simulation was utilized to predict the annual heating and cooling performance of the heat pumps. The model was later used to simulate the heat pump performance in different climates. The simulation results indicate that the ASHP delivered 2289 kWh of cooling while consuming 434 kWh of electricity. The seasonal cooling COP therefore was 5.27. When including the indoor fan electricity consumption (without control issues), the seasonal COP was 3.5. In heating mode, the ASHP delivered 17,579 kWh of heat while consuming 5,442 kWh of electricity. The seasonal COP therefore turned out to be 3.23. When including the indoor fan electricity consumption (without control issues) the seasonal COP was 2.1. The GSHP model resulted in 2,459 kWh of cooling output while consuming 425 kWh of electricity. The resulting seasonal COP turned out to be 5.78. When including the electricity consumption of the pump to buffer tank, pump to AHU, and the AHU fan (without control issues), the seasonal COP turned out to be 2.71. In heating mode, the GSHP outputted 18,764 kWh of heating and consumed 5,460 kWh of electricity resulting in a seasonal COP of 3.44. When including the electricity consumption of the pump to buffer tank and pump to in-floor heating (without control issues), the seasonal heating COP turned out to be 3.14. It is noticed that the GSHP overall system COP in cooling mode is relatively low. An explanation to this observation is that cooling is delivered to the spaces using a multizone AHU where dampers are used to control air flow to zones. It is therefore common for the AHU fan as well as the AHU circulation pump to operate frequently. However, the AHU fan is multispeed and can adjust its airflow to the desired capacity. The circulation pump on the other hand is not variable speed and is the main reason for such high electricity consumption in the overall system. The ASHP and the GSHP were simulated in different Canadian climates. The ASHP performed ideally in the Vancouver climate, both in heating and cooling. The system did however show weakness during the heating season in Edmonton. In fact, the ASHP could not meet the set-point temperature and required back-up heating due to the -30˚C ambient temperature experienced in Edmonton. Similar to the ASHP simulation, the GSHP had the lowest heating COP in Edmonton, due to a lower annual mean surface temperature of 2.6˚C. On the contrary, the system had the highest cooling COP in Vancouver because of a lower mean monthly temperature of 16.6˚C.

7.4 Payback Analysis

RETScreen was used to investigate the simple payback of the two heat pump systems. By assuming an all electric conventional system with 100% efficiency, the ASHP resulted with a payback period of 12.2 years, while the GSHP had a much longer payback period of 27.8 years. Although the GSHP results in higher annual energy saving over the ASHP, the initial investment cost is significantly higher. It is also worth mentioning that the ASHP would often be combined with a backup heating device (as in the case of the Archetype House). The initial cost and payback period of a backup heating device should also be considered in the overall ASHP case.

7.5 Contribution of Study

This study has contributed a fair amount of results that is considered new in the literature. The Archetype Twin Houses have allowed for a direct and side-by-side comparison of equipment performance in a real residential setting. The capability of the monitoring system has greatly contributed in collecting clean and accurate data. The heat pump systems tested are both considered new sustainable technologies for residential applications. These equipment include an ASHP with a two-stage variable compressor designed to perform well in cold climates, and a horizontal looped GSHP using both a multi-zone AHU and in-floor radiant heating. The ASHP was tested for cold climate performance and part load performance, areas that are uncommon in the literature. The GSHP utilized a horizontal ground loop heat exchanger which often requires large amount of land that is costly. Issues with control systems of both equipment were mentioned, and potential energy savings were shown through the use of data extrapolation. This information is beneficial to home owners, contractors, and consultants who often overlook the commissioning process of HVAC system installation. The commissioning process is particularly important with high efficiency designed homes such as the Archetype House which is a LEED Platinum certified home. The TRNSYS house and heat pump models were validated and tested in various Canadian climates. This analysis allows for a better understanding of how each system can perform in different climates. Most importantly, the simulation and cost analysis informs homeowners interested in installing such systems about the feasibility of their investment.

7.6 Recommendations

The following recommendations are made based on the results of this study:

- It is recommended that all installed HVAC systems are commissioned after installation. In this case, commissioning would ensure that intended design follows LEED energy credits.
- It is highly recommended that an aquastat be used in the buffer tank to control water set-point temperature. The current system checks tank temperature by often circulating water to and from the buffer tank.
- To obtain a more accurate result in measuring the AHU-A air flow, a flow measuring device should be used instead of an air velocity meter which measures the velocity at one point of the duct.

- In climates that experience winter temperatures below -20˚C, it is recommended to have supplementary heating if an ASHP is the only source of heating.
- It is recommended that a variable speed circulation pump be used when delivering conditioned water to the multi-zone AHU/in-floor heating system. When using a variable speed circulation pump, the control of flow through the coils will have to be coordinated with the damper control system to deliver enough cooling /heating to the zones.

7.7 Future Work

- Installation of a separate power meter on the outdoor ASHP fan to investigate the variable capacity capability.
- Comparison of horizontal vs. vertical ground loop configuration.
- The use of solar collectors to recharge the ground temperature near the pipes during the winter.
- Test and analyze the GSHP in-floor system in cooling mode.
- Analyze the thermal comfort of the multi-zone in-floor system and compare the results to House A thermal comfort.
- Analyze the performance of the GSHP with a desuperheater in cooling mode.

Appendix A

A.1 Fluid Properties

As referenced in the methodology section, the properties of fluids used in the heat pump equations are given in this section. Table A1 compares the density at atmospheric conditions and the density of moist air at an altitude of 347 ft (Toronto Altitude). Due to such a small percentage difference, the density at standard atmospheric conditions was used in the calculations.

Table A 1 Density of Air

Temperature (˚C)	Density Atm. Condition (kg/m^3)	Density of Moist Air at 347 ft (Kg/m^3)	Percentage difference
-20	1.395	1.378375235	1.191739408
0	1.293	1.279321131	1.05797185
5	1.269	1.25732588	0.919946386
10	1.247	1.236464785	0.84484483
15	1.225	1.216781113	0.67[illegible]929536
20	1.204	1.198337792	0.470283046
25	1.184	1.18121918	0.234866513
30	1.165	1.165532898	-0.045742356
40	1.127	1.139015256	-1.066127433
50	1.109	1.120181364	-1.00823842
60	1.06	1.11091602	-4.803398103
		Avg =	1.119457565

A graph was created as shown in Figure A1 to illustrate the relationship between the density of water at various temperatures. This relationship is used to calculate the heating and cooling of water systems for the GSHP.

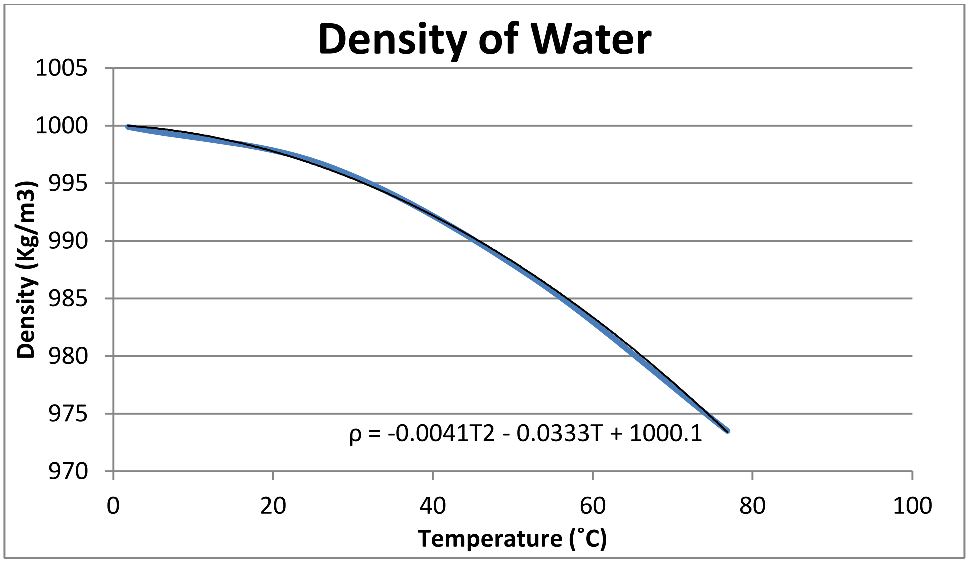

Figure A 1 Density of Water (Moran & Shapiro, 2004)

The density and specific heat of water at various temperatures is given below in Table A 2.

Table A 2 Density and Specific Heat of Water (Moran & Shapiro, 2004)

Temperature (K)	Temperature (˚C)	Density (kg/m^3)	Specific Heat (kJ/kg.K)
275	1.85	999.9	4.211
300	26.85	996.5	4.179
325	51.85	987.1	4.182
350	76.85	973.5	4.195

A.2 Ground Loop Fluid

The ground loop fluid of the GSHP uses a 30% propylene glycol/water mixture. Figure A 2 illustrates the relationship of the PG density with respect to fluid temperature. This density function is used to calculate the heat extracted from and rejected to the ground from the GSHP.

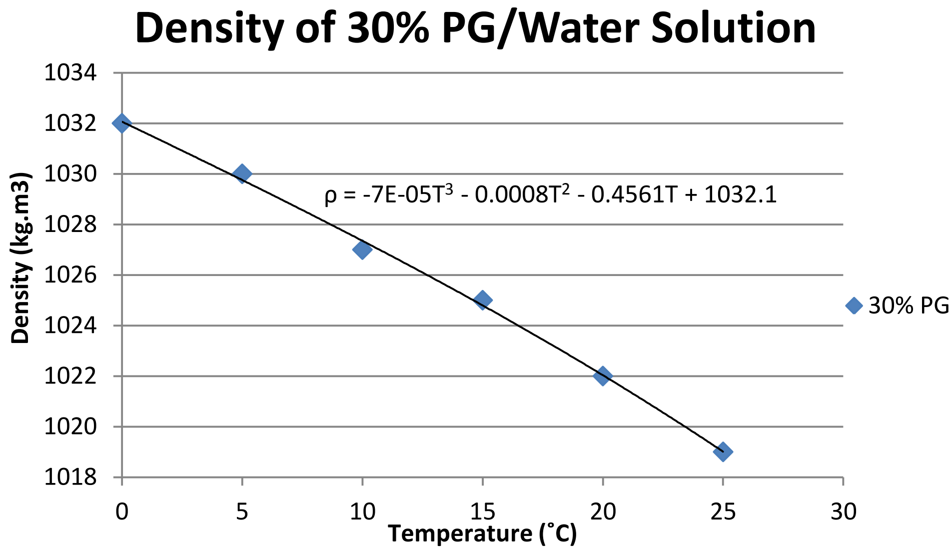

Figure A 2 Density of 30% Propylene Glycol/Water Solution (Curme & Johnston, 1952)

Appendix B

B.1 Uncertainty Analysis

In this section, uncertainty analysis is performed on the two heat pumps. During the data collection, it is assumed that the only source of uncertainty is generated from the sensors installed on the heat pumps. Random error is neglected in this analysis. The sensors used on the equipment all have manufactured sensor accuracy. Using equations for combined uncertainties (Bell, 1999), the heat pump uncertainty analysis can be performed. A list of the sensors used in the experiment along with their accuracy is given below in Table B 1.

Table B 1 Sensor Accuracy

Sensor name	Sensor type	Manufacturer	Location	Model number	Sensor Accuracy
Air velocity transmitter	Air velocity	Dwyer Instruments Inc.	AHU-A Main Supply Duct	AVU-1-A	±5.0%
Turbine type flow rate	Liquid/water flow rate	Omega/Clark Solution	GSHP to load Pipe	CFT110	±3.0%
Metering flow switch	Liquid/water flow rate	Proteus Industries Inc.	GSHP Ground Loop	800 Series	±0.5%
Air temperature (AT)/Relative humidity (RH)	AT and RH	Dwyer Instruments Inc.	AHU Supply/Return Duct	Series RHT-D	AT: ±1.5% RH: ±3.0%
Wattnode	Electrical energy	Continental Control Systems	Devices Consuming Electricity	WNB-3Y-208-P	±1.0%
RTD sensor (Pt.-100, directly immersed)	Temperature	Omega	On GSHP Pipes	PRTF-10-2-100-1/4-6-E	±0.1%

Individual standard uncertainties can be combined by using the root sum of squares. The result of this is called combined standard uncertainty (Bell, 1999). For addition and subtraction the combined uncertainty is given by: $\mu_c = \sqrt{A1^2 + A2^2 + ..etc}$ where A1 and A2 are the uncertainties from the sensors. In multiplication and division, the combined uncertainty is given by: $\frac{\mu_c(B)}{B} = \sqrt{(\frac{u_c(C)}{C})^2 + (\frac{u_c(D)}{D})^2}$ where B = C * D or C/D and $u_c(C)$ is the uncertainty of C while $u_c(D)$ is the uncertainty of D. Using the methods shown above, the uncertainties of some of the equations in section 4 are shown below in Table B 2**.**

Table B 2 Uncertainty in Heat Pump Calculations

Variable	**Uncertainty (%)**
ASHP Heating Output	±9.34
ASHP COP	±9.39
GSHP Heating Output	±3.01
GSHP COP	±3.17

Appendix C

TRNSYS Model Input Parameters

C.1 ASHP Model

ASHP: Split system with variable capacity compressor and direct expansion coil AHU

Performance: See Figure 7 & 49 for COP versus temperature relationship

C.2 GSHP Model

Horizontal Loop Heat Exchanger:

Depth of Pipe: 6 ft

Length of Pipe: 1000 ft

Fluid Type: 30% propylene glycol, 70% water

Fluid Density: 1024 kg/m^3

Fluid Specific Heat: 3.915 kJ/kg.K

# of Pumps: 2 at 325 W power draw

Ground Source Heat Pump:

Source Fluid**:** 30% propylene glycol, 70% water

Source Flow Rate: 15 GPM

Load Fluid: Water

Load Flow Rate: 12 GPM

# of Pumps: 1 at 185 W power draw

Performance: See Figure 19 & 65 for source and load relationships

Buffer Tank:

Tank Volume: 270 Litters

Tank Fluid: Water

Tank Heating Set point: Higher limit 45 ˚C, Lower limit 25˚ C

Tank Cooling Set point: Higher limit 15 ˚C, Lower limit 9˚ C

Number of Temperature Nodes: 5

In-Floor Radiant Heating:

Fluid Flow Rate: 2 GPM per valve

AHU-B:

Type: Fan Coil system with multi-zone control

Appendix D

Sample One Hour ASHP/GSHP Heating Operation

The two heat pumps were investigated for operational behaviour in mild, moderate, and cold winter temperatures. Here, the performance was concentrated in a one hour test period.

D.1 ASHP

The first ASHP test was completed on February 9, 2011 at 2:00 pm. During the one hour test period, the average temperature was -2.5˚C. From Figure D 1 it can be seen that the heat pump operated in single stage during the entire one hour and did not shut off during this period. The COP ranged from 2.76-3.03.

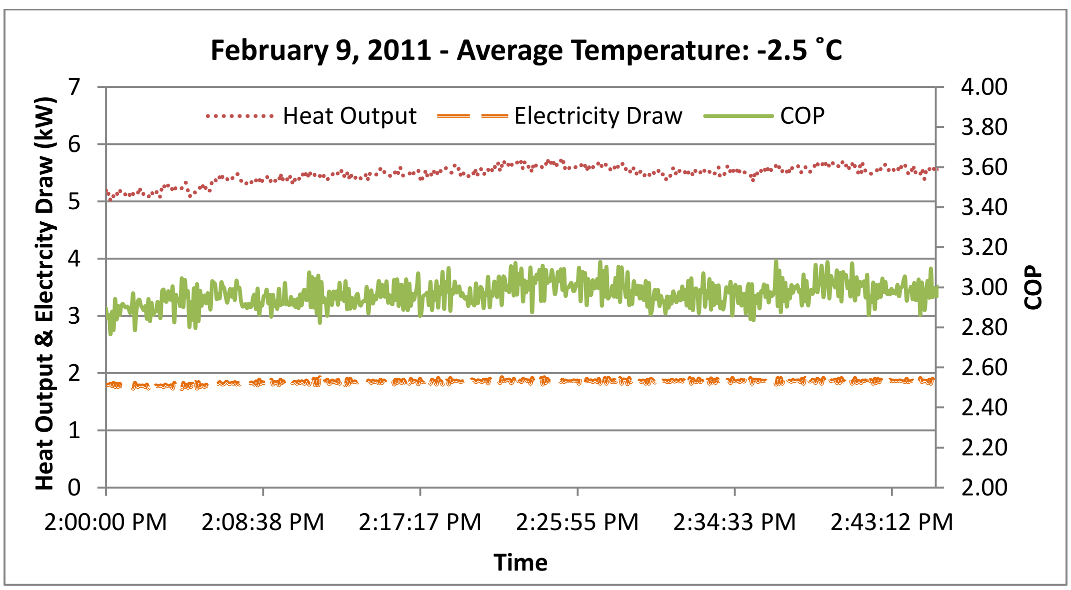

Figure D 1 ASHP One Hour Test at -2.5 ˚C

The second ASHP test was completed on January 30, 2011 at 12:00 am. During the one hour test period, the average temperature was -10.9˚C. From Figure D 2 it can be seen that the heat pump operated in single stage during the entire one hour, and similar to the previous case, did not shut off during this period. The COP however differed, ranging from 1.93-2.34.

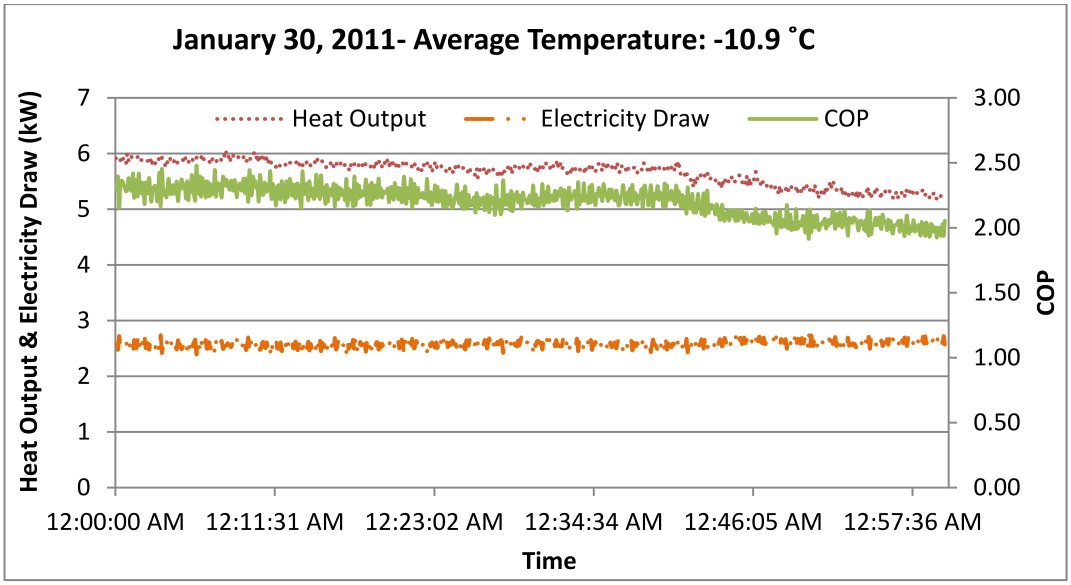

Figure D 2 ASHP One Hour Test at -10.9 ˚C

The last and most significant ASHP test was completed on January 31, 2011 at 4:00 am. During the one hour test period, the average temperature was -17.4˚C. From Figure D 3 it can be seen that the heat pump operated in the second stage during the entire one hour, and similar to the two previous cases, did not shut off during this period. The COP however was fairly low ranging from 1.58-2.01. It should also be noted that initially the heat pump outputted at a high heating rate (above 12 kW) and gradually decreased its output to match the heating load.

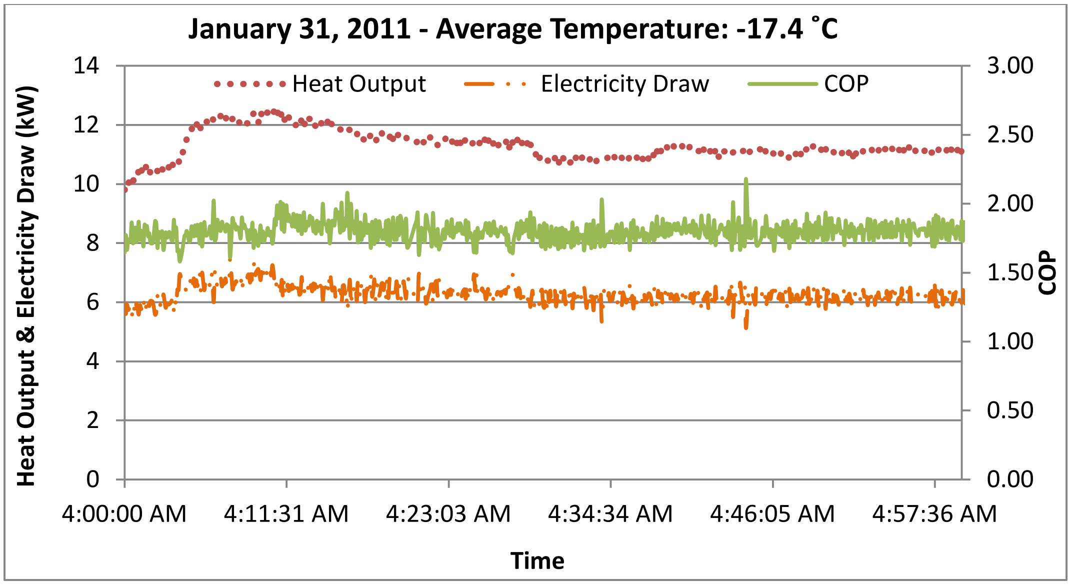

Figure D 3 ASHP One Hour Test at -17.4 ˚C

D.2 GSHP

Similar to the ASHP, the GSHP was also tested at three temperature ranges in a one hour test period. The first GSHP test was completed on December 8, 2010 at 7:00 pm. During the one hour test period, the average temperature was -4˚C. From Figure D 4 it can be seen that the heat pump was initially operating and turned off for about 30 minutes before the system called for heating once again. The COP ranged from 2.71-3.08.

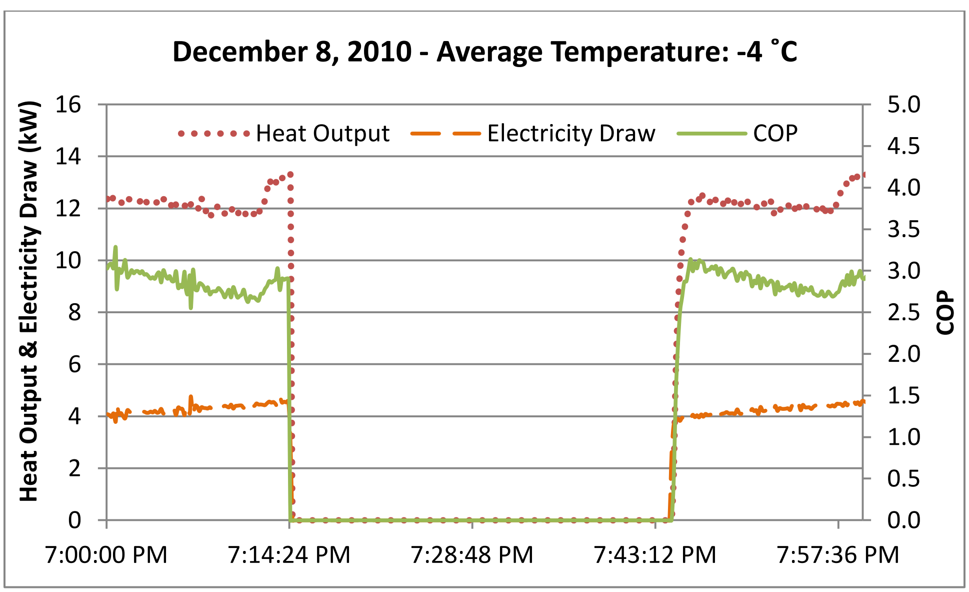

Figure D 4 GSHP One Hour Test at -4 ˚C

The second GSHP test was completed on December 13, 2010 at 10:00 pm. During the one hour test period, the average temperature was -12˚C. From Figure D 5 it can be seen that the heat pump cycled on and off once in this one hour. The COP ranged from 2.93-3.2.

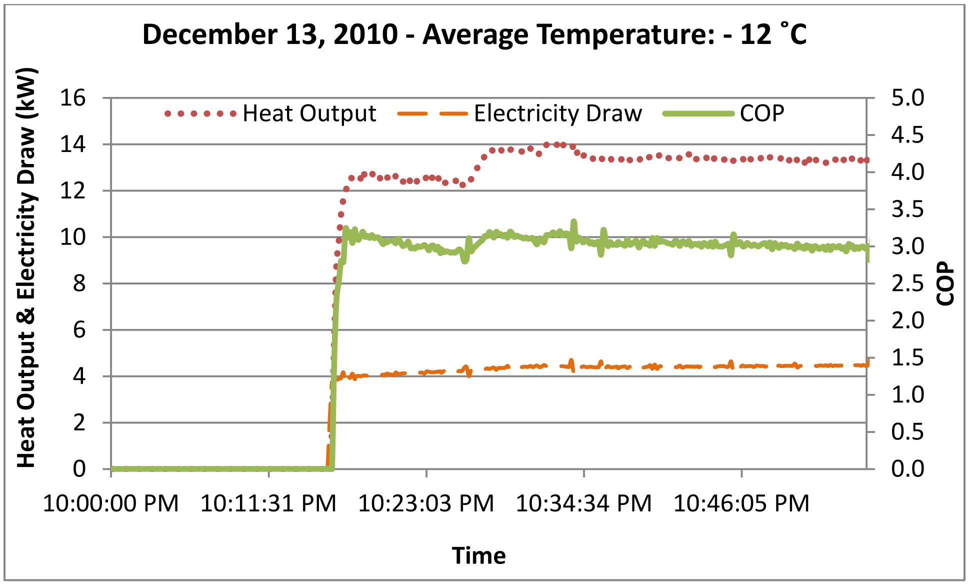

Figure D 5 GSHP One Hour Test at -12 ˚C

The last GSHP test was completed on December 15, 2010 at 7:00 am. During the one hour test period, the average temperature was -15˚C. From Figure D 6 it can be seen that the heat pump cycled on and off twice in this one hour. The COP ranged from 2.63-3.44.

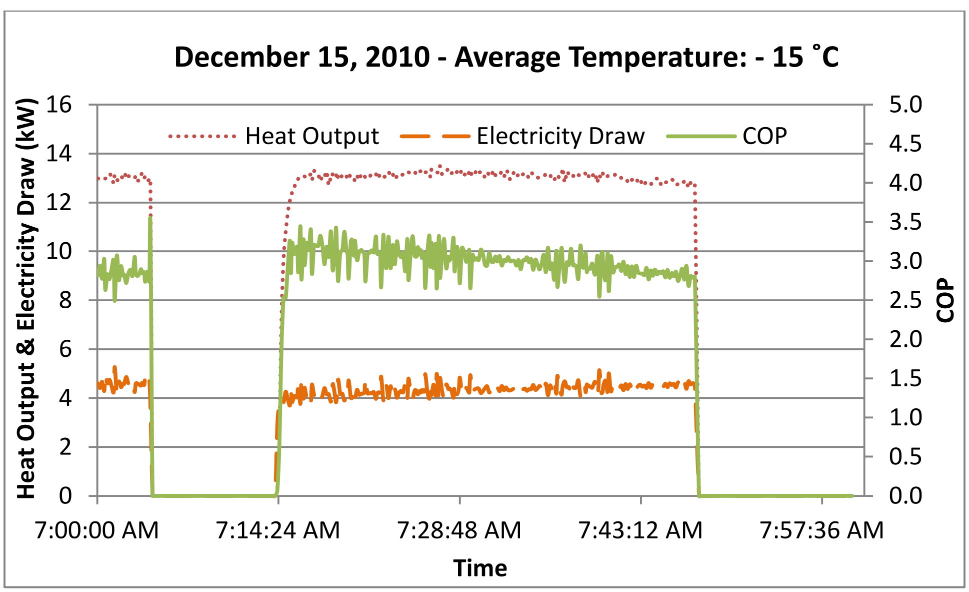

Figure D 6 GSHP One Hour Test at -15 ˚C

From the results of the 1 hour test period, it can be concluded that the ASHP COP is reduced in cold outdoor temperatures, while the GSHP's is fairly constant. Also, the variable capacity capabilities of the ASHP can be noticed depending on the building load. The second stage only turned on in colder ambient temperatures. It was also noted that the ASHP never cycled in the 1 hour test periods. The GSHP however cycled at least once in all three test periods.

Appendix E

Heat Pump Cooling and Heating Output Comparison

The daily cooling and heating outputs of the heat pumps obtained from the data collection earlier are shown in Figures E 1 and E 2. Figure E 1 illustrates the daily cooling output of the heat pumps while Figure E 2 illustrated the heating outputs.

E.1 Cooling

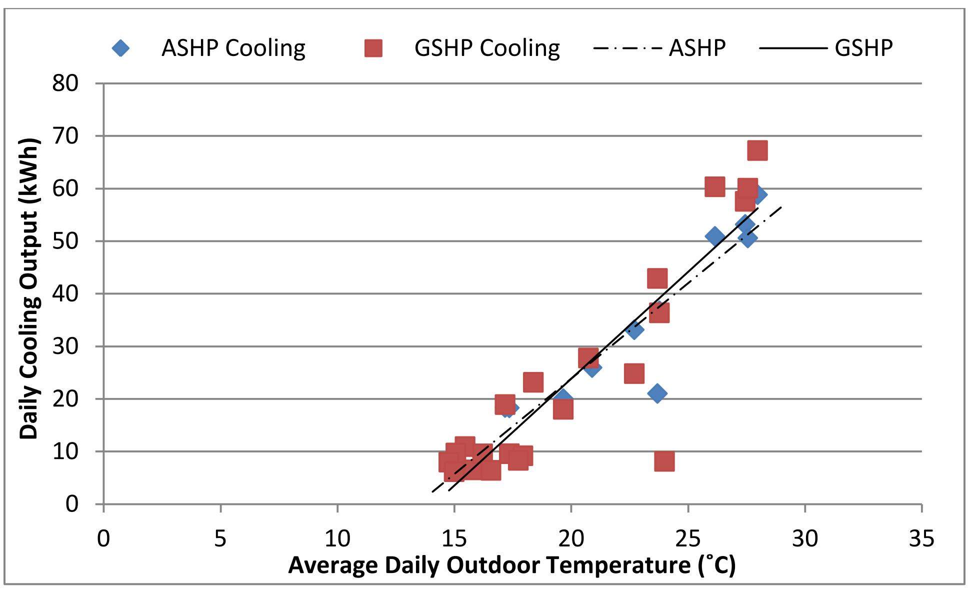

Figure E 1 ASHP/GSHP Cooling Output vs Average Daily Temperature

E.2 Heating

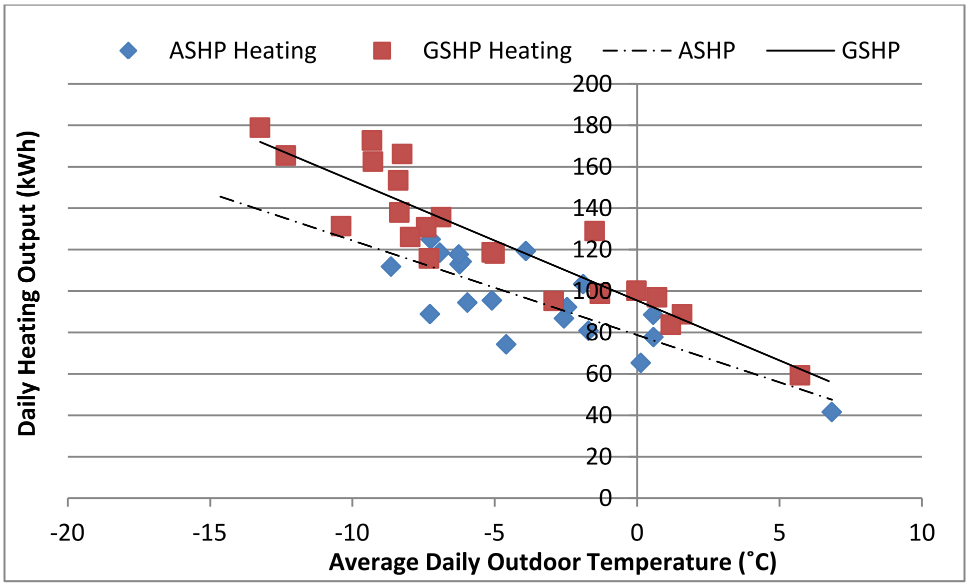

Figure E 2 ASHP/GSHP Heating Output vs Average Daily Temperature

References

Air Density and Specific Weight . (n.d.). Retrieved August 19, 2010, from The Engineering Tool Box: http://www.engineeringtoolbox.com/air-desity-specific-weight-d_600.html

American Society of Heating, Refrigerating, and Air-Conditioning Engineers Inc. (2009). 2009 ASHRAE Handbook: Fundamentals.

ASHRAE. (2009). *2009 ASHRAE Handbook - Fundamentals.* American Society of Heating, Refrigerating and Air-Conditioning Engineers, Inc.

Aydinalp, M., Ferguson, A., Fung, A., & Ugursal, V. (2001). Characterization of Energy Load Profiles in Housing Literature Review. *Canadian Residential Energy End-Use Data and Analysis Centre* .

Aye, L., Fuller, R., & Canal, A. (2010). Evaluation of a Heat Pump System for Greenhouse Heating. *International Journal of Thermal Sciences* , 202-208.

Bakirci, K. (2010). Evaluation of The Performance of a Ground-Source Heat-Pump System with Series GHE (Ground Heat Exchanger) in the Cold Climate Region. *Energy* , 3088-3096.

Barua, R. (2010). *ASSESSMENT AND ENERGY BENCHMARKING FOR TWO ARCHETYPE SUSTAINABLE HOUSES THROUGH COMPREHENSIVE LONG TERM MONITORING.* Toronto: Ryerson University.

Baxter, V. D. (1984). Comparison of Filed Performance of a High Efficiency Heat Pump With and Without a Desuperheater Water Heater. *ASHRAE Transactions* , 180-190.

Bell, S. (1999). *A Beginner’s Guide to Uncertainty of Measurement.* Middlesex, United Kingdom: National Physical Laboratory.

Bertsch, S., & Groll, E. (2008). Two-Stage Air-Source Heat Pump for Residential Heating and Cooling Applications in Northern U.S Climates. *International Journal of Refrigeration* , 1282-1292.

Biaoua, A., & Bernier, M. (2008). Achieving Total Domestic Hot Water Production With Renewable Energy. *Building and Environment* , 651-660.

CanmetENERGY . (2009, 6 3). A Review of Low and Net-Zero Energy Solar Home Initiatives. Varennes, QC, Canada.

Conservation Physics. (n.d.). *Moisture in air calculations* . Retrieved August 28, 2010, from Equations describing the physical properties of moist air: http://www.conservationphysics.org/atmcalc/atmoclc1.php

Crarley, D., Hand, J., Kummert, M., & Griffith, B. (2005, July). Contrasting the Capabilities of Building Energy Perfromance Simulation Programs. Washington , United States of America.

Curme, & Johnston. (1952). *Technical Data Propylene Glycol.* NewYork: Reinhold Publishing Corp.

Dembo, A., NG, R., Pyrka, A., & Fung, A. (2009). The Archetype Sustainable House: Investigating its potentials to achieving the net-zero energy status based on the results of a detailed energy audit. West Lafayette: Purdue University.

Deng, S., Song, Z., & Tant, K. (1998). Air-Cooled Heat Pump With Desuperheater: Retrofit For Year-Round Service Hot Water Supply. *Building services engineering research & technology* , 129-133.

Doherty, P., Al-Huthaili, S., Riffat, S., & Abodahab, N. (2004). Ground Source Heat Pump—Description and Preliminary Results of the Eco House System. *Applied Thermal Engineering* , 2627-2641.

D'Valentine, M., & Goldschmidt, V. (1990). Desuperheater Water-Heater and Air-to-Air Heat Pump System: Representative Performance Data. *ASHRAE Transactions* , 417-421.

Energy Shop. (2011, December 4). *Electricity Prices for Toronto Residential Customers*. Retrieved September 12, 2011, from Enrgy Shop: http://www.energyshop.com/electricity-prices-toronto-residential.cfm

Engineering Toolbox. (n.d.). *Propylene Glycol based Heat-Transfer Fluids*. Retrieved Jully 5, 2010, from The Engineering Toolbox: http://www.engineeringtoolbox.com/propylene-glycol-d_363.html

Enyu, W., Fung, A., Qi, C., & Leong, W. (2012). Performance prediction of a hybrid solar ground-source heat pump system. *Energy and Buildings, In Press* .

Erbs, D., Bullock, C., & Voorhis, R. (1986). New Testing and Rating Procedures for Seasonal Performance of Heat Pumps with Variable Speed Compressors. *ASHRAE Transactions* , 696-705.

Fadel, G., Cowden, E., & Dymek, A. (1986). Analysis and Simulation of Variable Speed Drive Heat Pumps. *Advanced Energy Systems* , 71-80.

Guoyuan, M., Qinhu, C., & Yi, J. (2003). Experimental Investigation of Air-Source Heat Pump For Cold Regions. *International Journal of Refrigeration* , 12-18.

Hwang, Y., Lee, J.-K., & Jeong, Y.-M. (2008). Cooling Performance of a Vertical Ground-Coupled Heat Pump System Installed in a School Building. *Renewable Energy* , 578-582.

Judkoff, R., & Neymark, J. (1995). A Procedure for Testing the Ability of Whole Building Energy Simulation Programs to Thermally Model the Building Fabric. *Journal of Solar Energy Engineering* , 7-15.

Kavanaugh, S., & Raffferty, K. (1997). Ground Source Heat Pumps: Design of Geothermal Systems for Commercial and Institutional Buildings. *ASHRAE* , 167.

Kavanaugh, S., Falls, R., & Parker, J. (1994). A Variable-Speed Ground-Source Heat Pump. *ASHRAE Transactions* , 1588-1596.

Kent, E. (1995). Performance Evaluation of a Compact Air-To-Air Heat Pump. *Energy Conversion and Management* , 341-345.

Kjellsson, E., Hellstrom, G., & Perers, B. (2010). Optimization of Systems with the Combination of Ground-Source Heat Pump and Solar Collectors in Dwellings. *Energy* , 2667-2673.

Klein, S., Beckman, W., Mitchell, J., Duffie, J., Duffie, N., Freeman, T., et al. (2006, June). TRNSYS 16 - A Transient System Simulation Program. Madison, Wisconsin, U.S.A.

Magranera, T., Monterob, A., Quilis, S., & Urchueguíac, J. (2010). Comparison Between Design and Actual Energy Performance of a HVAC-Ground Coupled Heat Pump System in Cooling and Heating Operation. *Energy and Buildings* , 1394–1401.

Marrone, J. (2007). *Getting to Zero: Defining the Path to Net Zero Energy Home Construction.* Natural Resources Canada.

McQuiston, Parker, & Spitler. (2005). *Heating Ventilating, And Air Conditioning.* New Jersey: John Wiley & Sons.

Meteotest. (2010). *Meteonorm: Global Meteorological Database for Engineers, Planners and Education*. Retrieved 11 29, 2010, from Meteonorm: http://www.meteonorm.com/pages/en/meteonorm.php

Michopoulos, A., Bozis, D., Kikidis, P., Papakostas, K., & Kyriakis, N. (2007). Three-Years Operation Experience of a Ground Source Heat Pump System in Northern Greece. *Energy and Buildings* , 328-334.

Moran, J., & Shapiro, N. (2004). *Fundamentals of Engineering Thermodynamics.* New Jersey: John Wiley & Sons, Inc.

Mountford, D., & Freund, P. (1981). The performance of an Air-Water Heat Pump Installed in an Experimental House. *Building Services Engineering Research & Technology* , 174-180.

Natural Resources Canada. (2005). *CLEAN ENERGY PROJECT ANALYSIS: Ground Source Heat Project Analysis.* Minister of Natural Resources Canada.

Ontario Energy Board. (2011, 07 28). *Smart Meters and Time-of-use (TOU) Prices*. Retrieved 10 2, 2011, from http://www.ontarioenergyboard.ca/OEB/Consumers/Electricity/Smart+Meters

Rad, F., Fung, A., & Leong, W. (2009). Combined Solar Thermal and Ground Source Heat Pump System. *11th International IBPSA Conference Building Simulation* , 2297-2305.

Roth, K., Dieckmann, J., & Brodrick, J. (2009). Heat Pumps for Cold Climates. *ASHRAE* , 69-72.

Sakellari, D., Forse, M., & Lundqvist, P. (2006). Investigating Control Strategies for a Domestic Low-Temperature Heat Pump Heating System. *International Journal of Refrigeration* , 547-555.

Salsbury, T., & Diamond, R. (2000). Performance Validation and Energy Analysis of HVAC Systems Using Simulation. *Energy and Buildings* , 5-7.

Tassou, S., Marquand, C., & Wilson, D. (1984). Part-Load Performance Analysis of Air-to-Water Heat Pump Systems. *Journal of the Institute of Energy* , 364-367.

Tong, Y., Kozai, T., Nishioka, N., & Ohyama, K. (2010). Greenhouse Heating Using Heat Pumps with a High Coefficient of Performance (COP). *Biosystems Engineering* , 405-411.

Toronto Facts & Figures. (2010). Retrieved August 22, 2010, from A View on Cities: http://www.aviewoncities.com/toronto/torontofacts.htm

Ugursal, V. I., Ma, B., & Li, C. (1992). Thermal Performance and Economic Feasibility of A Low Energy House Equipped with An Air-Source Heat Pump. *American Society of Mechanical Engineers* , 111-117.

Umezu, K., & Suma, S. (1984). HEAT PUMP ROOM AIR-CONDITIONER USING VARIABLE CAPACITY COMPRESSOR. *ASHRAE Transactions* , 335-349.

Wang, Ma, Z., Jiang, Y., Yang, Y., Xu, S., & Yang, Z. (2005). Field Test Investigation of a Double-Stage Coupled Heat Pumps Heating System for Cold Regions. *International Journal of Refrigeration* , 672-679.

Wang, R., Xie, G., Wu, Q., Wu, Y., & Yuan, J. (2011). An Air Source Heat Pump with an Advanced Cycle for Heating Buildings in Beijing. *Energy Conversion and Management* , 1493–150.

Wang, X., Ma, C., & Lu, Y. (2009). An experimental study of a direct expansion ground-coupled heat pump system in heating mode. *INTERNATIONAL JOURNAL OF ENERGY RESEARCH* , 1367–1383.

Wibbels, M., & Braven, K. (1994). The Effect of Cycling Operation of a Horizontal Ground Loop on Ground Coupled Heat Pump Performance. *ASME* , 33-44.

Zhang, D., Barua, R., & Fung, A. (2011). TRCA-BILD Archetype Sustainable House: Overview of Monitoring System and Preliminary Results for Mechanical Systems. *ASHRAE Transaction, Volume 117* .

Zogou, O., & Stamatelos, A. (2007). Optimization of Thermal Performance of a Building with Ground Source Heat Pump System. *Energy Conversion and Management* , 2853-2863.